QUANTIFICATION AND ANALYSIS OF HAND GRASP DYNAMICS AND ARM REACHING KINEMATICS FOLLOWING HEMIPARESIS USING A NOVEL ASSISTIVE ROBOTICS APPROACH

by

NAM – HUN KIM

A Dissertation submitted to the

Graduate School – New Brunswick

Rutgers, The State University of New Jersey

and

The Graduate School of Biomedical Sciences

University of Medicine and Dentistry of New Jersey

In partial fulfillment of the requirements

for the degree of

Doctor of Philosophy

Graduate Program in Biomedical Engineering

written under the direction of

Professor William Craelius

and approved by

_____

_____

_____

_____

_____

New Brunswick, New Jersey

May, 2007

ABSTRACT OF THE DISSERTATION

Quantification and Analysis of Hand Grasp Dynamics and Arm Reaching Kinematics Following Hemiparesis Using a Novel Assistive Robotics Approach

by Nam – Hun KIM

Dissertation Director: Professor William Craelius

Conventional upper extremity rehabilitation methods provide limited choices for training regimes with poor recovery outlook in regaining motor ability for persons with stroke, compared much wider and elaborative lower limb training options. Moreover, the existing upper limb rehabilitation paradigms often focus only on bulk motions with maximal force generation, neglecting on a more fine motor control over the whole spectrum of various force levels. Considering the fact that the focus on the upper extremity should be based on the finer control than lower extremity, an imbalance exists in the current rehabilitation regime. To balance this shortcoming and to achieve better overall results in rehabilitation training regime, a more refined and well-designed training system is required to ensure more practical and effective outcome with finer motor control as well as to quantitatively address the theoretical aspects of motor control.

To address these issues in terms of developing a better rehabilitation platform as well as to deliver more quantifiable metrics, this study investigated application and development of a novel upper limb rehabilitation training system for the restoration of daily fine motor function for hemiparetic persons using assistive robotic approaches on rehabilitation instrumentation to effectively quantify human kinetic and dynamic motor functions at the elbow, forearm, and hand.

Conventional Fitts' speed vs. accuracy trade-off (SAT) test was adapted for this research for both kinematic and dynamic aspects of human motor control. First, kinematic speed vs. accuracy trade-off (KSAT) test was performed at the elbow flexion and extension level, then dynamic speed vs. accuracy trade-off (DSAT) test was performed at the palmar force level, both with visual feedback.

Specifically, four hypotheses will be tested in this research: (1) Stroke groups' log-linearity trend from KSAT test will follow Fitts' law with differing slopes from normal groups' performance. (2) Second hypothesis will test normal groups' log-linearity from DSAT test to see whether the dynamic aspects of Fitts' paradigm will correlate to conventional kinematic Fitts' type behavior. (3) Third hypothesis will test

on the reproducibility of the direct hand grip force from extrinsic force signals at the forearm to see the functionality of the force myography (FMG) which detects extrinsic force signals at the end-effector sites. (4) Last hypothesis will test the stroke group's improvements in terms of important functional metrics produced by the devices to show the efficacy of the system.

The overall system is called HARI (Hand and Arm Rehabilitation Interface) with accompanying sub-components; MAST (Mechanical Arm Supporter and Tracker) for the base platform and lower arm movement detection with the embedded goniometer at the elbow, FMG (Force Myography) cuff sleeve for forearm musculature detection, and the Gripper for direct hand grip force detection. Instrumental development for HARI as a whole upper-limb rehabilitation system was successful, that all the individual sub-devices were able to gather a reliable and repeatable, high quality physiological data with good signal-to-noise (SNR) as well as excellent patient comfortness, to the level of imminent marketability for hospital, laboratory, or home settings, as an efficient and innovative rehabilitation tool.

Keywords – stroke, hemiparesis, paralysis, upper limb rehabilitation, kinematic, dynamic, Fitts' Law, fine-motor control.

Acknowledgement / Dedication

I would like to thank my Thesis Director Dr. William Craelius for his kind advices and management skill not only for the research but also for living in the US in general. I would also like to thank Drs. Nicki Newby, Kathryn De Laurentis, James Flint for their professional supports. Drs. Gary Drzewiecki, John Semmlow, and Dennis Carmody who gave me many invaluable comments on the instrumentation as well as relevant theoretical motor control and clinical aspects of my research.

I am also very grateful to Nian-Crae Inc. for the financial support throughout this project.

Thanks also go to my lab mates, Michael Wininger, Tiffany Morris, Don Yungher, Nuria Royo and Adam Shain who shared their most precious time, effort and knowledge whenever I needed their consultation. They also influenced me to balance between work and leisure in a synergetic way. Thus I wish fruitful results on their researches in the future, as well as growth in their chess skills so that someday, any one of them could finally beat me.

I cannot thank more to my family in Korea; my father, mother, sister and my late-canine brother Eggy. All of them sacrificed themselves to encourage and support me to concentrate on this research for many years. Especially, I was very sad that I was not with them when Eggy passed away in January last year. But I still remember that when I was visiting my home in Seoul during my coursework years, he was having few seconds of memory resetting process of me with his eyes fixed on me entering at the door, with frozen pointing posture, then started to wag his tale so vigorously.

I also feel very much in debt to my very close friends Teresa Suyon Lee and her adorable maltese Valentine I met along the course of my life, for giving me such amazing warm and secure feelings that without their presence, everything would have been much less accomplishment.

Education is not a transient thing but must be a life's endeavor, so I consider this moment as a new starting point. Tremendous challenges lie ahead of me that I am more than willing to face with my full force no matter how hard and difficult they will be. Everybody is welcome to join me or be a witness as I go along, so in the end you and I should confidently say that I did my best without any regrets nor fear so I did good, and I would gladly do it all over without hesitation if I am allowed to, that it will be another exciting journey which will be a much different yet a much better one in view of my scope as well as under god's scrutiny.

Table of Contents

List of Tables

List of Equations

$$MT = a + b \cdot \log_2\left(\frac{2A}{W}\right) = a + b \cdot ID$$ Equation 1

$$C = H(signal) - H(noise) = BW \cdot \log_2\left(\frac{S+N}{N}\right)$$ Equation 2

$$ID = \log_2\left(\frac{D}{W} + 1\right)$$ Equation 3

$$W_e = \sqrt{2\pi\epsilon} \cdot \sigma = 4.133 \cdot \sigma$$ Equation 4

$$W_e = \begin{cases} W \times \frac{2.066}{z\left(1-\frac{Err}{2}\right)}, & Err > 0.0049\ \% \\ W \times 0.5089, & Otherwise \end{cases}$$ Equation 5

$$ID_e = \log_2\left(\frac{A_e}{W_e} + 1\right)$$ Equation 6

$$APRT = \frac{\sqrt{\langle M_e^2 \rangle}}{M_{Max}}$$ Equation 7

$$FMG\ output = \alpha + \beta \cdot \sqrt{\sum_{i=1}^{N} |Pressure_i(t)|^2}$$ Equation 8

$$S = k\frac{D}{T}$$ Equation 9

List of Illustrations

List of Abbreviated Terminologies (alphabetical order)

ADC : Analog to Digital Converter

ADL : Activities of Daily Living

ANOVA : Analysis Of Variance

APRT : Average Placement Removed from Target

CNS : Central Nervous System

DSAT : Dynamic Speed vs. Accuracy Trade-off

EMG : Electromyography

FMG : Force Myography

fMRI : functional Magnetic Resonance Imaging

fNIRS : functional Near-Infrared Spectroscopy

FSR : Force Sensitive Resistor

HARI : Hand and Arm Rehabilitation Interface

ID : Index (Indices) of Difficulty

KSAT : Kinematic Speed vs. Accuracy Trade-off

MAST : Mechanical Arm Supporter and Tracker

MISO : Multiple-Input Single-Output

MKI : Myokinetic Interface

MOA : Minute Of Angle

MT : Measurement (Movement) Time

%MVC : percentile Maximal Voluntary Contraction

PET : Positron Emission Tomography

QPS : Quadrature Phase Shift

SAT : Speed vs. Accuracy Trade-off

SISO : Single-Input Single-Output

SNR : Signal to Noise Ratio

VI : Virtual Instrument (in LabVIEW)

1. INTRODUCTION

1.1 Statement of Need

Stroke attacks more than 700,000 Americans every year, resulting in 5 million stroke survivors struggling to get back to their life right now in US alone. Stroke impacts a person's body, mind, their behavior, their ability to perform everyday routines and sports activities such as driving, cooking, rock climbing and so on, with symptoms such as paralysis, deteriorated musculoskeletal integrity since the onset of the stroke through learned disuse over time.

Many stroke survivors recover ambulation for their legs through intensive rehabilitation, but the upper body rehabilitation is less prioritized, precluding a complete return of functionality. But evidence shows that our brain is sufficiently plastic to exert a significant fine-motor control functional reversal from paralysis, if proper stimuli are given. Repetitive attempts to move their arms can trigger their brain to reorganize and re-learn to control their limbs. But a comprehensive upper limb rehabilitation system is very rare, which makes the recovery outlook for upper limbs very poor. This clear imbalance and the reason for the corrective measures can be supported by considering the fact that humans are bipedal animals with legs mainly for location changes or travelling which involves crude walking or running, while hands and arms are used to manipulate finer environments.

Given this unbalanced proportion between lower and upper limb rehabilitation training available as well as considering the fundamentals of human motor behavior that involve both kinetic and dynamic aspects of human actions, a new rehabilitation system for upper limb is necessary. Also, the modality of the training should focus more on regaining finer motor control, less on crude maximal force generation.

Two distinct but comparable protocols (KSAT and DSAT) will evaluate upper limb function using an optimized myokinetic interface, with an advanced data assessment tools including motion analysis and statistical signal processing. This research also seeks a better systemic approach to facilitate upper-limb rehabilitation area by developing a noble metrics that can be used by clinicians to give quantitative information about subject progress.

1.2 Backgrounds of Speed vs. Accuracy Trade-off

Movement speed versus accuracy during reaching and targeting is a central issue in neuromotor control with a broad range of research (Duarte and Freitas 2005), and there are many theories attempting to describe the fundamental laws governing human motor control. Among them, Fitts' Law has been widely tested for the application of speed accuracy trade-off under various conditions

with normal subjects. However, the application of Fitts' Law to post-stroke patients has been rare. Furthermore, the conventional Fitts' Law addresses only the kinematic aspect (spatial displacement control) wherein the focus is to determine the ability of the subject to move their limbs spatially to targets, which neglects a dynamic aspect (force control), where the interest is in the amount of muscular tone being generated. Thus it is worthwhile to perform both kinematic speed vs. accuracy trade-off (kinematic SAT) test and dynamic speed vs. accuracy trade-off (dynamic SAT) test separately and then compare results.

If there is too much isometric myokinetic effort, rapid fatigue will ensue that will lead to positional oscillations resulting in erroneous behavior. This should not only be avoided because it is very hazardous in daily life situations for stroke patients, but also should be treated and remedied in the course of the rehabilitation process. Moreover, training stroke patients to regain their motor control ability should involve both dynamic and kinematic aspects in terms of force and positional controls which are two essential elements of any volition. Thus, a comprehensive rehabilitative treatment should encourage stroke subjects' ability to produce a possibly small, but stably controlled force rather than only encouraging them to produce their maximum amount of force they can exert. This focused fine motor control aspect is vital for the development of an overall rehabilitation regime in a sense that the purpose of rehabilitation is to help patients regain their basic function from small, intermediate to maximal, not necessarily only maximal motor abilities. Because activities of daily living (ADL) demands production of the whole range of force, such as picking up an egg without crushing it, or driving a car for an extended of time without fatiguing their hands or other complications. Thus it is important for current rehabilitation regimes available to re-focus on the ability to train the full-range of dynamic motor controllability in conjunction with their kinematic abilities

1.3 Hypotheses

Four hypotheses are proposed along with other research goals to investigate applicability of Fitts' law on hemiparetic patients, in both conventional kinematic and adapted dynamic Fitts' paradigm experiments to compare various statistical points of interests.

Traditional Fitts' paradigm tests will be named as kinetic speed vs. accuracy trade-off test (KSAT test) for the elbow kinematic Fitts' paradigm, and DSAT test for dynamic version of Fitts' paradigm.

1.3.1 Hypothesis (1): KSAT is log-linear in stroke, similar to Fitts' paradigm, but has higher slope compared to healthy subjects.

Main hypothesis of this research is the correlation between normal and stroke groups performance characteristics from kinematic and dynamic Fitts' paradigms. Between-group characteristics (normal vs. stroke) will be correlated or comparable for each Fitts' paradigm (kinematic SAT and dynamic SAT tests separately).

Fitts' paradigm performance results from kinematic SAT will be gathered, and then their group-specific log-linearity will be compared to find any differences/similarities between them. Same procedure will be repeated for dynamic SAT test. The tools to be implemented to test this hypothesis will be the execution of two modes of Fitts' law, kinematic SAT and dynamic SAT tests.

1.3.2 Hypothesis (2): Correlation between dynamic and kinematic Fitts' paradigm performances (DSAT is also log-linear).

Secondary hypothesis is that between-mode comparison (KSAT vs. DSAT) will be similar or comparable to each other from normal subjects.

Because it is unknown whether hemiparetic subjects would follow Fitts' Law at the elbow level movements to show any effects of hemiparesis, test on the hypothesis 2 will be limited only on normal groups' results. This will reveal the adaptability of dynamic aspects of Fitts' paradigm style test (dynamic SAT) to conventional Fitts' law style test (kinematic SAT).

1.3.3 Hypothesis (3): Extrinsic muscles in the forearm can reproduce hand grip force using myokinetic interface (MKI).

Third hypothesis will show that extrinsic musculature force output signal from forearm can reproduce/follow end-effector force from direct handgrip. Myokinetic Interface (MKI) cuff sleeve using force-myography (FMG) will be used to acquire force output signature from the forearm, while the Gripper monitors direct handgrip force simultaneously; Gripper-Cuff correlation.

1.3.4 Hypothesis (4): Efficacy of HARI (Clinical utility of HARI system).

Efficacy of HARI in general over the course of training with stroke patients will be tested. A number of functionality metrics will be measured and are expected to show statistically significant improvements. Measures will include range of motion (ROM), elbow flexion and extension, amplitude of force, and some other indicative metrics including log-linearity and velocity profiles

from SAT tests, smoothness, etc. More importantly, ability to control grip force level, which is essential in targeting task, measured in dynamic SAT, is expected to improve for stroke subjects after 6 weeks of training.

1.3.5 Summary of Hypotheses

These 4 hypotheses from KSAT, DSAT, and Gripper-Cuff correlation will provide useful measures for the study of human motor behavior and control.

Statistics analysis will be used with specific metrics from kinematic SAT and dynamic SAT tests as well as from HARI efficacy and Gripper-Cuff correlation test.

Implementation of the above experiments will involve a development of novel rehabilitation assistive robotic devices to detect subjects' extrinsic hand grip force to perform dynamic SAT test using a force-sensing modality, which consists the Hand and Arm Rehabilitation Interface (HARI) system to effectively monitor stroke patient's actions. In addition to this, commercialization prospects of HARI as an effective rehabilitation system for stroke-stricken patients in a clinical as well as home-based training platform will be considered.

2. LITERATURE REVIEW

2.1 Fitts' Paradigm: Speed vs. Accuracy Tradeoff (SAT) Test

The fundamental laws in human motor behavior can be found as analogous to the laws of physics, in the same manner through scientific tests and verification with theories and experiments. However, the field of motor behavior involving human physiology is different from physics which deals with the environment in a very rigorous way and is not governed by human psychology. Thus, principles in motor behavior are not as many in number, nor are they as precisely stated as their counterparts in physical sciences.

Fitts' paradigm or Fitts' law (Fitts 1954) is an example of an accepted principle describing human performance (Gouiard & Lafon, 2004). Fitts' law states that the more rapidly we move, the less accurate we become, so to speak 'haste makes waste', a tradeoff between speed vs. accuracy. This is an important aspect of Fitts' paradigm that makes it a semi-fundamental principle that describes the efficiency of human motor skill, which has been tested and verified to be true in various physiological cases including different muscles, fitting a peg into holes, or even under microscopic conditions (Langolf, Chaffin, & Foulke, 1976), since Fitts' first publication in 1954. All these variations from Fitts' original tapping set up shown in Figure 1, makes Fitts' paradigm a validated empirical principle so far in the field of motor behavior.

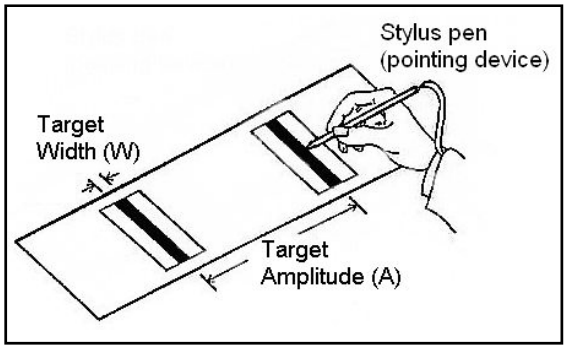

Figure 1. Conceptual diagram for Fitts' paradigm action

The conventional SAT test has been the spatial test in which the subject is repeatedly moving a specific body part in oscillating manner (back and forth or left and right, etc) between two targets. The SAT test monitors the subject's targeting ability between two stationary targets. Targets are 2 rectangular bars of varying width (W) and movement amplitude (A) as target center-to-center distance as shown in Figure 1. The task is to

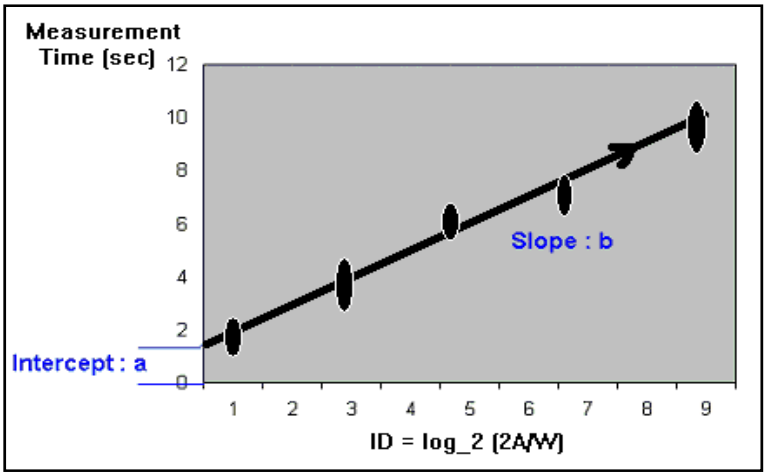

Figure 2. Typical log-linearity from Fitts' paradigm result

hit each bar alternately as many times as possible without interruption within given period of time. From this paradigm, Fitts found a logarithmic relationship between the speed and accuracy, a typical diagram shown in Figure 2, the speed relative to the number of hits within given time period and the accuracy being controlled by target arrangements (variations of A and W).

$$MT = a + b \cdot \log_2\left(\frac{2A}{W}\right) = a + b \cdot ID \qquad \text{Equation 1}$$

Where, MT = movement time

A = distal amplitude of movement between targets

W = width of the target

a = intercept

b = slope

The term $\log_2\left(\frac{2A}{W}\right)$ is called 'the index of difficulty (ID)', because it takes more time (MT becomes longer) for wider A or narrower W, as seen in the Figure 1. The important metric here are the slope 'b', and the intercept 'a' of the ordinate. The slope 'b' tells the subject's adaptive ability under changing difficulty in targeting, and the intercept 'a' shows the initial responsive agility of the subject. Later in the result sections for SAT, fitting constants p_1 and p_2 are used instead of b and a, to represent the linear-regression equation; $y = p_1 \cdot x + p_2$.

Fitts' milestone paper (Fitts 1954) was widely cited, tested, and evolved into a good empirical law that tells us how human motor systems conduct an action. Fitts viewed his paradigm as a test of one's information capacity to manipulate his/her limb, specifically under rapid movement protocol. In this point of view, an action is performed under a motor control command signal generated at motor cortex of the brain, and then the signal passes through neuromuscular channels of one's body down to the end effectors where the actual action is taking place. In his paradigm, Fitts found the MT/ID relationship mentioned above reveals a straight line, where the MT/ID can be viewed as one's task-specific information handling capacity in bits per second (Fitts and Peterson 1964), thus using the base of 2 in the log scale, a corollary to precedent Shannon's information theory (Shannon and Weaver 1949).

2.2 Shannon's information theory: theoretical basis of Fitts' law

Shannon's information theory states that the information capacity (C) of a continuous channel in the presence of noise is equal to the difference between the entropy (H) of the signal and the noise as following equation (Shannon and Weaver 1949) as a reduction of uncertainty at the endpoint of movement, or the difference of entropy (Crossman 1960).

$$\mathrm{C} = \mathrm{H}(\mathrm{signal}) - \mathrm{H}(\mathrm{noise}) = \mathrm{BW} \cdot \log_2\left(\frac{\mathrm{S+N}}{N}\right) \qquad \text{Equation 2}$$

Where, BW is the bandwidth of the system.

Shannon's formulation of index of difficulty (ID) uses D and W for target distance and width, respectively.

$$\mathrm{ID} = \log_2\left(\frac{\mathrm{D}}{W} + 1\right) \qquad \text{Equation 3}$$

This is the theoretical background of Fitts law, which originally deals with noise and variability in communication channels. Fitts cited this formula as the basis of his law. Shannon's formulation has certain superiorities over Fitts' formulation. By looking at Equation 2-3, one can easily notice that it doesn't allow yielding a zero (or negative) ID where the log-linear intercept (*a*) contacts (or falls under) abscissa, meaning a zero (or negative) movement distance. By preventing a zero (or negative) intercept, we can avoid dealing with difficulties in interpretation of regression model with negative intercepts. On the contrary, Fitts' formulation (Equation 1) can yield a negative intercept and some explanations have been made to describe it, such as, unavoidable delay in the psychomotor system (Fitts and Radford 1966), reaction time (Fitts and Peterson 1964), theoretical plausibility of reaction time required in zero movement distance (MacKenzie 1992), time required in repetitive tapping 'in place' (Zhai, Sue et al. 2002).

2.3 Standardized metrics in reporting Fitts' type experiments

2.3.1 International Standards on Ergonomics (ISO 9241-9)

Standardization toward designing physical input devices is important in two aspects. Firstly, any human-computer interface product from any country designed by the ISO guideline can be used in anywhere in the world without further ado of adjusting its dimensions, etc. Secondly, any physiological data generated by the standardized product can be analyzed directly by common tools also designed by the ISO guideline.

Considering the fact that given target parameters programmed by the tester are not necessarily identical to actual hit scatter results acquired from actual run. Thus analysis of the performance should take account of the differences between programmer's parameters and performer's effective hit landmarks, as originally suggested by Crossman (Crossman 1960) and reorganized by Soukoreff

(Soukoreff and MacKenzie 2004). These considerations are described in following sub-chapters, which will introduce more details about some suggested standardized metrics in reporting experiments using Fitts' type paradigm.

2.3.2 Effective variables

Errors between theoretical target parameters given during protocol and actual resultant performance values are considered. Actual hit scatter clouds from subject's results doesn't always coincide with 'suggested' target given as a rectangular box, forming a new sets of subject or session specific targeting results as shown in Figure 3.

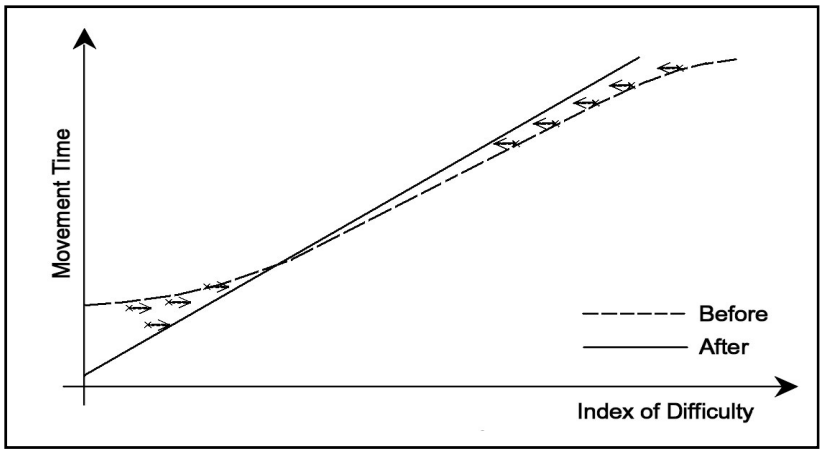

Figure 3. Adjustive effects on low and high ends of ID points for MT/ID profile using effective parameters.

Effective target width (W_e) is defined as follows.

$$W_e = \sqrt{2\pi\epsilon} \cdot \sigma = 4.133 \cdot \sigma \qquad \text{Equation 4}$$

Another way to acquire an effective target width is to use adjustment for accuracy determined by error rate;

$$W_e = \begin{cases} W \times \frac{2.066}{z\left(1-\frac{Err}{2}\right)}, & Err > 0.0049\ \% \\ W \times 0.5089, & Otherwise \end{cases} \qquad \text{Equation 5}$$

Effective amplitude (A_e) is calculated as the mean travel distance from the baseline (starting point) to end-point coordinate per hit where actual hit occurs. Each hit generates unique movement amplitude, then each of them are averaged to calculate A_e.

Effective index of difficulty (ID_e) are calculated using effective target width (W_e) and Effective amplitude (A_e), instead of given target width (W) and amplitude (A) as follows.

$$ID_e = \log_2\left(\frac{A_e}{W_e} + 1\right) \qquad \text{Equation 6}$$

2.3.3 Graphical interpretation of adjusted MT/ID score using effective variables

As mentioned above, this post-hoc analysis on Fitts performance is to normalize the target width to account for the resultant spread of actual end-points for various ID conditions. It is necessary to calculate the information content of the distribution of the movement end-points by assuming the resultant movement end-points are normally distributed with a centered mean (center of the target) with its particular standard deviation (width of the target). Using Equation 2-3, then the maximum entropy becomes 4.133 times larger than the standard deviation for each case.

2.3.4 Corrected MT using effective Index of Difficulty (ID_e)

According to Shannon's information theory (Shannon and Weaver 1949), the index of difficulty was equivalent to the information to be carried through the channel in bits. Fitts himself used these adjusted variables in his later works (Fitts and Peterson 1964) (Fitts and Radford 1966) and acquired a lower intercept at lower ID which was beneficial to a better fit of linear regression.

3. INSTRUMENTATION

3.1 Design Criteria for Rehabilitation Device

Implementation of the devices will require a specific novel force-sensing device development to detect subjects' handgrip force during dynamic SAT test. Also, upgrade and improvements on Hand and Arm Rehabilitation Interface (HARI) system to meet the required data conditions will be made.

In implementing these devices, there are certain aspects to consider when it comes to gathering physiological event data from human motor performance. First of all, the device should always be able to generate consistent and repeatable data sets over long period of time, without much between-subjects error as well as within-subject error. Secondly, the device itself should not burden the tester's performance, or altering the actions in unexpected way due to its own unwieldy form factor. As a simple analogy to Heisenberg's uncertainty principle, a detector or probe is bound to alter the entity being detected, which is also true for physiological event monitoring. Thus designer should consider these facts and ensure the amount of influence to be minimal that the subject's performance being tested should not be altered by the methodology itself.

A rehabilitation tool that is perfectly ideal for every user or every situation is not realistic; however, there are some common characteristics that are sufficiently general and fundamental to provide design specifications for a device to be useful and effective enough to achieve certain tasks. Although compiled data on the characteristics of stroke patients are limited, some generalizations can be made as listed in the following Table to ensure the efficacy and ease of use for the system to effectively monitor physiological phenomenon.

Table 1. Characteristics of stroke patients

Various Characteristics	Possible Residual Ability	Potential Solutions
Irreparable damage to areas of the brain that formerly controlled one or more limbs.	Central nervous system (CNS) plasticity; Sensory perception intact.	Re-learning movements through proper training and sensory feedback to reduce conflict. Sustained attempts at re-activating task-oriented motion; playing in a virtual environment.
Fixed flexure of affected elbow and generally stiff joints.	Usually can be extended by unaffected arm.	Anti-flexion orthotic device for elbow.
Co-contraction of agonist and antagonist muscle during movement, i.e. 'synergy'	Muscle spindle afferents are intact, but possibly anomalous.	Stretching, weight bearing, and exercise to reset muscles.
Loss of wrist and hand dexterity	Some extrinsic muscles are usually active, even in early recovery.	Staged protocols that begin with restoring reaching ability and progress to hand grasping.

3.2 Digitized Motion Analysis

A Canon Optura20 digital video camera was used with a wide-angle lens to record subject's video data. Canon ZoombrowserXL software was used in pc to optimize the video data. Optimized video data was then loaded into EHuman software and adjusted to scale for modeling. A digitized model of the upper limb and the MAST was created using markers on the strategic points of the body (subject's shoulder, elbow, and wrist, MAST's upper arm joint, elbow joint, and wrist joint). EHuman then created stick figure model, to perform numerous calculations over the stick figure model. With the help of the custom-modified basic models supplied as a built-in module in EHuman, plots of flexion-extension, velocity, acceleration, and displacement for each angle points were created for final analysis. This analysis was performed multiple times over the course of therapy with number of subjects to determine how effective the MAST was as a rehabilitative assisting device that will be used for SAT tests later on.

3.3 Hand and Arm Rehabilitation Interface (HARI)

All four experiments shared the Hand and Arm Rehabilitation Interface (HARI) with different utilizations of the HARI's sub-parts. HARI consists of several sub-systems. The backbone of HARI is the Mechanical Arm Support and Tracker (MAST) which offers a frame for other sub-components attached to MAST as Myokinetic Interfaces (MKI) with force sensitive resistors (FSR), as well as an analog to digital (ADC) device and accompanying custom LabVIEW program in personal computer (PC), described in turn in the following sub-chapters.

3.3.1 Mechanical Arm Supporter and Tracker (MAST)

3.3.1.1 1st generation MAST (2004~2005)

Figure 4 shows a 1st generation MAST device. It has 5 joints that locks or frees corresponding joints from shoulder to elbow and wrists. For the purpose of SAT tests, only joint 3 (elbow) was used whereas other joints were locked in neutral position.

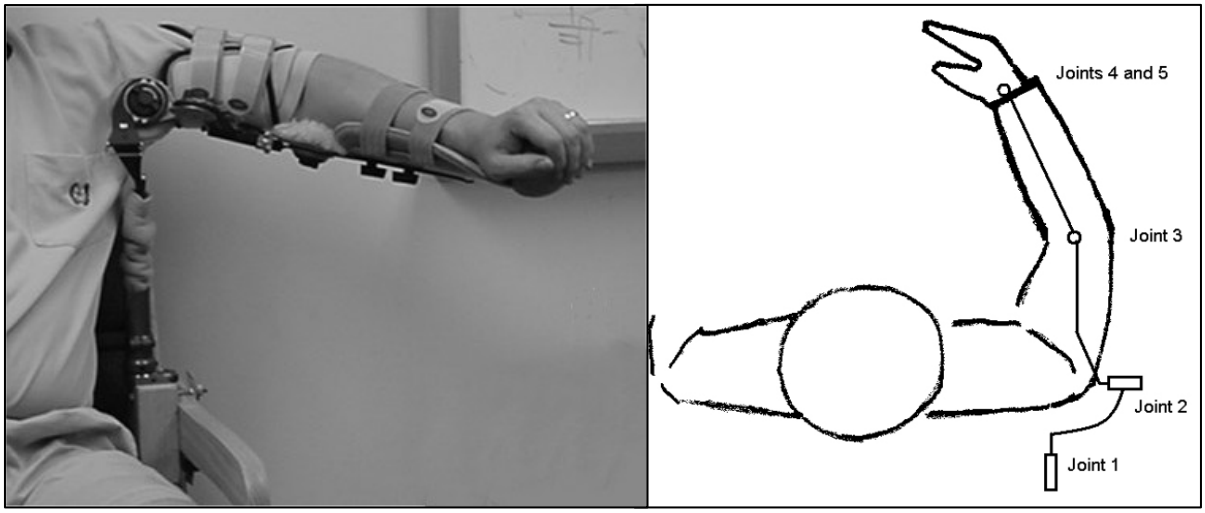

Figure 4. 1st generation MAST with subject and it's diagram with 5 lockable joints.

3.3.1.2 2nd generation MAST (2005~2006)

Unnecessary adjustment functionality at joint 1 and 2 around the shoulder area was removed from 1st generation MAST design. These adjustable latches allowed users to choose to fix or free a certain degree of freedom, but this lock-free mechanism possessed an intrinsic mechanical looseness, which gave unfavorable infinitesimal yet large enough displacement errors related by the movement forces from the user. This optimized design reduced complexity in fabrication as well as increased efficiency on site while getting in and out of MAST (Figure 5).

Figure 5. 2nd generation MAST with improved adjustment features (joint 1 and 2 for shoulder locking is discarded in the 2nd generation MAST).

3.3.1.3 3rd generation MAST (2006~2007)

Design consideration was focused mainly on efficiency of the MAST as a support platform to other sub-components to gather data from subject's elbow actions and securing the wrist. The resultant modification led to a new design (Figure 6) with only one goniometer sensor at the elbow,

shoulder height and arm length adjustability, with more stability to withstand dynamic subject movements. This latest generation of the MAST was especially focused on its ability to offer a comfortable yet a stable platform for stroke subjects to execute an isolated extension and flexion of the lower arm at the elbow point with the anti-gravity support which is essential for stroke patients to concentrate on the Fitts' paradigm movements.

Figure 6. 3rd generation MAST with improved mechanical stability and optimal quick-adjsustable features for shoulder height, upper & lower arm length.

3.3.2 Myokinetic Interface (MKI)

Definition of MKI: The term MKI is a used widely to describe any force signal detection modality that utilizes neuromuscular physiological phenomenon where muscular activation occurs (either contraction or relaxation) which deviates from its resting state, generating a voltage signal interpreted as an in-situ force output.

Various types of MKI devices: Signal detection was made by force sensitive resistor (FSR; Interlink Electronics, Carpinteria, CA), a type of force transducer. Overall form-factor of each MKI device varies as the detection site changes. For example, a glove with FSR attached on the fingertip can be used as a typing force detector, or a cylindrical rod with FSR on its surface is used for the detection of handgrip force, etc.

For our application, myokinetic interface of the arm was done by an arm sleeve (the Cuff) containing an array of force sensitive resistors. Sensor sleeves were fabricated from a forearm/wrist orthosis (Orthobionics, Dallas, TX). FSR sensors (1.4 cm diameter) were prepared by attaching a 1 cm layer of silicone foam to their active portion and then inserting them between the thin mesh inner lining and a compliant foam layer, to ensure close contact between skin and sensor (Curcie 2001).

3.3.2.1 Force Sensitive Resistor (FSR)

HARI system utilizes piezo-resistive force-sensing resistors (FSRs) to monitor subject's muscular force resulted from myokinetic activity generated from the hand and forearm.

Mechanical characteristics: Dynamic response of FSR was determined over a frequency range of 0.5 to 20 Hz with sinusoidal pressure applied to the sensors with approximately 0.5~1.0 PSI (50~5000 g force). Sensor to sensor difference was also tested, showing 0 ~ less than 1 % differences under same condition (50~5000 g force range) shown in Figure 7.

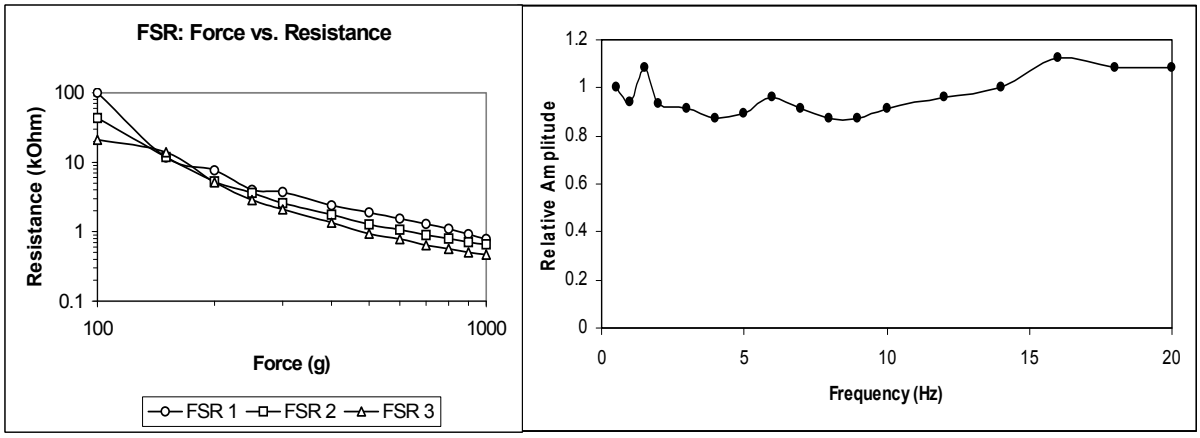

Figure 7. Dynamic response of FSR over loading (left) and spectral characteristics (right).

FSR responded fairly linearly at loads up to 1000 g (~10 psi) then becomes non-linear at loads greater than 1000 g, as shown below. Dynamic pressure response of FSR is appropriate without any additional signal conditioning for myokinetic muscle recording, especially for the arm, where the actual force signal generated onto the device is relatively smaller. Dynamic response was approximately linear to at least 20 Hz, and thus the bandwidth was adequate to register most of myokinetic activities, that seldom exceeds 10 Hz, which was minimum sampling rate for SAT tests.

Force Myography (FMG): The term FMG is used to denote an MKI device where the sensing area necessitates a utilization of multiple force transducers, generating a more than one force signal, which covers usually over relatively large area of the body. Thus, a single fingertip force sensing device would not generate more than one data stream, so it cannot be called as an FMG device, while an MKI arm sleeve with multiple FSR sensors would generate a matrix of force signals, which is adequate to be called an FMG signal.

In the following contexts, the term Force Myography (FMG) will be used to distinguish the Cuff from the Gripper, where the Cuff generates a matrix of force signals while the Gripper is a single channel device.

3.3.3 FMG Cuff

The Cuff is an MKI device that uses force myography (FMG) to detect in situ muscular activity on the forearm as an alternative to EMG. Myokinetic interfacial sleeve (Figure 8) with an array of circular FSRs (Figure 9, Model #402, Interlink Electronics) was implemented. FSRs were strategically placed in 14 detection sites (7 anterior and 7 posterior) to cover most of the major muscle groups involved in power grip shown in Figure 10.

Figure 8. FMG cuff sleeve

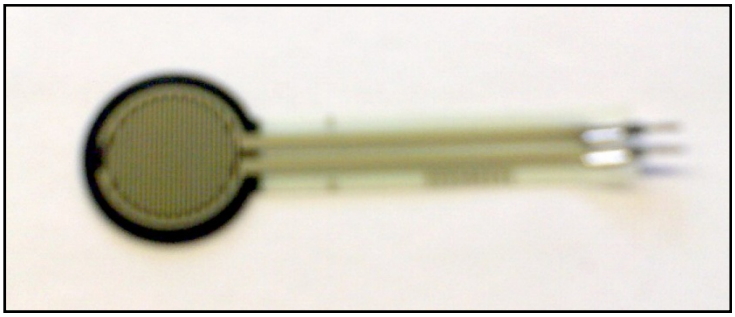

Figure 9. Circular FSR unit for the Cuff (Model #402, , Interlink Elec. Inc.)

Mounting variation errors were treated by baseline initialization for each mounting generates a unique baselines. However, within subject baseline variation was much less or minimal compared to between subjects baseline variations. Overall force output value was calculated as square mean deviation from resting value.

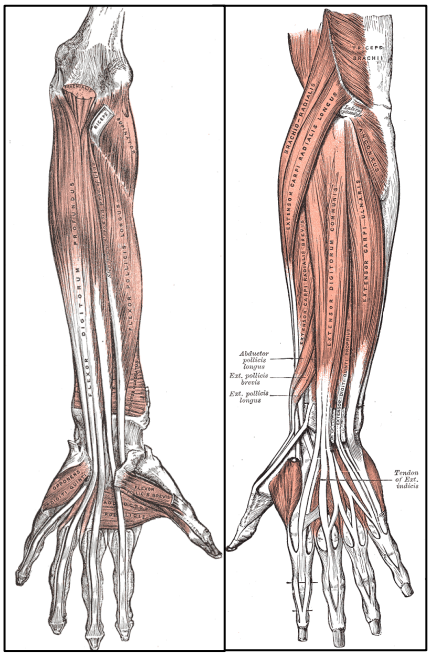

Figure 10. Superficial and deep muscle groups Responsible for hand manipulation (Left hand)

Detailed data processing was previously reported (Flint, 2004) and briefly described here. The basic operating principle of FMG is based on the ability of acquiring a force matrix registered by the FSR sensor array as user exerts force over the sensing area. Each matrix shows a specific pattern, which represents a unique muscular activity of interest. This intrinsic feature of the Cuff is capable of deciphering different types of grip according to user volition (Craelius 2002; Flint JA 2003). However, due to the accompaniment of the Gripper, this research utilized only one type of MKI generated by cylindrical grip.

The resultant signals represent dynamic images of muscular activity, whose patterns can be learned by an adaptive processor, and associated with specific muscles. Specifically, MKI can substitute for EMG for the following exemplar applications:

• Detection of volitional muscular force output (Kuttuva, Burdea et al. 2005).

• Monitoring biofeedback of neuromuscular effort related to elbow, wrist and fingers (Kuttiva 2003).

• Distinction between agonist and antagonist muscle activity during co-activations (Flint, Phillips et al. 2003).

3.3.3.1 Coverage of the Cuff

Due to the nature of the physical modality of the Cuff (outward volumetric detection capability of the pressure sensors), detectable muscle groups by the Cuff are not limited to superficial muscles but also span into deep muscles including but not limited to flexor pollicis longus (fpl) from anterior, or flexor digitorum profundus (fdp) from posterior of the forearm as well as other superficial muscles such as flexor carpi ulnaris (fcu), flexor digitorum superficialis (fds), palmaris longus (pl), flexor carpi radialis (fcr), pronator teres (pt), brachio radialis (br) for anterior region, and extensor carpi radialis longus (ecl), extensor carpi radialis brevis (ecb), extensor digitorum (edi), extensor carpi ulnaris (ecu), anconeus (cubitalis rolani) for posterior region (Figure 10). Moreover, the nature of FMG modality enables this unique MKI device sensitive to other muscular structures such as tendon and bone rearrangements.

3.3.4 The Gripper

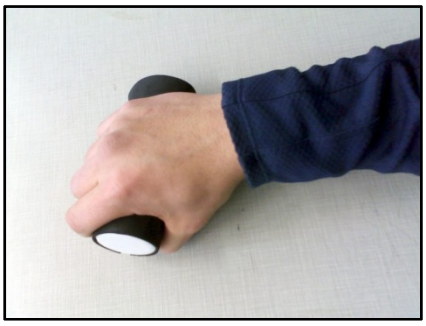

Figure 11. The Gripper in use with cylindrical palmar grip.

The Gripper was developed to detect direct hand grasping force signature (Figure 11). Four strip FSRs (Figure 12, Model #408, Interlink Electronics.) were placed longitudinally on the surface of a PVC cylinder (4 cm diameter x 10 cm longitudinal) as a quadruple parallel sensor arrangement, with the half-bridge circuitry with a single fixed resistor.

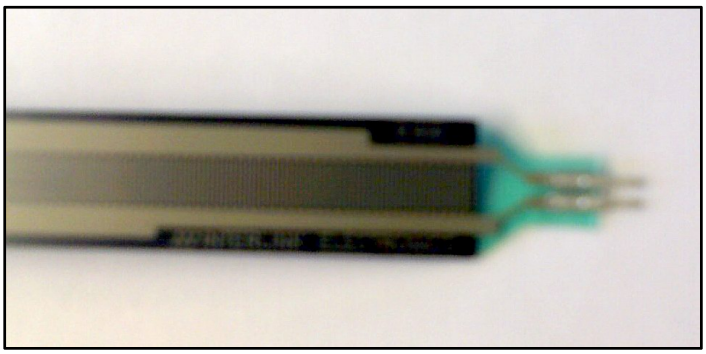

Figure 12. FSR strip used for the Gripper (Model #408, Interlink Elec. Inc.)

The diameter of the Gripper was selected to ensure the most stress-free palmar grip actions from most of the general population. For the selection of

the material, structural rigidity was necessary for the base material to ensure isometric force detection, thus PVC pipe was selected. Due to its cylindrical morphology which allows the user to wrap around it with maximal palmar contact area, the Gripper gives true cylindrical grip force detection. Conventional unidirectional force transducer setup makes most of the contacts mainly at intermediate phalanges only, neglecting distal and proximal phalanges' contribution, as well as missing contacts with most parts of metacarpus bones. Thus it is safe to say that the Gripper offers a true radial contact between the whole five metacarpus bones with sensor. Using a cylindrical detection methodology to monitor cylindrical grip force is the only direct and straightforward way to measure the whole event with clear mechanical and anatomical advantages without any loss of physiological effort. The raw voltage output was fed into the commercial ADC device (NI-DAQ-USB-6008) to save the data.

3.3.4.1 Orientation error in using the Gripper

Orientation error was tested when gripping to gripping difference occurs when FSR positions at certain angle in the palm. The error ratio was tested with different latitudinal setups of 0º and 45º in reference to longitudinal center of reference FSR. 90º and 135º and so on are cyclic and redundant as part-to-part error among FSRs was negligible. Multiple data points per each orientation were acquired, then ensemble averaged shown as the average values per each orientation, then the total average was calculated as 0.75 ± 1.03 % difference (Table 2).

Table 2. Angular orientation error on the Gripper

%MVC / Orientation	0	10	20	30	40	50	60	70	80	90	Total % difference
0º	4.70	3.60	3.00	2.60	2.15	1.74	1.34	1.00	0.65	0.32	0.75 ± 1.03 (%)
45º	4.60	3.50	3.00	2.60	2.14	1.74	1.35	1.00	0.65	0.36	
% difference	2.20	2.80	0	0	0.50	0	0.70	0	0	1.30	

3.3.4.2 Linearization of the Gripper

Although, individual FSR's dynamic response up to 1000g was fairly linear, the Gripper's dynamic response reaches into the non-linear region of FSR due to its physiological in-situ characteristics of the signal, that it detects the direct force output from the palm. Thus, the Gripper requires a calibration to linearly represent user's %MVC in its full range.

To show the actual force readings out of user %MVC, Gripper linearization was done in a separate LabVIEW program prior to the main protocol. Raw force signature (Figure 13, left) was fed through the half-bridge force-to-voltage circuitry, then calibrated pressure (forces per area) in PSI applied to force gauge dynamometer (FG-5000, Extech Instruments) capable of detecting 50~5000g

force range, was recorded to generate scaled filter (Figure 13, middle), resulting a linearized force signature to display %MVC proportional to user force level (Figure 13, right). Linearized Gripper after this process was used in the main protocol LabVIEW VI program throughout the experiment. The filter equation was 3rd order; $y = 59373.6\,x^3 - 3003.7\,x^2 + 2701.5\,x + 88.565$, where x is gripper tank coordinate (1/100 of %MVC), and y is the actual force in grams.

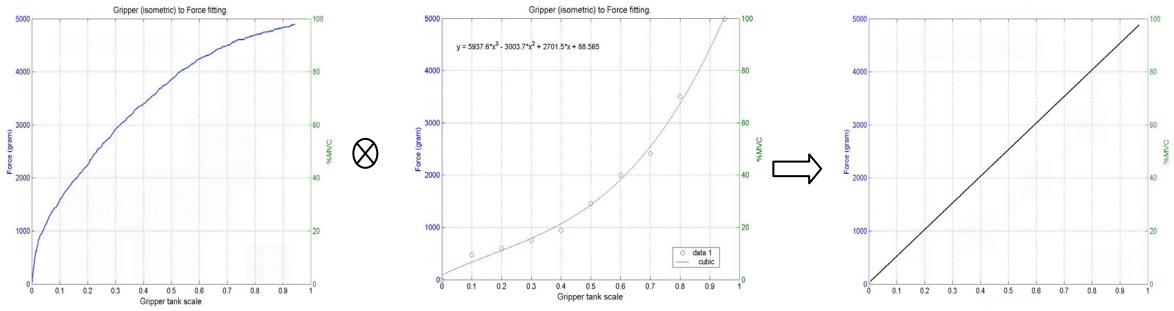

Figure 13. Linearization filtering of the Gripper.
Raw Gripper output signal (left) × Linearization filter (middle) = Linearized Gripper

3.3.5 Elbow Goniometer

As mentioned before, any physiological detector should effectively be able to monitor the interested physiological phenomenon with somatic compatibility to the subject, mechanical reliability to the signal per se. Considering these aspects of signal conditions, three elbow angular sensors were tested and fabricated, including custom and commercial optical encoders, and variable resistor (potentiometer) as follows.

3.3.5.1 Custom-built Optical Encoder

A custom built optical encoder was tried using two photo-darlington optical interrupter sensors (H22B2, Fairchild Semiconductor, South Portland, Maine U.S.A) side to side with 90° out-of-phased signal output from each detectors generated by rotating a fine-printed wheel gate. The unit was able to measure angular rotation displacement, as well as rotation direction. A Quadrature Phase Shift (QPS, Figure 14) was used to identify a two-way discrete movement of the data stream, proportional to the rotation of the wheel, as two data streams shifted by 90 degrees with each other and modulated by a single clock. Number of total changing bits gives total amount of angular rotation, and the pattern distinguishes the direction of the rotation which reads differently from clockwise (00 01 11 10 00…) to counterclockwise (00 10 11 01 00…) depicted in a conceptual diagram in Figure 14.

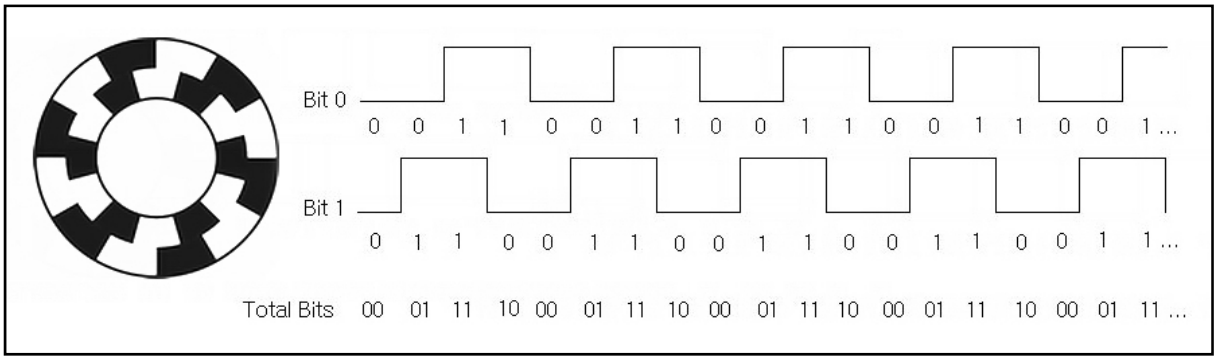

Figure 14. Diagram of dual photo-darlington optical encoder wheel gate and schematics of resultant signal read with Quadrature phase shift (QPS) signal capable of decode directionality and angular speed of the wheel

AutoCAD was used to design a wheel gate composed of a number of radial shades calculated to function as the QPS encoder wheel, then printed on a transparent film to switch (toggle) the laser diode signal on and off as it rotates.

Figure 15 shows the calculation of the angle from the wheel gate. Wheel gate have N number of shades (notches) and also same N number of transparent windows (gaps), both with same circumferential width of d (= rθ, assuming the angle θ is small enough), thus each shade-window pair will occupy 2θ angle out of a whole circle (2πr or 360°). The number of shades N dividing the whole 360-degrees decides angular resolution of an optical encoder. For example, a wheel with 256 notches will give an angular resolution of $1.406°\left(=\frac{360}{256}\right)$. To print N number of shades with fine angular resolution on a circular wheel, the radius r needs to be large enough to be able to actually print on a transparent film, which requires a non-conventional fine printing. A rough calculation yields the radius to be at least 25cm to make the angular resolution to be 1°, which allows one shade to have about 1 mm circumferential length (d), which is as fine as any fine laser printing on a transparent film due to physical limitations by toner blending and diffusion on the film. Also, the actual setup of the goniometer around subject's elbow only allows the radius up to certain sizes. Although this custom approach was favorable considering HARI's future prospect on commercialization that runs initially through the whole

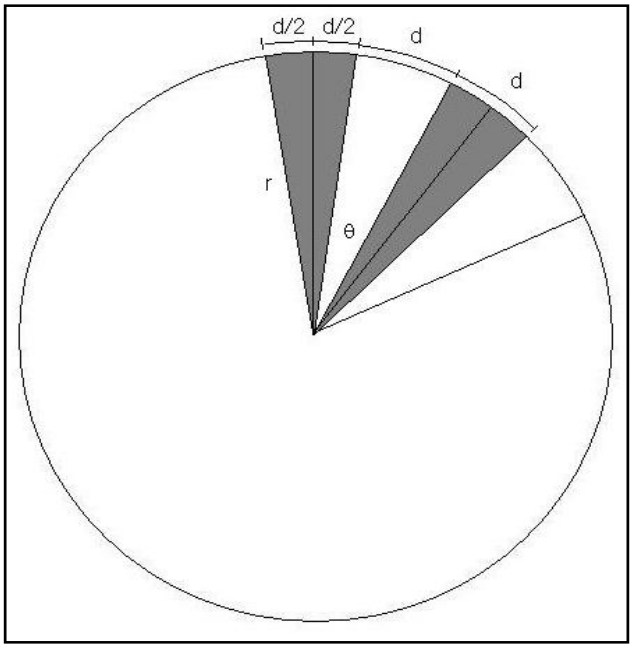

Figure 15. Diagram of the wheel gate for the calculation of angular displacement.

system development processes, customizing the wheel gates with individual photo-darlington sensors turned out to be ineffective and improbable in terms of mechanical feasibility. Thus better equipment for the detection of elbow angle was necessary.

3.3.5.2 Commercial Optical Encoder

Next candidate for elbow goniometer was the commercial optical encoder from US Digital Inc, CA (Figure 16). Ready-made optical goniometer has certain advantages over previous approach such as superior angular resolution (about a quarter degree) and completeness as one whole commercial package with high SNR, ready to be used right out of the box, regardless of the much higher cost.

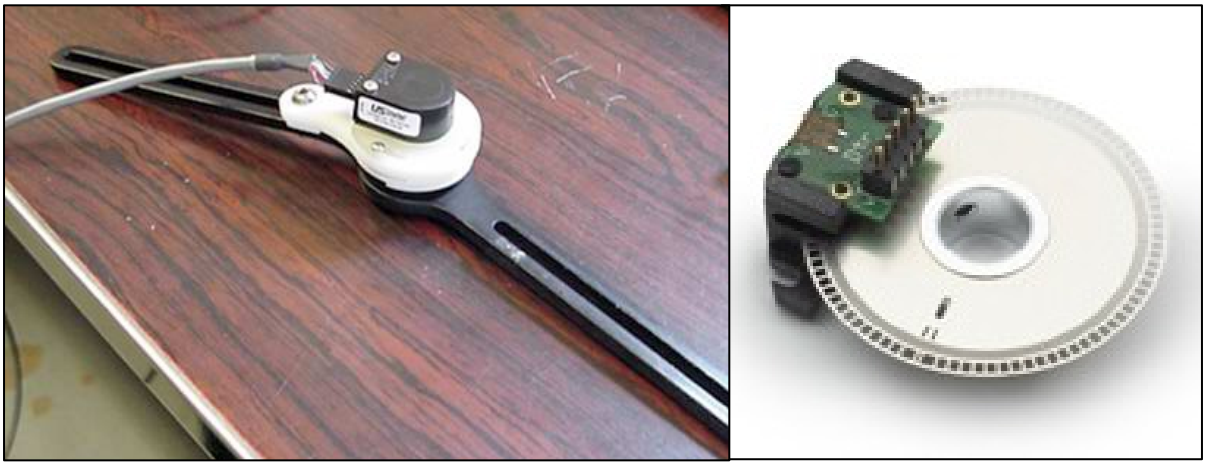

Figure 16. Optical encoder attached as the MAST elbow unit.

However, actual trial of this one on the MAST elbow unit revealed a critical flaw of this optical encoder. While laser optics within the package ensured high angular resolution and high signal to noise (SNR) ratio with accompanying signal conditioning box, reading of the encoder wheel was not consistent between flexing and extending motion by losing a few degrees per repetition. There were two reasons, which resulted in the loss of angles. First, the wheel has to be placed a perfect mid-offset position between laser diode and detector. In our application, it is prone to be exposed to down force on the unit generated during normal usage, the required precise placement of the wheel relative to optical sensors were easily compromised, without extra heave-duty skeletal support. Secondly, the encoder itself showed some loss of MOA (minute of angle = $\frac{1}{60}$ of one degree) when it returns to the home position (full flexion) even under load-free set up, accumulating and deviates too much from 0° after a dozen repetitions, which rendered the optical encoders unsuitable for our application.

3.3.5.3 Variable Resistor (Potentiometer)

Second candidate for our elbow sensor was an old-fashioned variable resistor, trim-pot. Although it's very basic, simple element of electrical engineering design, trim-pot served very well as our elbow angular sensor and met our standards for its purpose described at the beginning of this chapter. Potentiometer gave us a fairly good angular resolution of about 2 degrees, and most importantly, without any change of its reference values when the arm returns to its base position (90° flexed position).

3.3.6 LabVIEW Interface

Gripper-Cuff correlation and both spatial/dynamic SAT tests will be performed in their own custom written LabVIEW programs which integrate data acquisition and initial analysis. All LabVIEW interfaces offer an introductory remark at the beginning of each protocol to guide the performer or helper with relevant information, such as mounting the device on a patient, custom adjusting each joint to fit different shape of different subjects' physique, and tweaking other variables of the console. The screen with targets that users actually see is called 'front panel', as opposed to 'block diagram' where a programmer composes, edits or debugs the LabVIEW program as necessary.

Data is saved for post-hoc analysis in MATLAB. LabVIEW interface saves numerous streams of data as a Microsoft Excel file depending on the protocol as follows:

- Raw voltage-out data from the MSAT (KSAT) or from the Gripper (DSAT)
- Elbow angle data (in KSAT)
- %MVC data (in DSAT)
- Scaled data (front panel coordinates)
- Time stamp (in milliseconds, used to calculate Measurement Time per ID)
- Measurement Time (MT) per ID = $\frac{\text{Time given per ID (15 sec)}}{\text{Number of hits per ID}}$
- Number of hits (used to calculate Measurement Time)
- Index of difficulty stamp (1st ID ~ 5th ID)

4. PRELIMINARY EXPERIMENT: SYSTEM EVALUATION

4.1 Subject recruitment for preliminary experiment

Two post-stroke hemiparetic subjects were recruited along with six normal volunteers within university for the preliminary study to evaluate the system reliability. Informed consents from normal subjects were also gathered prior to the experiment under the provision and guidelines of the Rutgers University Institutional Review Board (IRB) and UMDNJ. There was no discomfort or complaints during or after the experiment from both subject groups.

4.2 Methods for preliminary experiment

To test the system quality, a preliminary test was performed with normal (n = 6) and hemiparetic (n = 2) subjects at the wrist velocity profile, elbow extension and flexion and grasp force control.

4.3 Protocols for Preliminary Results

Elbow flexion and extension of both normal and stroke-affected upper limbs were analyzed in the horizontal plane. The extent of gross movement rehabilitation was quantified by comparing the velocity and angular profiles of normal upper limbs to those of the afflicted limbs. To measure grasp control, subjects squeezed a ball to maintain a target of 50% effort at various grasp strengths ranging from light to near sub-maximal.

A new method for quantifying grasp force control was created, called Average Placement Removed from Target (APRT) shown in Equation 7. Based on muscular error and maximum muscular effort, APRT allows users to quantify control and evaluate their performance, thus witnessing improvement over the course of therapy. The APRT scores were calculated to assess the degree of grasp control.

$$\mathrm{APRT} = \frac{\sqrt{\langle \mathrm{M}_e^2 \rangle}}{M_{Max}} \qquad \text{Equation 7}$$

Results showed that the velocity profiles of normal limbs were bell shaped, similar to that seen in unaided normal reaching. In contrast, results from affected limbs were a series of Euler functions decreasing in magnitude. Over the course of training, some improvements were noted.

In 6 subjects, APRT decreased with the strength level of the grasp, according to a power function, with exponent = 0.75. Over the course of MKI biofeedback training, stroke subjects improved their control over grasp, as measured by decreased APRT, which shows a purely active training of the upper-limb, assisted against gravity, can improve control.

Over the course of this preliminary therapy with HARI, a hemiparetic subject improved elbow mobility and control, going from a jerky motion to a smooth elbow movement. The elbow angle and wrist velocity profiles of the hemiparetic subject approached those of the normal subjects in the study. The relationship between APRT and grasp force control was defined through many normal subjects and established as a power function. In addition, by biofeedback of grasp force, the hemiparetic subject developed improved control over grasp at all tested levels of force. Preliminary results and analysis for wrist, elbow, and grip forces are shown below.

4.3.1 Wrist Velocity

Normal Subjects: Normal wrist velocity profiles resembled a bell curve of an Euler function (Figure 17). The peak is flat and smooth, which indicates a controlled, single movement.

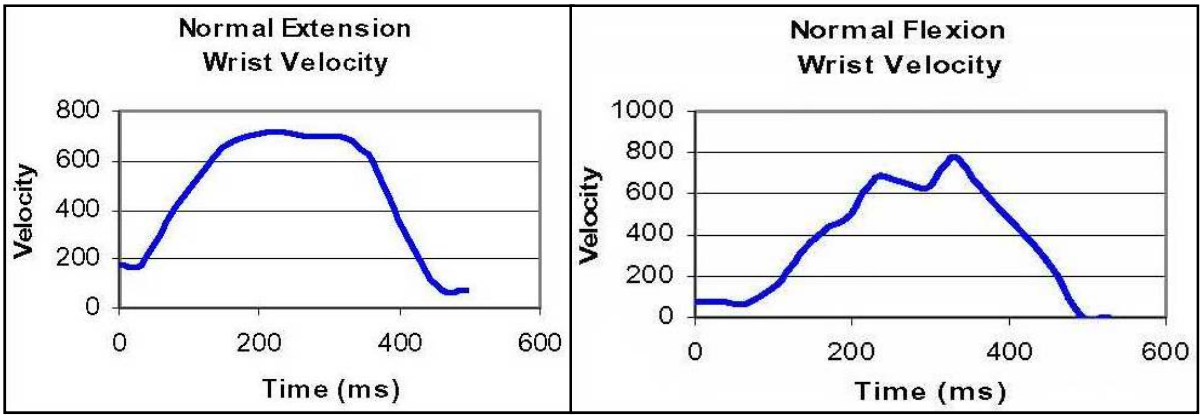

Figure 17. Normal subject motion analysis velocity profiles extension (left) and flexion (right).

Hemiparetic Subjects: The wrist velocity of a hemiparetic subject on day one of therapy was uncontrolled. Instead of the normal Euler function, the hemiparetic subject demonstrated a series of these functions decreasing in magnitude (Figure 18). This signified that both elbow extension and flexion are made up of multiple movements at this point in therapy.

After therapy, the wrist velocity profile in both extension and flexion changed dramatically. The profile in extension has expanded into two main motions. While the flexion wrist velocity profile is still 4 movements, the peaks of each motion have flattened, signifying more control and a smoother movement (Figure 19).

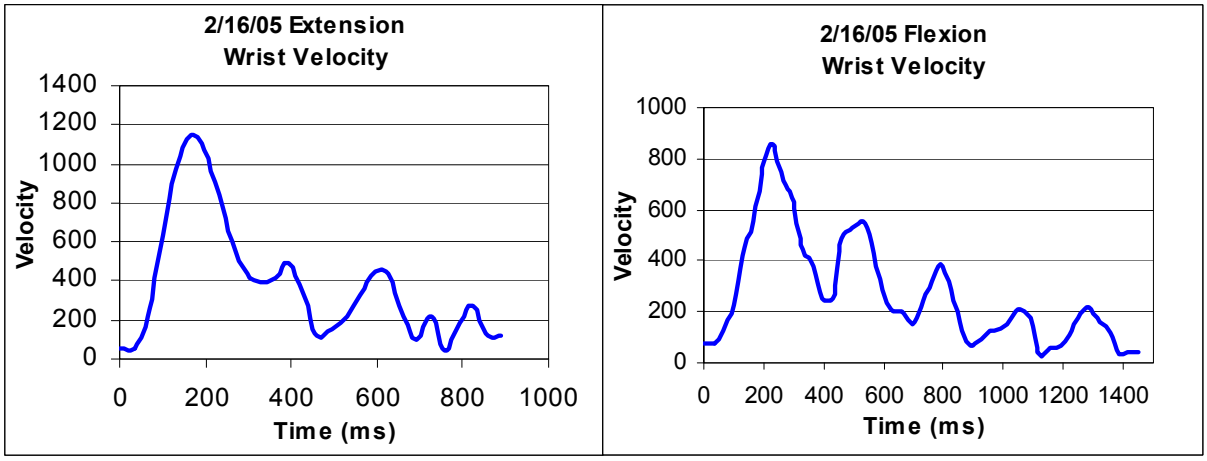

Figure 18. Wrist velocity profiles for hemi-paretic subject in extension (left) and flexion (right) for day one of therapy.

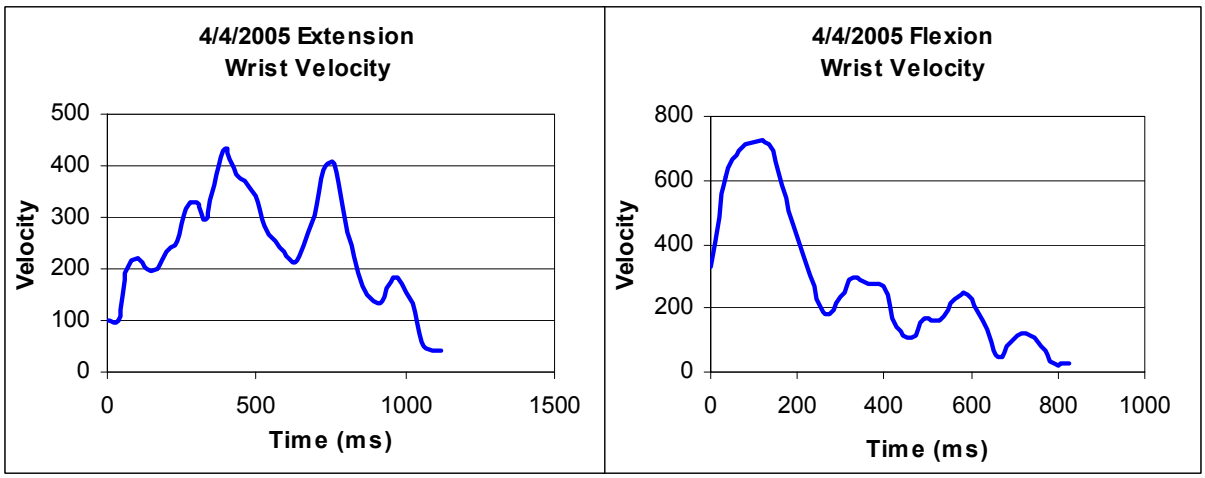

Figure 19. velocity profiles in extension (left) and flexion (right), after the therapy.

4.3.2 Elbow Angle

Normal Subjects: Normal subjects demonstrated a nearly linear elbow angle across the motion (Figure 20) for both flexion and extension. A single point of inflection was observed approximately midway through the motion.

Hemiparetic Subjects: On the first day of therapy for a hemiparetic subject, the elbow angle during both extension and flexion had a low linearity and was not a smooth function, as seen in Figure 21. However, at the end of the therapy, stroke subject's linearity markedly increased with very good linear-regression values shown in Figure 22.

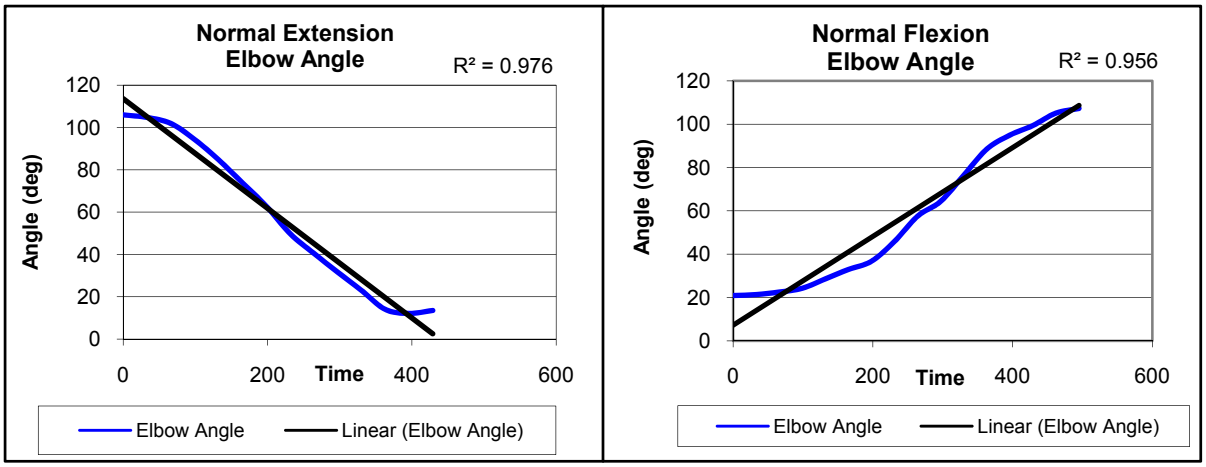

Figure 20. Normal subject elbow angle during extension (left) and flexion (right) with the linearity displayed.

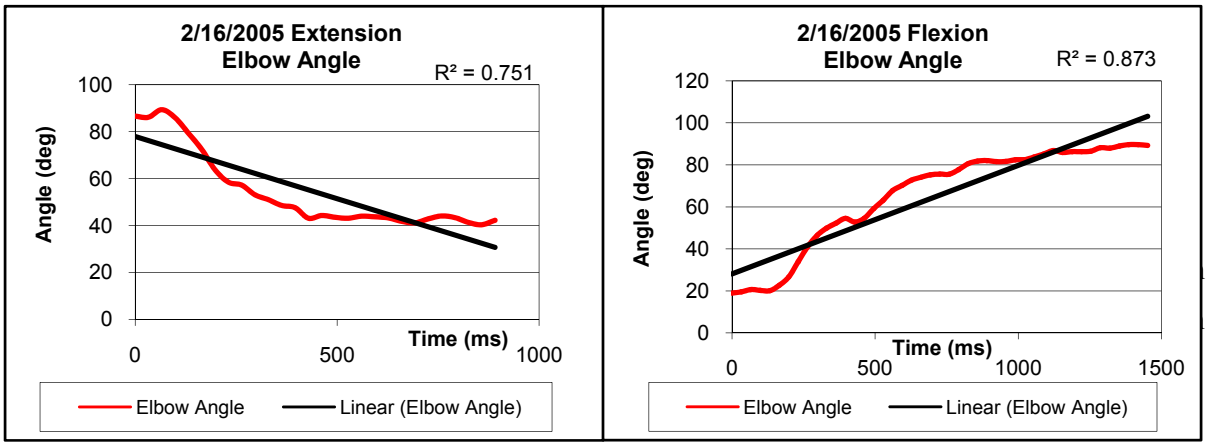

Figure 21. Elbow angle during extension (left) and flexion (right) on day one of therapy for hemi-paretic subject.

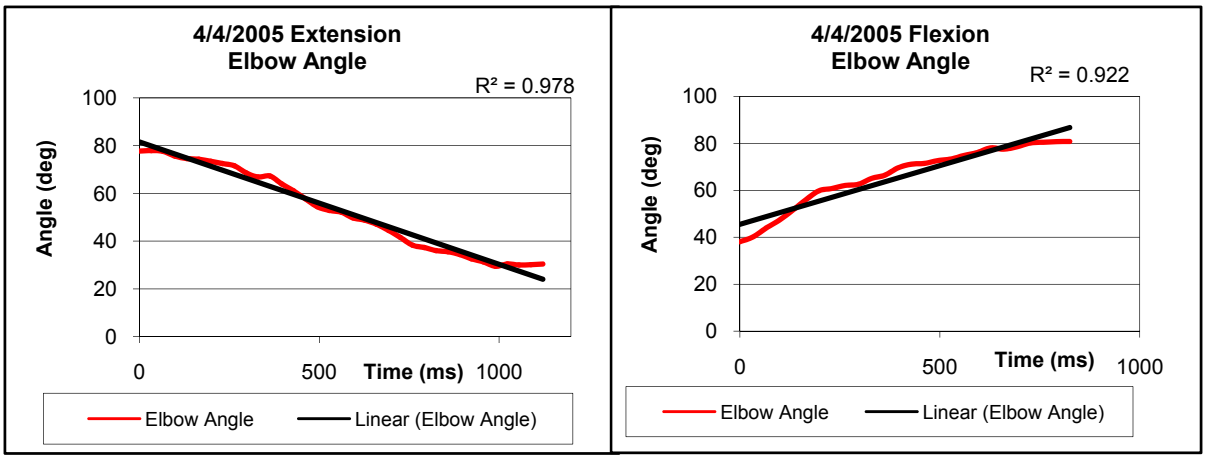

Figure 22. Elbow angle during extension (left) and flexion (right) for hemi-paretic subject. After the therapy.

The average APRT at many grasp forces was calculated for up to 5 subjects at each grasp force. It was found that APRT decreased with an increase in grasp force, and that the change was reminiscent of a power function $y = 2.689x^{-0.7542}$ (Figure 23).

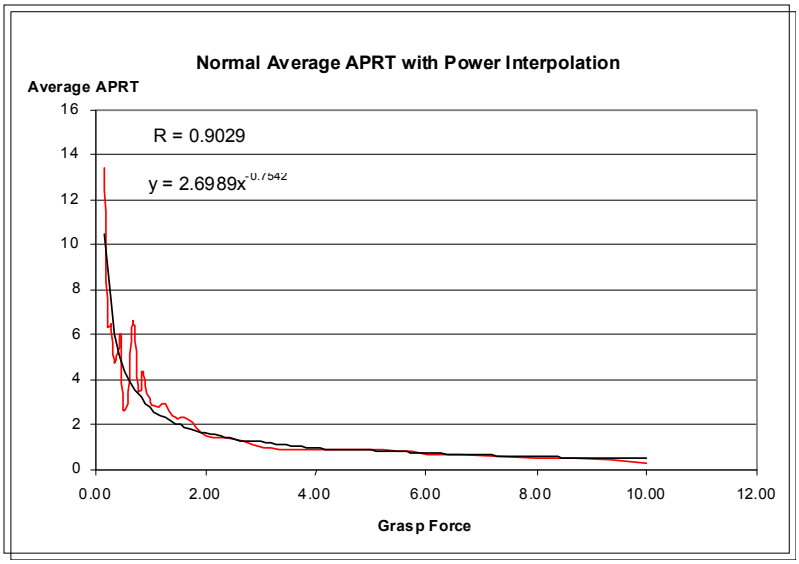

Figure 23. Normal average APRT (red line) followed a power function

Over the course of therapy for the hemiparetic subject, APRT decreased at each grasp force, demonstrating improved control. As seen in Figure 24, by the most recent testing date, the subject had exceeded the control of his normal, unaffected arm, with that of his affected arm (Figure 24).

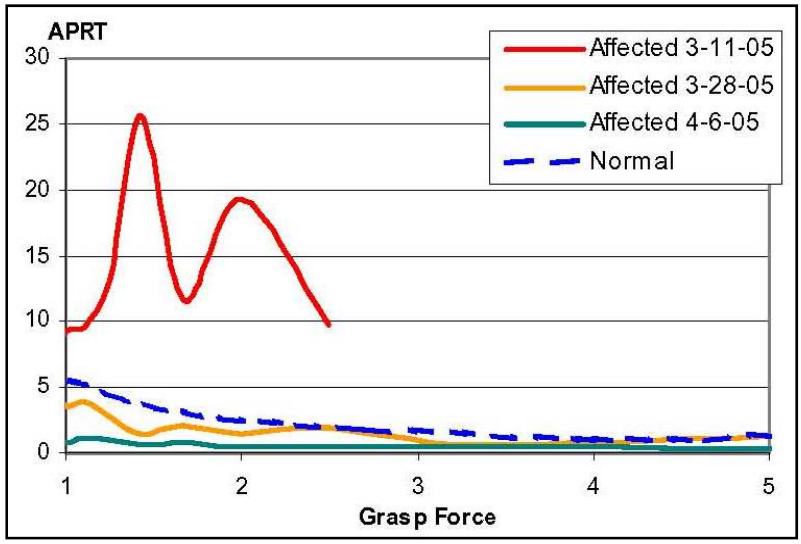

Figure 24. Change in APRT functions over therapy in hemi-paretic subject.

Compared to the control group, the hemiparetic affect arm showed a high APRT at the beginning of therapy and an inability to achieve higher grasp force.

By the end of therapy, the APRT of the affect arm decreased by 8.42 at grasp force 1 and the subject could achieve the high grasp force of 5 at a level comparable to normal subjects (Figure 25).

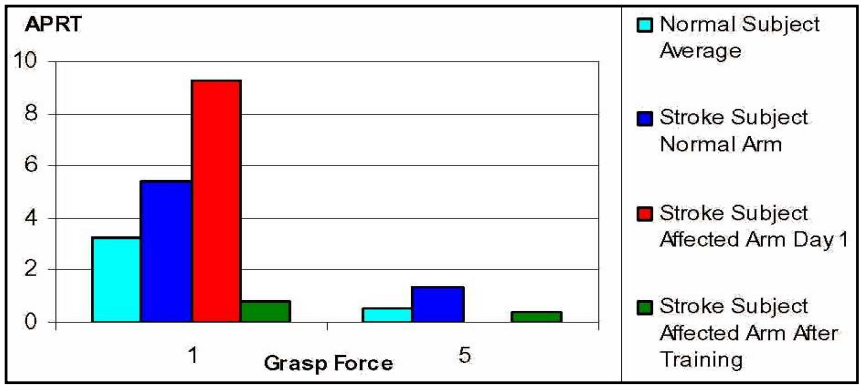

Figure 25. APRT at grasp force 1 and 5 for normal subject, hemi-paretic normal and affected arm at beginning and end of therapy.

4.4 Conclusion for preliminary experiment

The Hand and Arm Rehabilitation Interface (HARI) was an effective rehabilitation device with both elbow control with grasp force quantification capability. Mechanical Arm Support and Tracker (MAST) provided a gravitation-free horizontal support plane support to target specific actions with focused muscle group in the upper extremity. MAST also provided a good platform for motion analysis for the evaluation of upper body motor control in conjunction with Myokinetic Interfaces (MKI), which detects user biofeedback. Using these new technologies, HARI proved itself to be an excellent rehabilitation tool for subjects with impaired upper limb functionality.

Preliminary experiment was successful for HARI in development of quantifiable measures. Baseline data on normal subjects for elbow motion analysis and wrist velocity profiles followed the results from previous studies (Agnes et al. 2003). As expected, normal subjects' wrist velocity profiles followed an Euler function, which validates the motion analysis tools used in this project. A remarkable improvement in upper extremity control was also noticed; linearity of elbow angle was increased by 0.2271 in extension and 0.0486 in flexion. Shape profile of the velocity curve was also improved, which showed a better smoothness. Grasp force controllability was also improved seen by the APRT metric decreased by 8.42 from subject A, who could have achieved a higher grasp level of 10 by the end of therapy. These results indicate increased control of movement. APRT was sensitive enough to show progress changes over the course of training, but was not overly sensitive to produce any false trends.

In creating a baseline for grasp force control, which was new among motor control researchers either dealing with normal or hemiparetic subjects, APRT was able to produce baseline data in grasp force control, a useful guideline in further researches. A normal grasp force control followed a power function of $y = 2.689x^{-0.7542}$, with APRT decreasing with an increased grasp force. This is a significant finding in identifying the force signature error levels with respect to the amplitude of the command signal from the brain, which was critical because that trend can be used to evaluate how the end-effector manifests force output according to the incoming motor signal. This preliminary experiment successfully demonstrated the effectiveness of HARI in upper limb rehabilitation which will lead to the following experiments to quantify neuromotor control in more sophisticated way.

5. EXPERIMENT #1: KINEMATIC SPEED VS. ACCURACY TRADE-OFF (KSAT) TEST

Repetitive exercise training of skeletal muscles helps improve stroke patients' upper limb movements (Craelius 2002; Flint, Phillips et al. 2003). Fitts' paradigm of repetitive elbow motion was applied on hemiparetic patients to quantify their upper arm movement and improvement. A custom rehabilitation training tool for upper body, the Mechanical Arm Support Tracker (MAST) embedded with an elbow goniometer, was used. Fitts' paradigm was applied to monitor subject's targeting performance in speed vs. accuracy trade-off (SAT) test at the elbow (Fitts 1954).

SAT test was performed in spatial and dynamic modes. First, kinematic SAT test was performed to evaluate the subject's spatial aiming ability as in conventional Fitts' paradigm. In the next experiment, DSAT (dynamic SAT) test will monitor subject's ability to control force. Thus the viability of Fitts' Law with stroke patients will be tested by both kinetic and dynamic modes.

5.1 Subject recruitment for KSAT test

After informed consent gathering procedure from all subjects before the experiment under the provision of Rutgers IRB, four stroke subjects (S1~S4, age 61±10 yrs, 6±7 months since the onset of the stroke), along with eight normal healthy subjects (C1~C8, age 25±5 yrs) were recruited. Stroke population was tested by the acceptance criteria as higher than level 6 in the Chedoke-McMaster stroke assessment index (Gowland, Stratford et al. 1993) for each hemiparetic subject, due to the critical requirements that a performer should be able to go through kinematic SAT test without resulting any non-zero hit scores over all ID levels, by resulting an infinite MT $\left(=\frac{\text{ID interval time}}{\text{Number of hits}}\right)$ which would render the whole session invalid.

For the same analogy, any extended hesitations, jerkiness, or dwellings within a confined ROM would result in a similar invalidity which would compromise on the assumption of Fitts' paradigm. This was monitored throughout the test to ensure detection of any deviations from subject inclusion status, although not imposed to exclude any data sets. The assumption here is that each and every targeting motion in Fitts' paradigm experiment should be rapid enough without any kinds of self-invoked (subject taking time or resting due to fatigue), or outside environmental interruptions/perturbations.

5.2 Protocol for KSAT test

A custom LabVIEW Virtual Instrument (VI) was written in pc to test subject's kinetic targeting ability by controlling the elbow angle to position the forearm in virtual 2-D space as depicted in Figure 26 showing the front panel of the VI in fronto-parallel manner. The VI is programmed self-explanatorily, with instructions for subject (or physical therapies) on the first page is 'Instructions' tab that describes how to set up the MAST device, testing time, sampling rate (machine time delay), result reporting formats, etc. Actual run of the protocol is performed on the 'Operation' page. The other two pages ('Goniometer' and 'Configure') contain information for programmers to allow checking and tweaking of the goniometer mechanics and further fine-tuning of the VI.

Figure 26. LabVIEW interface for KSAT. Two green rectangle represent targets to be hit with red marker representing subject elbow position

After initial trial with hemiparetic patients, five indexes of difficulties (2.5 ~ 5.0) were selected to cover the widest range of target placement setup. Below $ID_{2.5}$ was improbable to perform by hemiparetic subjects for possibly numerous reasons; their intrinsic resting tremor (stationary motor variability), etc. In a same analogy, higher than $ID_{5.0}$ was discarded for apparently inevitable zero hit scores that they generated which would result an infinite value in MT (= Time per ID / # of hits) invalidating the whole session.

5.3 Results for KSAT test

According to the effective parameter adjustment described in Introductions, five *ad-hoc* ID values are generated as Table 3, and used to report the performances in the following chapters.

Table 3. Indices of difficulty for KSAT test

		1st ID	2nd ID	3rd ID	4th ID	5th ID
A	cm	5.0	7.4	14.6	20.5	27.5
W	cm	1.8				
2A/W	dimensionless	5.6	8.2	16.2	22.8	30.6
$\log_2(2A/W)$	bits	2.47	3.4	4.02	4.51	4.93
IDs	bits	**2.5**	**3.0**	**4.0**	**4.5**	**5.0**

As suggested by Fitts, any targeting test following Fitts' paradigm should be performed before any task-specific learning and after all the task-specific unfamiliarity are removed, i.e., their real neuromotor information process capacity can only be monitored only when subjects have just reached their stable performances after ample amount of trials which allows them to adapt themselves for any environmental variables that would hinder them to generate their optimal performances (Fitts and M.I. 1967). In this research, this was applied only to normal populations, due to the difficulty of defining a 'learning-effect' or 'adaptation-effect' from hemiparetic population, for their performance improvement is visible only after a very long extended period of training where the actual period cannot be easily identified. For stroke subjects, introduction to the protocol was minimized to one day, which was only to confirm that they are able to generate 'non-zero' hit scores from each all ID levels.

Note that each day has 5-sessions, and normal group did only single-day run total, while stroke group underwent 11 days total. Both groups did trial runs before regular day begins which were not counted in the data analysis.

5.3.1 Logarithmic relationship (log-linearity) of KSAT test

Figure 27 shows normal subjects' KSAT MT/ID score graph with one line per session plotted. Each subject showed various MT/ID score trends different from session by session, but general patterns reveal a good linearity which agrees with results from a numerous other reports on conventional Fitts' paradigm experiments which will be discussed later. Note that subject C1 ~ C4 exhibited one or two performance 'reversal' between $ID_{4.5}$ and $ID_{5.0}$, seen as an MT score drop. Also note that subject C2 showed a moderate or no change in the $ID_{4.0}$ ~ $ID_{5.0}$ region.

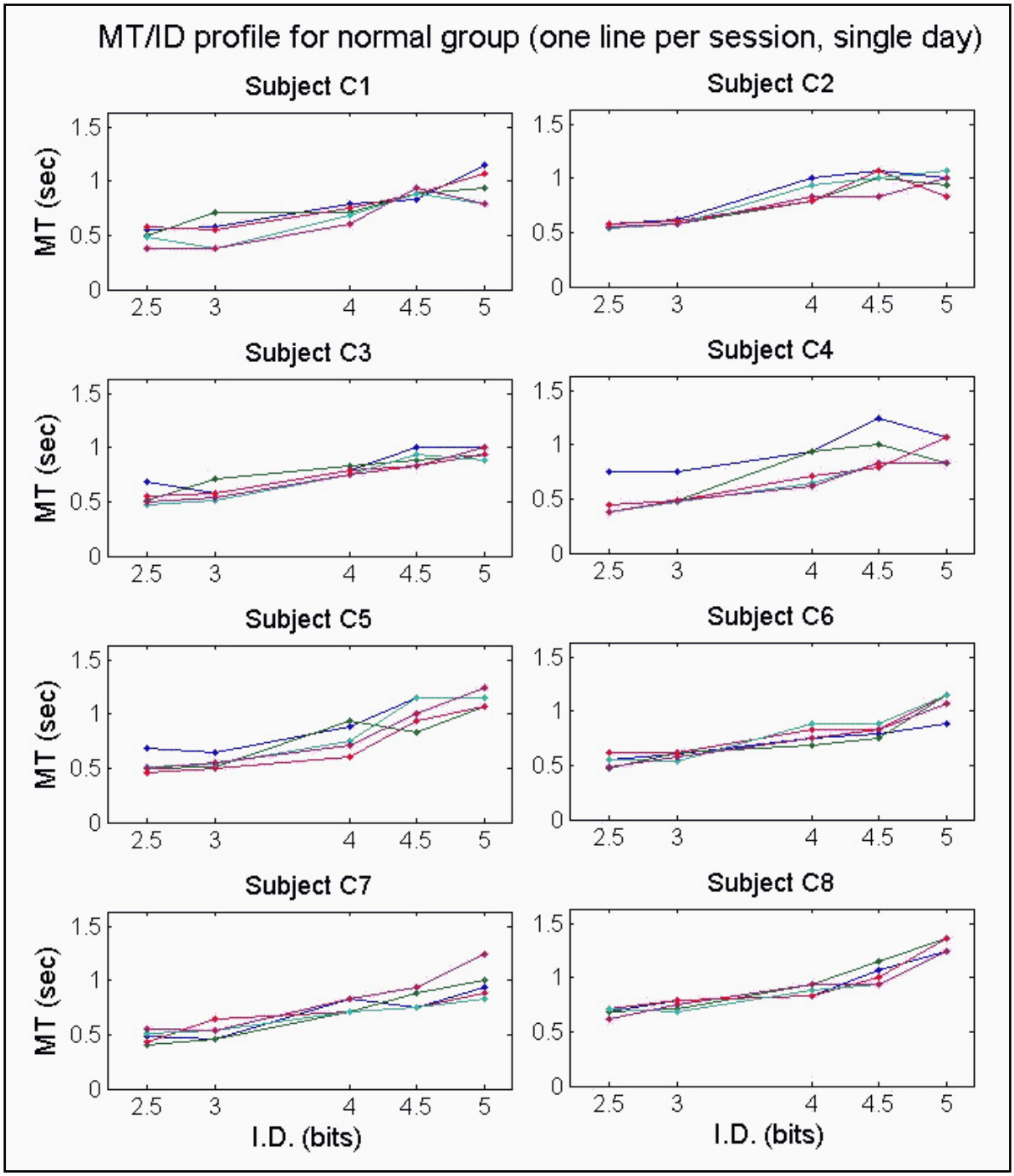

Figure 27. KSAT session-specific average MT/ID score showing each healthy subject's results (single day, one line per session). Note the overall superiority of MT scale compared to stroke subjects' performance plots.

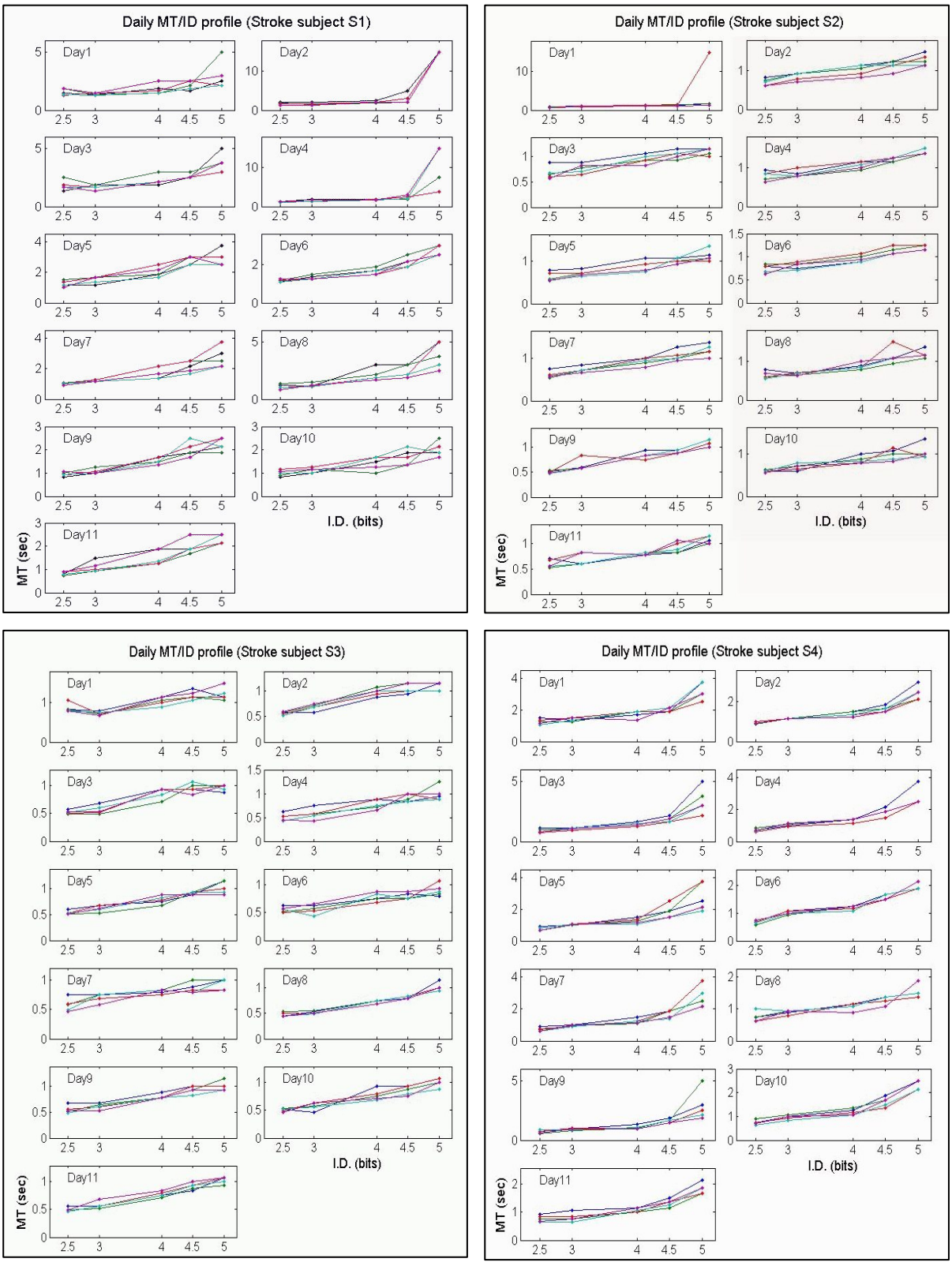

Figure 28. KSAT strok subjects' day by day MT/ID profiles (11 days total, 5 sessions per day, one line per session).

Figure 28 shows each stroke subject's daily MT/ID score with one line per session plotted. Note that unlike normal's results, many of stroke subjects shows 'flap-up' patterns at $ID_{5.0}$, resultant from low number of hits where the target distance was the highest.

Comparing these two groups of figures, note the overall ordinate amplitude of 1.5 seconds (= 10 hits per ID interval time of 15 seconds) for all normal subjects, while for stroke groups ordinate usually goes over 3 seconds (= 5 hits), 4 seconds (~ 4 hits), 6 seconds (= 2~3 hits), or up to 15 seconds (= only one hit) depending on the performances.

Statistical analysis of KSAT: Various way of statistical approach is introduced here to ensure that every aspects of mathematical rigor were considered in this research. But only **Method.1** is mainly used for the final analysis in this research, because the purpose of having 5-sessions per day was originally to gather a daily trend. Matlab statistical toolbox was used for following calculations.

There are mainly two ways to average post-hoc Fitts' paradigm results.

[**Method.1 ID-ensemble-average per each day**] Gather each day's ensemble-averaged MT/ID score, then plot a single line of ensembled MT/ID score graph per day to generate fitting constants (intercept a and slope b) with daily goodness of fit per subject.

[**Method.1' ID-ensemble-average for x-days**] It is a variation from method 1, gather all day's ensemble-averaged MT/ID score, then plot a single line of ensemble MT/ID score graph for all days to generate only one single value of goodness of fit per subject for the interested duration of the training.

This result is shown in Table 4 and 5 for normal and stroke groups, respectively. Note that it is invalid for normal subjects for normal group only ran a single-day protocol.

This method was also used to show stroke subject improvements, by setting the interested duration to be first 4 days and last 4 days separately and compare the results.

[**Method.2 Session-average per each day**] The other way does not use ID-ensemble method. But instead, gather each session's MT/ID score, to generate daily fit constants with goodness of fit.

[**Method.2' Session-average for x-days**] Similar variation, "session-averaged for all days" exists for this way as well; gather all day's non-ID-ensembled Session-averaged MT/ID scores, then plot a single line of graph for all days to generate only one fit constants with goodness of fit per subject.

Result from method 2s are shown in Table 6 and 7 for normal and stroke groups, respectively. Here, also note that same redundancy exists for normal subjects for the same reason (one-day only protocol for normal group) as before.

5.3.1.1 ID-ensemble-averaged performances for KSAT

MT/ID scores: Figure 29 shows ID-ensembled-averaged final MT score with linear-regression fit line for both groups corresponds to the right-most column data of Tables 4 ~ 7.

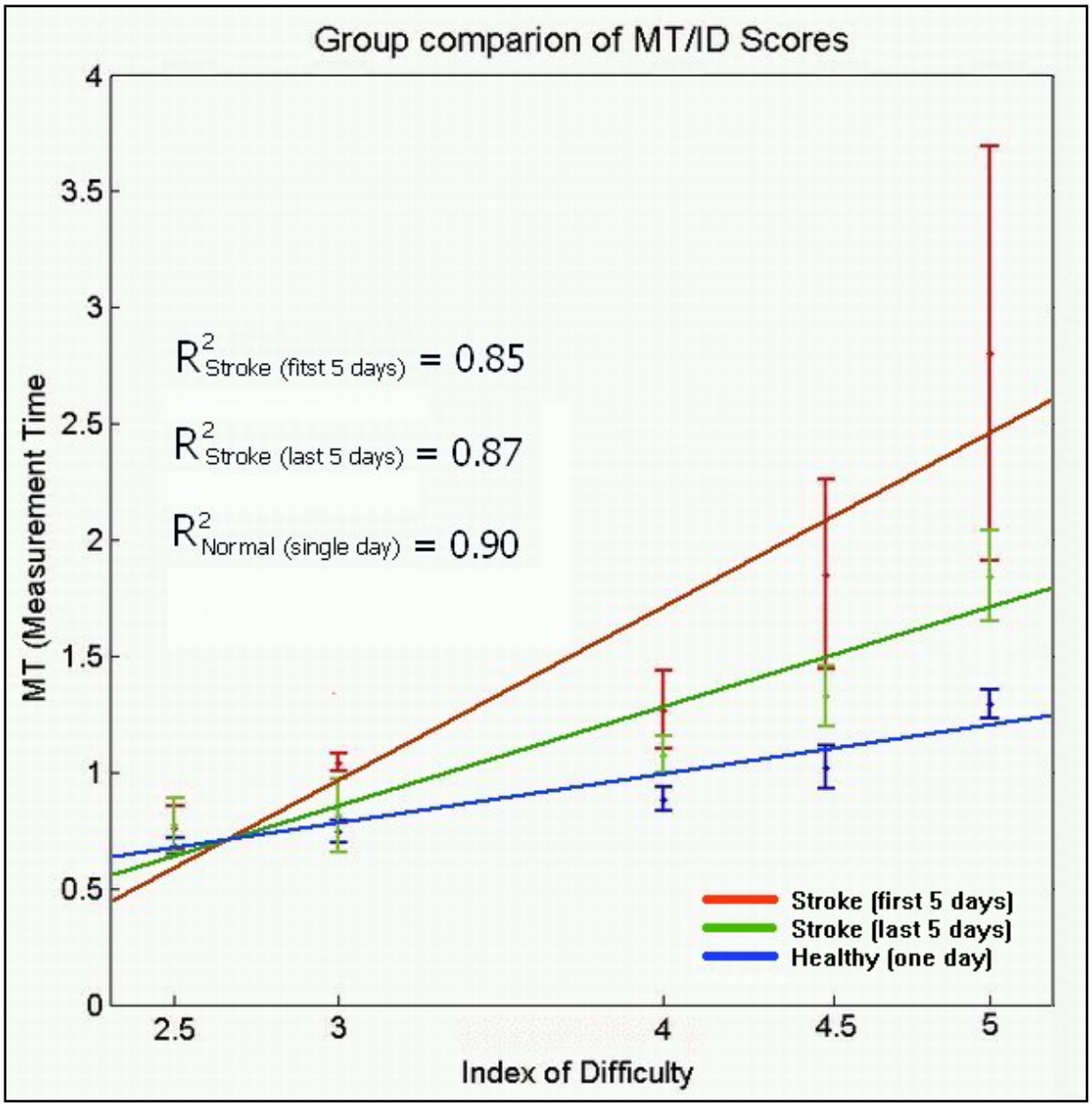

Figure 29. ID-ensembled MT/ID score plot of KSAT from both normal and stroke groups. Note the more linear fit from normal's with coefficient of 0.90, while strok group's log-linearity was only 0.85 for the first 5 days and 0.87 for the last 5 days.

ID-ensembled normal subjects performance was better than strokes' seen in blue fit line, with better consistency represented by smaller error bars, also with higher linear regression coefficient of 0.90 (Table 4). However, stroke subjects' ID-ensembled MT score trend was less adherent to a linear fit line with noticeable improvement in the linearity from over the course of training ($R^2_{\text{Stroke (first 5 days)}} = 0.85 \rightarrow R^2_{\text{Stroke (first 5 days)}} = 0.87$) seen in Tables 6 and 7.

Note the intercepts are not showing any meaningful trend. During the familiarization phase, more than one stroke subject reported an uneasiness to stick to the pre-determined starting position to be neither full extension nor full flexion, thus randomizing the starting position to each and every subject in both groups was necessary to maintain the data integrity. Due to this reason, the metric analyzed was the slope constant only.

Table 4. KSAT Single-day ID-ensenble-averaged MT scores from Normal (Cx) group (in seconds).

		C1	C2	C3	C4	C5	C6	C7	C8	ID-ensembled
IDs	2.5	0.5004	0.5604	0.5448	0.4784	0.5308	0.5380	0.4782	0.6834	0.5393
	3.0	0.5214	0.5912	0.5842	0.5342	0.5522	0.5926	0.5268	0.7448	0.5809
	4.0	0.7070	0.8696	0.7822	0.7730	0.7766	0.7794	0.7616	0.8844	0.7917
	4.5	0.8832	0.9950	0.8970	0.9410	1.0156	0.8174	0.8138	1.0198	0.9228
	5.0	0.9480	0.9682	0.9512	0.9282	1.1400	1.0830	0.9804	1.2956	1.0368
$R^2_{\text{linear, Normal}} = 0.90$										

Table 5. KSAT All-days ID-ensenble-averaged MT scores from Stroke (Sx) group (in seconds).

		S1	S2	S3	S4	ID-ensembled
IDs	2.5	1.2012	0.6601	0.5594	0.8131	0.8084
	3.0	1.307	0.7617	0.6106	1.0249	0.9260
	4.0	1.773	0.9445	0.8307	1.2701	1.2046
	4.5	2.2414	1.0768	0.9285	1.6639	1.4777
	5.0	4.4404	1.1963	1.0174	2.541	2.2988

Table 6. KSAT First 5-days ID-ensenble-averaged MT scores from Stroke (Sx) group (in seconds).

		S1	S2	S3	S4	ID-ensembled
IDs	2.5	1.5162	0.7116	0.5996	0.9184	0.9365
	3.0	1.5310	0.8320	0.6347	1.1466	1.0361
	4.0	2.0068	1.0288	0.8930	1.4291	1.3394
	4.5	2.5653	1.1426	1.0056	1.8346	1.6370
	5.0	6.7314	1.8162	1.0595	2.9179	3.1313
$R^2_{\text{linear, Stroke (first 5 days)}} = 0.85$						

Table 7. KSAT Last 5-days ID-ensenble-averaged MT scores from Stroke (Sx) group (in seconds).

		S1	S2	S3	S4	ID-ensembled
IDs	2.5	0.9734	0.5919	0.5200	0.7366	0.7055
	3.0	1.1399	0.6832	0.5953	0.9050	0.8309
	4.0	1.6655	0.8583	0.7786	1.1262	1.1071
	4.5	2.0444	1.0017	0.8784	1.5126	1.3593
	5.0	2.6174	1.1188	0.9984	2.2865	1.7553
$R^2_{\text{linear, Stroke (first 5 days)}} = 0.87$						

Slopes and Intercepts: Tables 8, 9 and Figure 30 are generated from linear-regression fitting results showing fit constants (slope p_1 and intercept p_2) from normal and stroke groups in KSAT test. The subject-specific fit equations $y = p_1 \cdot x + p_2$ at 95% confidence bounds (where p_1 is the slope and p_2 is the intercept) for the duration of interests (X-days) are acquired from each ID-ensembled MT/ID cases from Tables 4 and 5 for fit constants calculation. For normal group, only one-day data are used accordingly, shown in Table 8.

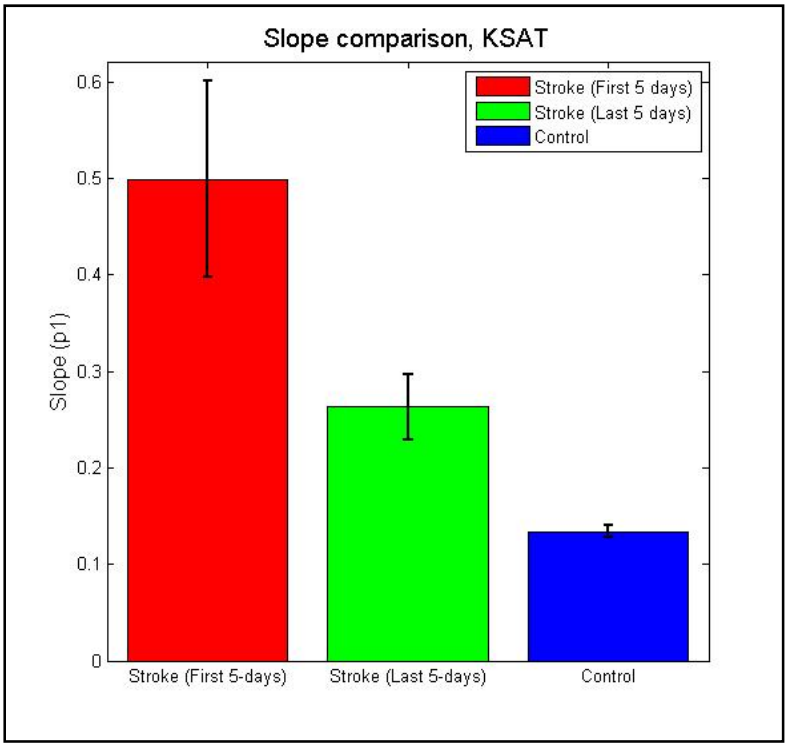

Figure 30. First-order linear-regression constant (p_1) between stroke group and control group comparison. Stroke group's data were devided into first 5-days and last 5-days, showing almost twice improvements over 6-weeks training.
Note that it is comparable to Figure 39.

For stroke group, all-days, first 5-days, or last 5-days fit constants are calculated and shown in Table 9, showing almost twice improvements over 6-weeks training. Figure 30 is the graphical representation of these results. First-order linear-regression constant (p_1) between stroke and normal group reveals a clear distinction between them. Also note that the variability depicted as error bars which can be considered as the reciprocal of stability also shows group distinction as well as stroke subjects' improvements.

The intercept constant p_2 was not analyzed further but tabulated here as well, because it does not represent the conventional notion of 'the time required to respond to given target' due to the indices of difficulties began from 2.5 bits ($ID_{2.5}$), not from 1.0 bits ($ID_{1.0}$) or less, also the movement cue was randomly given between 0~1 seconds due to the previously explained reason in protocol session, thus MT was not decomposed into 'reaction time', 'travel time', and 'homing time'.

Table 8. KSAT Linear-regression fit constants (slopes & intercepts) from Control (Cx) group.

	C1	C2	C3	C4	C5	C6	C7	C8	Group average
$p_{1\ (slope)}$	0.1257	0.1219	0.1126	0.1306	0.1682	0.1315	0.1291	0.1499	**0.1337** ± 0.0175
$p_{2\ (intercept)}$	0.3349	0.4311	0.4142	0.3390	0.2985	0.3676	0.3247	0.4758	0.3732 ± 0.0611

Table 9. KSAT Linear-regression fit constants (slopes & intercepts) from Stroke (Sx) group.

		S1	S2	S3	S4	Group averages
First 5-days	$p_{1\ (slope)}$	1.1465	0.2520	0.1291	0.4687	**0.4991** ± 0.4539
	$p_{2\ (intercept)}$	-0.5693	0.3503	0.4513	0.2432	0.1189 ± 0.4666
All-days	$p_{1\ (slope)}$	0.7472	0.188	0.1234	0.4905	0.3670 ± 0.2815
	$p_{2\ (intercept)}$	-0.0076	0.4132	0.4191	0.2341	0.2647 ± 0.2008
Last 5-days	$p_{1\ (slope)}$	0.4193	0.1372	0.1240	0.3708	**0.2628** ± 0.1540
	$p_{2\ (intercept)}$	0.4304	0.4391	0.3822	0.2011	0.3632 ± 0.1109

Velocity profiles: MT/ID data are analyzed further to create velocity profiles. Due to fact that it is not a reciprocal of MT/ID data but the target amplitude difference (A) per each index of difficulty are used in the calculation, velocity profiles seen in Figures 31 and 32 reveal another relevant motor functionality characteristics in reaching and targeting experiment.

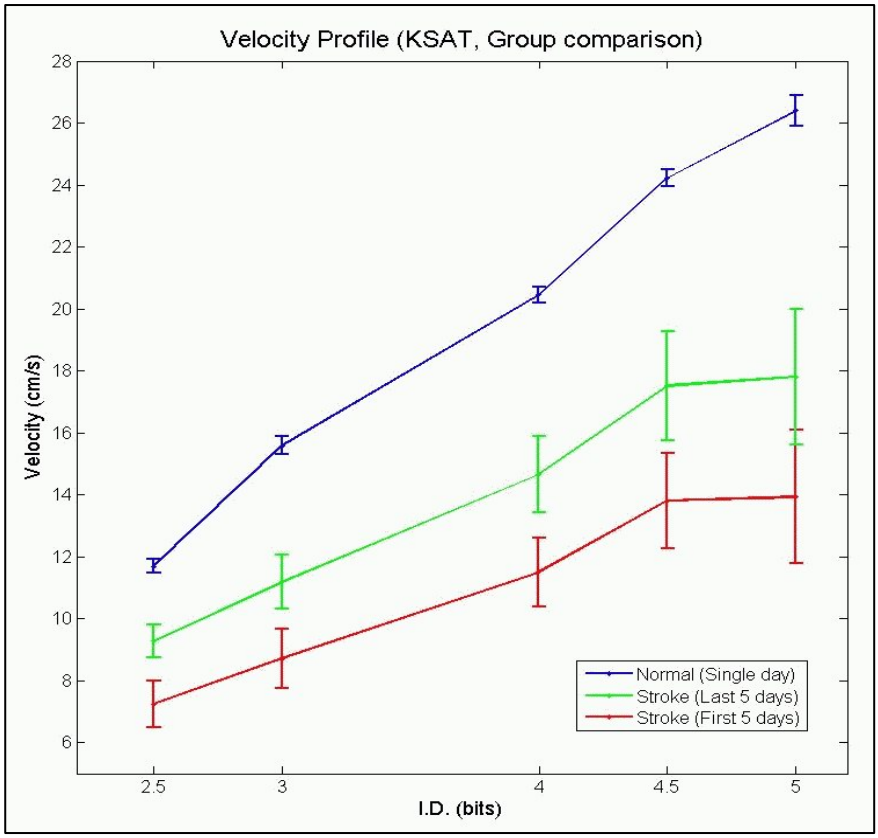

Figure 31. Velocity comparison from KSAT test, Normal (healthy) group (in blue) shows a definite superiority in the absolute value of velocity values as well as consistency (smaller standard error), compared to stroke subjects' 6 weeks' velocity profile. Note that stroke group showed a good improvement

Figure 31 shows a clear distinction within stroke group day-wise comparison (first 5 days vs. last 5 days) as well as between group comparison. Note that normal group's ability to make a faster action with much better consistency is once again visible in this analysis. However, within stroke group day-wise comparison (first 5 days vs. last 5 days) didn't show any consistency changes (error bars) over the course of training.

Figure 32 shows within stroke group and between groups' linear-regression results for their velocity profiles. Note that the log-linearity is much greater here than MT/ID profiles seen in Figure 29 identified as fitting constant R^2 for each profile lines.

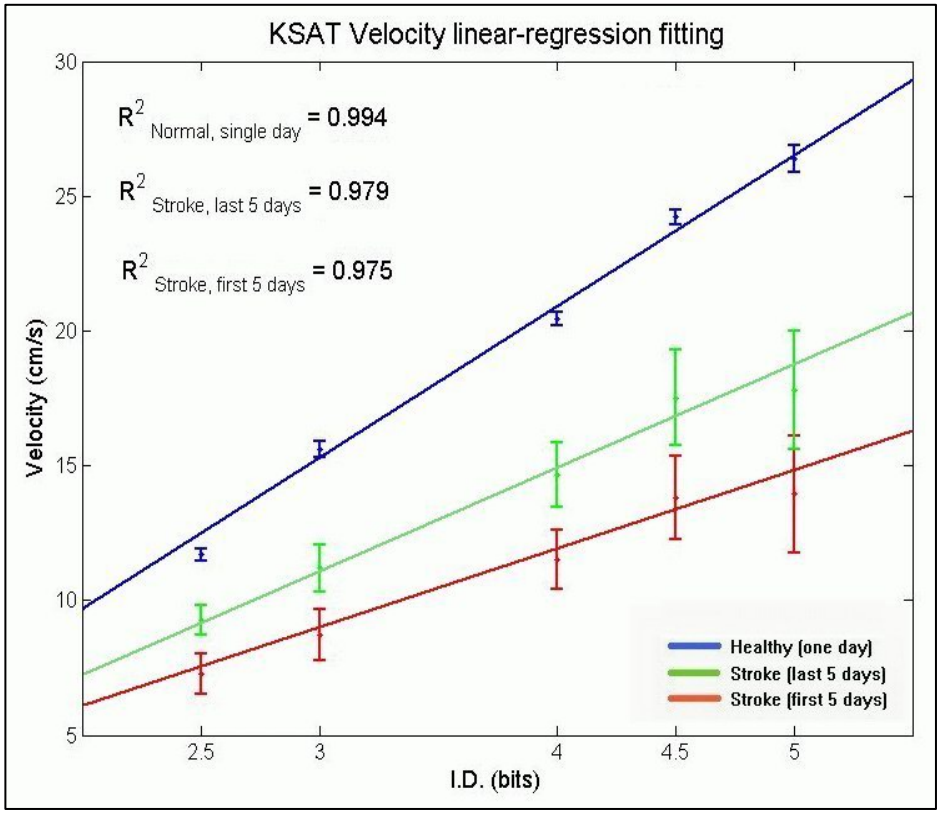

Figure 32. KSAT velocity linear-regression fitting shows a consistent hierarchy from between group trend to within stroke group improvement, a comparable trend to MT/ID score profiles. Note that fitting constants here are much higher in this velocity analysis than MT/ID score profiles.

5.3.2 Improvements of stroke group in KSAT test

Within stroke group (between first 5 days and last 5 days) was compared for MT/ID profile, slope constants and velocity profiles to find between group differences and test the main hypothesis. Other series of statistical methods such as analysis of variance (ANOVA) was considered and tested (McCall 1975) but **they revealed false Boolean** values toward the obvious trends seen in the graphical results with statistically insignificant p-values due to the non-normalcy and heterogeneous variances from the data set (Gibbons 1985). Thus a simple day-wise improvement ratio was calculated in the following chapters.

5.3.2.1 MT/ID ratio between first 5 days and last 5 days

Stroke subjects' measurement time performance over 6 weeks in KSAT test exhibited noticeable comparative improvements for average MT scores per hits $\left(= \frac{15 \text{ seconds}}{\#\ of\ hits}\right)$ shown in Table 10,

calculated as day-wise ratio over all stroke subjects. First 5 days over last 5 days MT was calculated, showing a 35% improvements in terms of the time spent per hits for all ID levels.

Table 10. KSAT MT/ID score improvements for stroke subjects over 6 weeks.

ID	2.5	3.0	4.0	4.5	5.0
$MT_{days\ 1\sim5}$	0.94	1.04	1.34	1.64	3.13
$MT_{days\ 7\sim11}$	0.71	0.83	1.11	1.36	1.76
$MT_{days\ 1\sim5}$/ $MT_{days\ 7\sim11}$	1.33	1.25	1.21	1.20	1.78
Averaged MT/ID ratio	**1.35 ± 0.24**				

5.3.2.2 Velocity ratio between first 5 days and last 5 days

Stroke subjects' velocity performance over 6 weeks in KSAT test also exhibited noticeable comparative improvements for velocity values per ID $\left(= \frac{\text{Total travel distance per ID}}{15\ seconds}\right)$ shown in Table 11, calculated as day-wise ratio over all stroke subjects. Last 5 days over first 5 days velocity was calculated, showing a 28% improvement in terms of the speed of elbow movements for all ID levels.

Table 11. KSAT velocity improvements for stroke subjects over 6 weeks.

ID	2.5	3.0	4.0	4.5	5.0
$Velocity_{days\ 1\sim5}$	7.2509	8.7092	11.5052	13.8020	13.9325
$Velocity_{days\ 7\sim11}$	9.2728	11.1904	14.6543	17.5107	17.805
$Velocity_{days\ 7\sim11}$/$Velocity_{days\ 1\sim5}$	1.2788	1.2849	1.2737	1.2687	1.2779
Averaged Velocity ratio	**1.28 ± 0.01**				

5.4 Conclusion for KSAT test

At the end of the 6 weeks of training, stroke subjects' performance in all of MT/ID profile, linear-regression slope and velocity profile improved markedly, with their later days of the training performance becoming closer to the log-linear Fitts' behavior and to healthy group's performance. Also note that some of stroke patients' performance after training matched or exceeded that of the normal's due to task-specific adaptation. Even though all these results are pointing out the evident improvements on their motor abilities, other conventional post-training rehabilitation assessment such as Chedoke-McMaster rehabilitation scaling didn't show much change on their grading, indicating the inefficiency and insensitivity of these assessment systems. It is due to the qualitative nature of these assessments that depends on the assessor's subjective opinions.

Along with the obvious trend from stroke group to normal groups' linear-regression results, the 'reaction time' (between 'action' cue and actual 'onset' of the movement) might have been played a role if it had been acquired in a systematic manner. Possible trend might have been shown in the

reversed order of p_2 from stroke group being higher to normal groups' lower p_2 values, because it has been noticed that stroke subjects' reaction time was very irregular and also higher which would result in a similar trend monitored in slope (p_1) comparison. Once again, the intercepts are not analyzed for it does not show any meaningful metric in this research due to the randomized starting positions during the protocol.

Velocity analysis showed an overall higher regression results compared to the MT/ID score profiles, indicating that the adapted Fitts' paradigm used in this research as KSAT test might represent the speed itself better than conventional measurement time as originally suggested to be log-linear in Fitts' original test. Although much consideration and adjustments were made to eliminate any irrational discrepancies between actual elbow angle and fronto-parallel screen coordinates, the intrinsically required additional process to translate the elbow angle outputs into the circular coordinate on the rectangular (transversal) screen coordinates actually given as the visual feedback environment might have been the reason for the velocity's superior log-linearity. One research on the effect of virtual environment in performing Fitts' type experiments shows related effects on the scaling factor which brings a reversal or over-performance on the MT/ID score profiles (Balakrishnan 2004). Although this research doesn't suggest any adjustments to original Fitts' formula or their new models, application of Fitts' law to facilitate more effective human-computer interface environments is meaningful and worthwhile.

In summary, the main hypothesis that movement time (MT) increases as a function of index of difficulty (ID) is proven. Also hemiparetic subjects' movement times were significantly slower and more affected by increased ID than normal subjects.

Upper limb actions at the elbow level in reaching and targeting approximately followed Fitts' type behavior for both healthy and hemiparetic groups using the MAST system. Third hypothesis was also proven that stroke subjects' Fitts' type exercise showed an improved performance by key metrics generated by the MAST system. Thus this experiment successfully proved that the MAST system can produce quantifiable metrics with intuitive, simple, and effective training platform in upper arm rehabilitation regime.

6. EXPERIMENT #2: DYNAMIC SPEED VS. ACCURACY TRADE-OFF (DSAT) TEST

6.1 Subject recruitment for DSAT test

Same acceptance criteria identical to kinematic SAT experiment were applied to dynamic SAT test, as specified by higher than level 6 Chedoke-McMaster index (Gowland, Stratford et al. 1993) as well as the same requirements as Fitts' paradigm performance which requires interruption-free actions either by self-invoked or from outside perturbations (Fitts, 1967). All four subjects who performed KSAT test met those criteria for DSAT as well, thus participated here. Normal subjects (n=8) were also recruited, not necessarily same individuals from KSAT test. Informed consent was gathered from all subjects before the experiment under the provision of Rutgers IRB.

6.2 Protocol for DSAT test

DSAT test was performed using a LabVIEW VI interface with a vertical tank display shown in Figure 33. DSAT test's unique aspect on the representation of subject's actual movements as a whole-body isometric action must be noted here that in dynamic SAT test, no part of subject's body is moving, because the Gripper only monitors direct isometric handgrip force generated from the subject's palmar force of the hand, while the subject's arm is at rest on the MAST (all other joints of the upper-arm on the MAST is fixed in neutral position) with wrist, elbow, and shoulder not moving. The force signal is interpreted to move the blue tank bar in proportion to subject %MVC. The target arrangement was in a similar manner to kinematic SAT test, but in dynamic SAT test, the cursor (top edge of the force tank) traveled vertically as subject's grip force changes.

Figure 33. LabVIEW interface (front panel) for DSAT, showing the lower target hit-registration.

6.3 Results for DSAT test

Adjusted (*ad-hoc*) indices of difficulty for DSAT test shown in Table 16 were matched from KSAT's IDs (Table 3), but from different target dimensions. Matching those indices of difficulties for both KSAT and DSAT was a necessary process to be able to compare the two experiments for information capacitive aspects to test the 2nd hypothesis; Correlation between KSAT and DSAT tests. Note that instead of target width (W) in KSAT test, target height (H) is used here in DSAT test.

Table 12. Indices of difficulty for dynamic SAT test

		1st ID	2nd ID	3rd ID	4th ID	5th ID
A	cm	3.5	4.9	9.5	13.5	18.0
H	cm	1.2				
2A/H	dimensionless	3.9	8.17	15.8	22.5	30
$\log_2(2A/H)$	bits	2.54	3.03	3.98	4.49	4.91
IDs	bits	2.5	3.0	4.0	4.5	5.0

Figure 34 shows exemplary dynamic SAT signal trends per each index of difficulties for 5 sessions (one-day) overlapped altogether from a single subject. Noticeable dynamic features are revealed in this sample waveforms generated by actual run, that it is not an ideal perfect sinusoidal waves but has many important landmarks such as overshoots, undershoots, dwelling on the target, etc. With this ID-decomposed force profile plot, we can monitor subject's qualitative and quantitative force targeting characteristics at different force levels such as events around the moment of target hit registrations, between target-hits dynamic features,

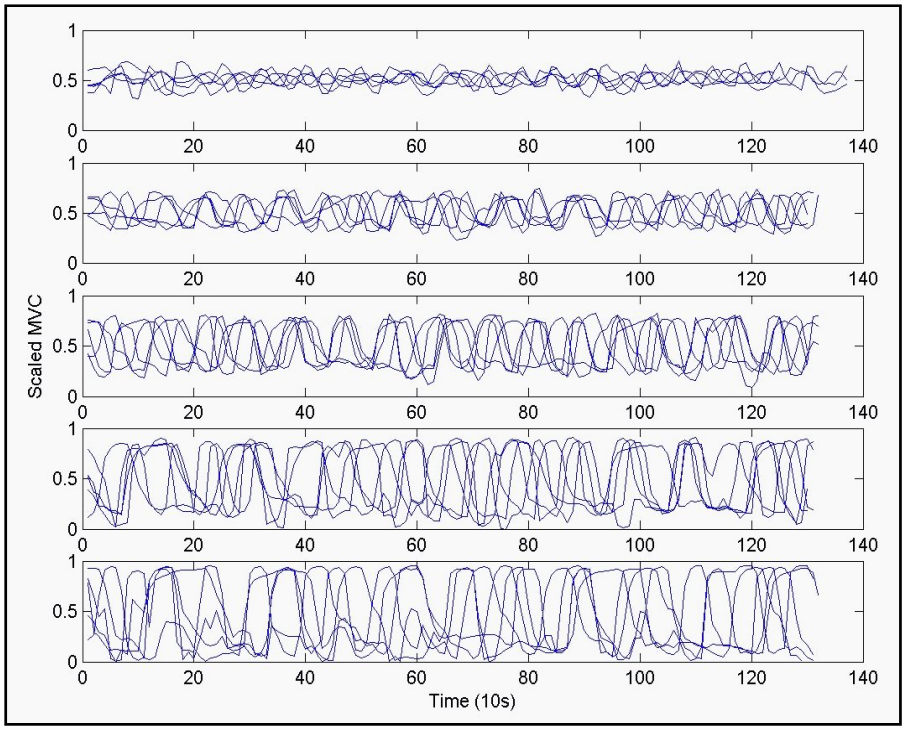

Figure 34. . Examplar Force profile of DSAT decomposed over 5 IDs. These types of force profiles from subjects were collected and used to perform statistical analyses in the result section. (lower to higher ID levels shown from top to bottim).

variability characteristics as a measure of motor system repeatability or stability, and so forth.

6.3.1 Logarithmic relationship (log-linearity) of DSAT test

Statistical analysis of DSAT: Statistical analysis used in KSAT was also applied here in DSAT. Main analysis method was identical to KSAT test's analysis to maintain consistency as follows.

[**Method.1 ID-ensemble-average per each day**] Gather each day's ensemble-averaged MT/ID score, then plot a single line of ensembled MT/ID score graph per day to generate fitting constants (intercept a and slope b) with daily goodness of fit per subject.

[**Method.1' ID-ensemble-average for x-days**] It is a variation from method 1, gather all day's ensemble-averaged MT/ID score, then plot a single line of ensemble MT/ID score graph for all days to generate only one single value of goodness of fit per subject for the interested duration of the training.

6.3.1.1 ID-ensemble-averaged performances for DSAT

MT/ID scores: Table 17 shows the MT/ID score of DSAT performance from normal groups with the corresponding plot in Figure 35. Note that subject C3 showed large between session variations compared to other normal subjects.

Table 13. DSAT Single-day ID-ensenble-averaged MT scores from Normal (Cx) group (in seconds).

		C1	C2	C3	C4	C5	C6	C7	C8	ID-ensembled
IDs	2.5	0.4526	0.5072	0.5352	0.4950	0.4918	0.4250	0.3854	0.4576	0.4687 ± 0.0483
	3.0	0.7206	0.6958	0.7724	0.6476	0.5544	0.4700	0.6134	0.6802	0.6443 ± 0.0968
	4.0	0.7372	0.7920	0.9446	0.7386	0.6552	0.4918	0.6982	0.7530	0.7263 ± 0.1275
	4.5	0.9276	0.9402	1.0032	0.7936	0.6774	0.6308	0.7466	0.8196	0.8174 ± 0.1319
	5.0	0.8914	0.9052	1.4502	0.8358	0.7374	0.7192	0.8618	0.8920	0.9116 ± 0.2288
ID-ensembled $R^2_{linear, Normal} = 0.9540$										

Figure 36 shows each stroke subject's daily DSAT MT/ID profiles per sessions. Note that unlike normal group's result, many of stroke subjects shows 'flap-up' patterns at $ID_{5.0}$, due to the same reason as in KSAT, from low number of hits where the target distance was the highest.

Similar to KSAT's result, the overall ordinate amplitude between groups are different in DSAT as well which represents group performance differences.

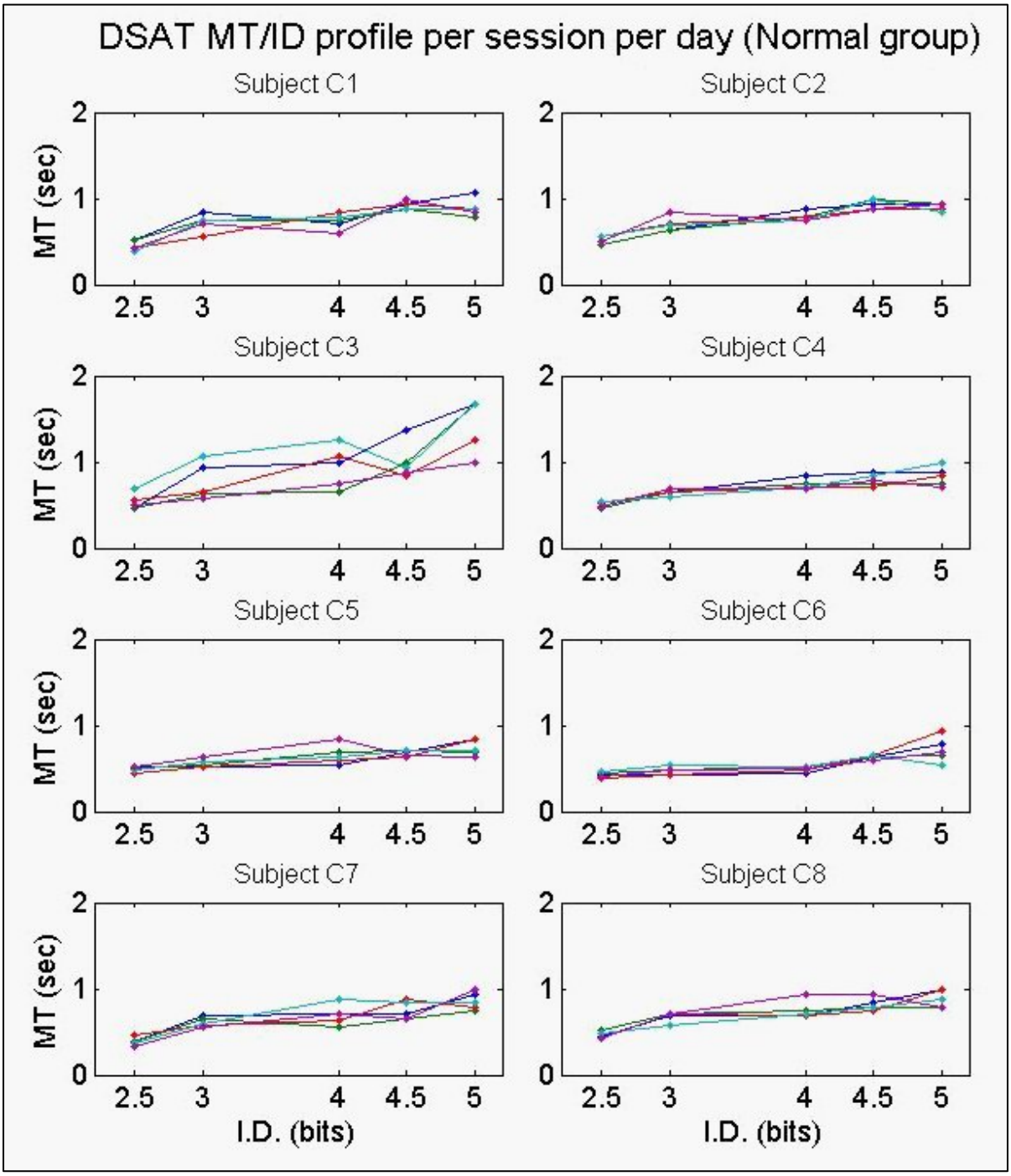

Figure 35. DSAT session-specific MT/ID score showing each healthy subject's results (single day). Note the overall superiority of DSAT MT scale compared to following stroke subjects' performance plots.

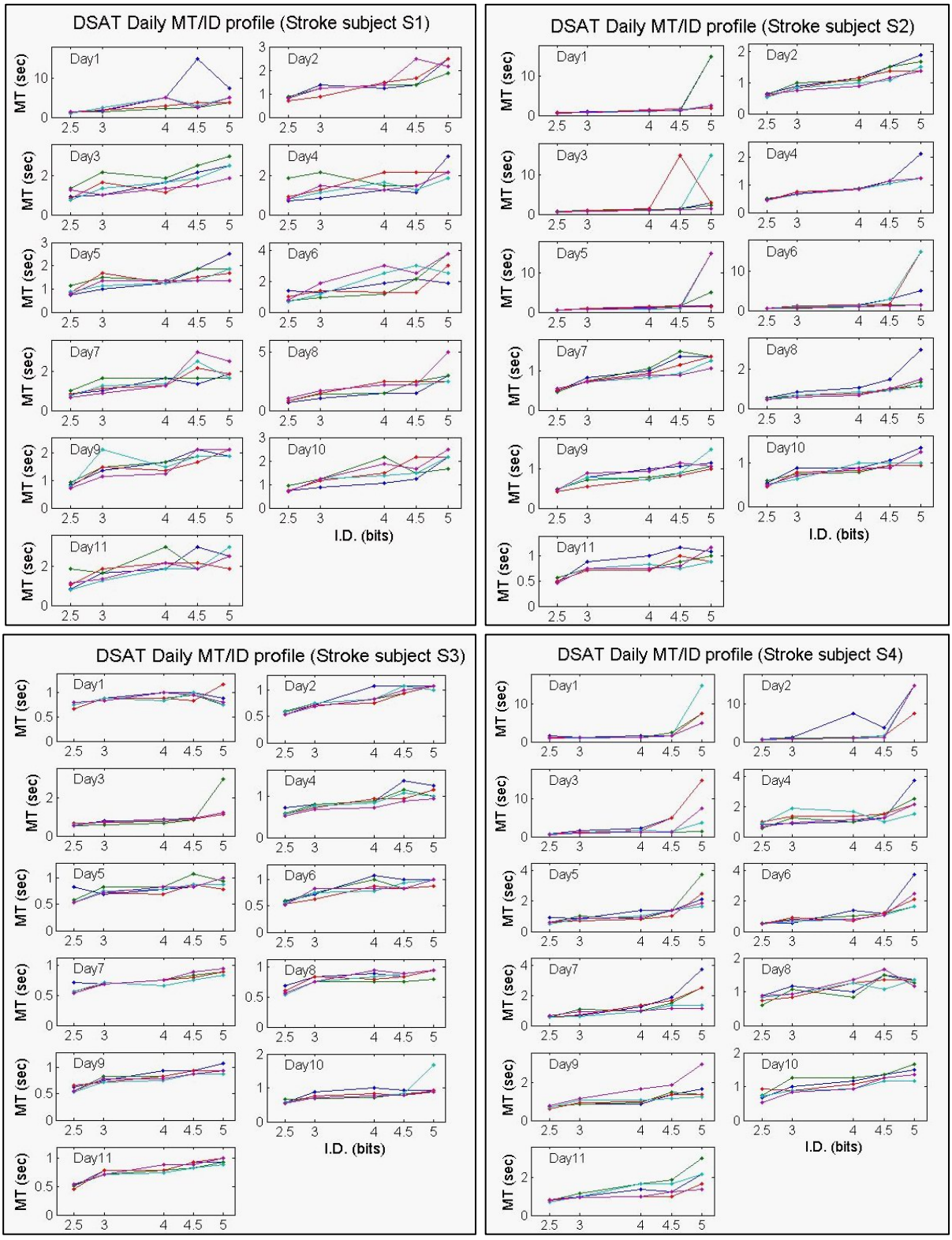

Figure 36. DSAT day-specific MT/ID profiles from each stroke subject.

Table 14. DSAT All-days ID-ensenble-averaged MT scores from Stroke (Sx) group (in seconds).

		S1	S2	S3	S4	ID-ensembled
IDs	2.5	0.9490	0.5238	0.5841	0.7326	0.6974 ± 0.1893
	3.0	1.4041	0.7864	0.7506	0.9789	0.9800 ± 0.3000
	4.0	1.8582	0.9840	0.8282	1.2710	1.2353 ± 0.4539
	4.5	2.2289	1.4946	0.9107	1.5698	1.5510 ± 0.5395
	5.0	2.5902	3.3306	1.0214	4.2198	2.7905 ± 1.3545

Table 15. DSAT First 5-days ID-ensenble-averaged MT scores from Stroke (Sx) group (in seconds).

		S1	S2	S3	S4	ID-ensembled
IDs	2.5	1.0136	0.5587	0.6076	0.7836	0.7409 ± 0.2059
	3.0	1.4461	0.8138	0.7596	1.0557	1.0188 ± 0.3126
	4.0	1.9600	1.0716	0.8378	1.4559	1.3313 ± 0.4905
	4.5	2.4625	1.8596	0.9663	1.8118	1.7751 ± 0.6151
	5.0	2.7648	4.5839	1.0985	7.0634	3.8777 ± 2.5567
$R^2_{\text{linear, Stroke (first 5 days)}} = 0.7144$						

Table 16. DSAT Last 5-days ID-ensenble-averaged MT scores from Stroke (Sx) group (in seconds).

		S1	S2	S3	S4	ID-ensembled
IDs	2.5	0.8908	0.4887	0.5660	0.7230	0.6671 ± 0.1781
	3.0	1.3797	0.7398	0.7448	0.9505	0.9537 ± 0.3005
	4.0	1.7368	0.8573	0.8012	1.1541	1.1374 ± 0.4286
	4.5	1.9996	1.0174	0.8598	1.4137	1.3226 ± 0.5080
	5.0	2.3386	1.2343	0.9533	1.7510	1.5693 ± 0.6101
$R^2_{\text{linear, Stroke (first 5 days)}} = 0.9672$						

Figure 37 shows DSAT ID-ensembled-averaged final MT scores per each group (also day-wise improvement comparisons for stroke group) with linear-regression fit lines correspond to the right-most column data of Table 17 (normal) and Tables 19 and 10 (stroke). Note here that the intercepts are again meaningless due to the identical reason given in KSAT analysis. Also note that the linear regression coefficient for all days from stroke group was not calculated in Figure 37 for they are less meaningful than day-wise data subsets, due to another identical reasoning to KSAT's method of analysis.

Graphical and linear-regression analysis showed very good linear fitting result with R^2 value of 0.954 along with stroke group's last 5 days result with higher linear-regression coefficient of 0.9672 which shows a log-linearity reversal resultant from stroke group's task-specific adaptability in DSAT. Meanwhile, stroke subjects' first 5 day result shows a low linear-regression coefficient of 0.7144, due to an outlier-type score at $ID_{5.0}$ difficulty level compared to $ID_{2.5} \sim ID_{4.5}$ levels.

Slopes and Intercepts: Tables 21, 22 and Figure 38 are generated from DSAT's linear-regression analysis and its corresponding constants from normal and stroke groups. Same as in KSAT

analysis, the subject-specific fit equations ($y = p_1 \cdot x + p_2$ at 95% confidence level) each for groups are acquired here in DSAT from ID-ensembled DSAT MT/ID values of Tables 17 ~20 for fit constants calculations.

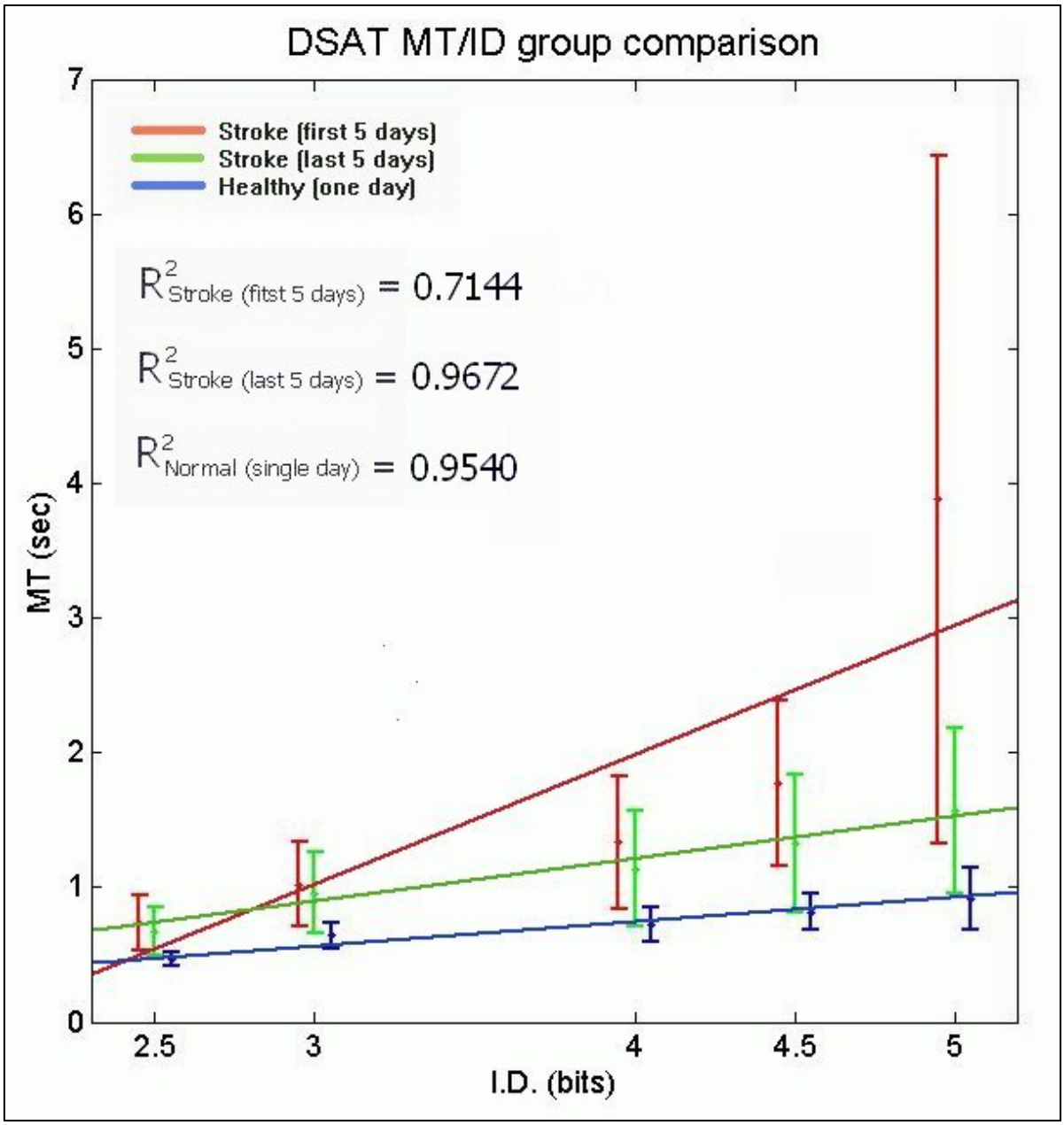

Figure 37. Linear-regression group comparison of ensemble-avereaged DSAT MT/ID profile

Stroke group's first 5-days vs. last 5-days fitting quality comparison reports more than three-fold improvements from Table 18. Figure 38 shows the graphical comparison from Tables 21 and 22. First-order linear-regression constant (p_1) between stroke and normal group reveals a clear distinction

between them. In addition to the p1 values, the variability in errors as stability also shows group differences as well as improved stability within stroke group.

Consistently as in KSAT analysis, the intercept constant p_2 of DSAT performance was not analyzed here in DSAT but tabulated for the record. Same as in KSAT test, DSAT test's movement cue in the protocol was randomly distributed between 0~1 second based on the identical reasoning explained previously in KSAT's result. Once again, the given reasoning is proven and depicted here in DSAT's regression analysis with negative p_2 values, due to the SAT test performed here is not a discrete single action but an oscillatory targeting movements as a connected whole wave form under continuously increasing ID levels, seen in the sample wave forms in Figure 34, which renders the meaning of the intercept void for this research.

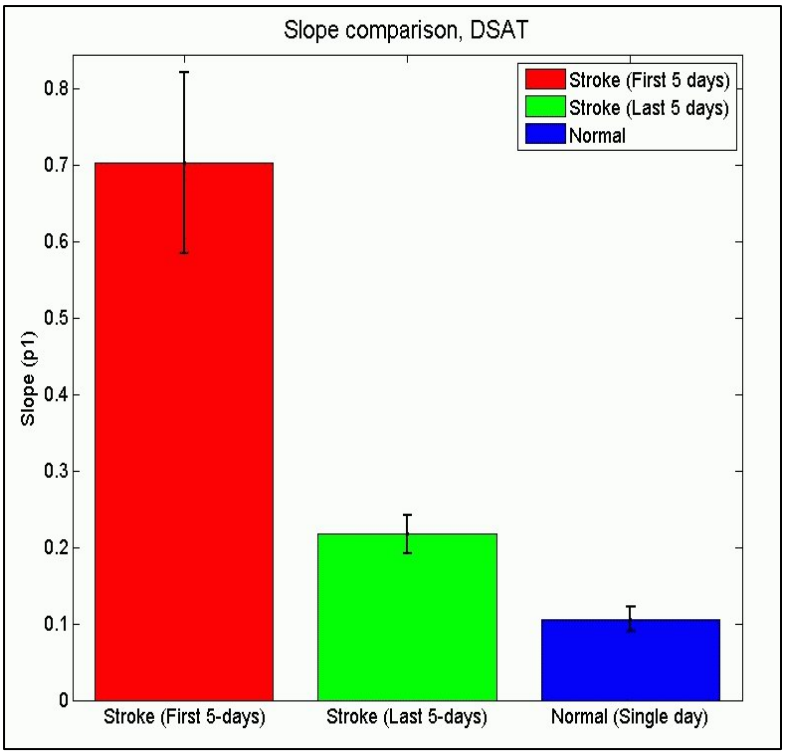

Figure 38. DSAT Slope group comparison. Note the more prominent (higher) slope for stroke group's first 5 days compared to KSAT. Similar downward trend visible in both the bar graph and the error level.

Table 17. DSAT Linear-regression fit constants (slopes & intercepts) from Control (Cx) group.

	C1	C2	C3	C4	C5	C6	C7	C8	Group average
$p_{1\ (slope)}$	0.1085	0.1040	0.2061	0.0828	0.0614	0.0749	0.1086	0.1008	**0.1059** ± 0.0055
$p_{2\ (intercept)}$	0.4205	0.4560	0.3229	0.4538	0.4390	0.3226	0.3353	0.4180	0.3960 ± 0.0074

Table 18. DSAT Linear-regression fit constants (slopes & intercepts) from Stroke (Sx) group.

		S1	S2	S3	S4	Group averages
First 5-days	$p_{1\ (slope)}$	0.4519	0.9096	0.1189	1.3316	**0.7030** ± 0.1059
	$p_{2\ (intercept)}$	0.5737	-0.9513	0.4974	-1.5606	-0.3602 ± 0.2128
All-days	$p_{1\ (slope)}$	0.4107	0.6322	0.1035	0.7565	0.4757 ± 0.2864
	$p_{2\ (intercept)}$	0.5739	-0.4727	0.5086	-0.5152	0.0237 ± 0.5985
Last 5-days	$p_{1\ (slope)}$	0.3516	0.1769	0.0890	0.2519	**0.2173** ± 0.0223
	$p_{2\ (intercept)}$	0.6144	0.3369	0.5181	0.4427	0.4780 ± 0.0235

Velocity profiles: DSAT MT/ID data are analyzed further in the same manner from KSAT analysis to monitor sectional (ID-wise) velocity performances. Here, the same analogy applies as in KSAT that it is not just a reciprocal of MT/ID data but dealt with the target amplitude difference (A) per each index of difficulty. Thus velocity profile in Figures 39 and 40 reveal more relevant and better representation of the subject motor function characteristics in Fitts' paradigm experiment.

Figure 39 shows the same clear distinction as seen in KSAT test for within stroke group day-wise velocity profile comparison (first 5 days vs. last 5 days) as well as between groups comparisons. Note that normal group's velocity was clearly superior (faster) in DSAT test as well, with better consistency (smaller error bars). However, last 5 days of stroke velocity at $ID_{2.5}$ showed smaller green error than normal's blue error at $ID_{2.5}$ in Figure 40, indicating a task-specific performance reversal at low-force level (low information load) between hemiparetic and non-hemiparetic functionality.

Within stroke group's day-wise velocity comparison (first 5 days vs. last 5 days) also showed a moderate consistency changes (error bars) over the course of training, seen in the trend of red to green error differences, which was not prominent in KSAT's result.

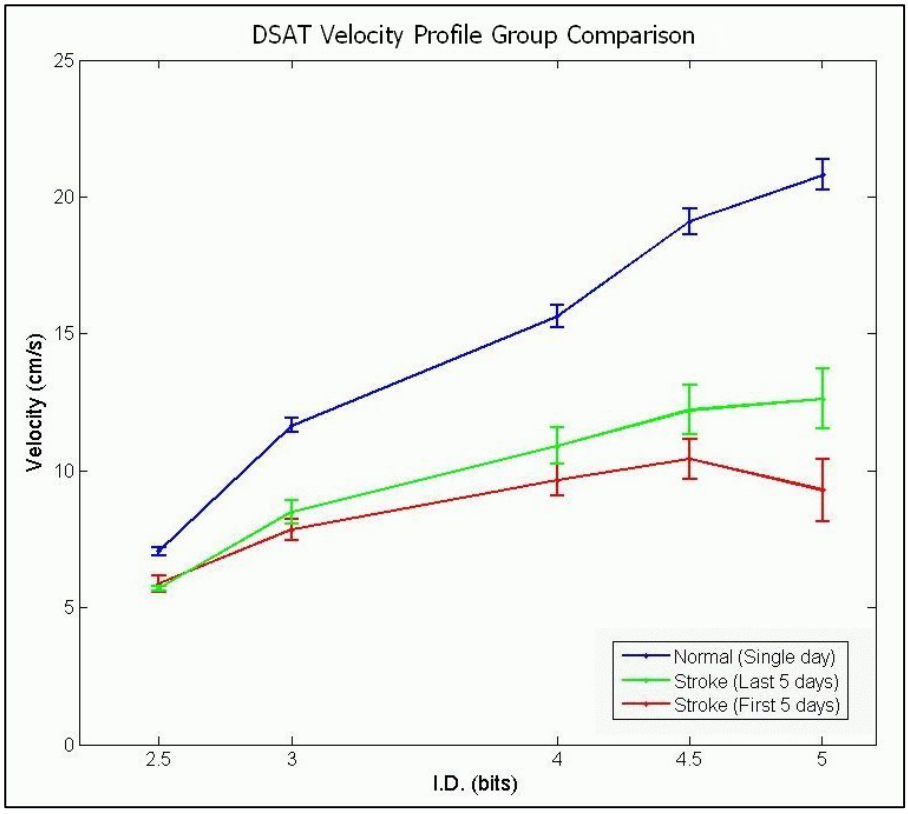

Figure 39. Velocity profile group comparison for DSAT. Note the similar performance trend (superiority in normals, compared to strokes, within stroke group day-wise improvement) seen in KSAT.

Figure 40 shows linear-regression fittings of DSAT velocity profile for the same comparison (within stroke group as well as between groups comparison). Note that the log-linearity is once again much greater in velocity analysis than MT/ID profiles which is clearly visible by fitting constants for each profiles.

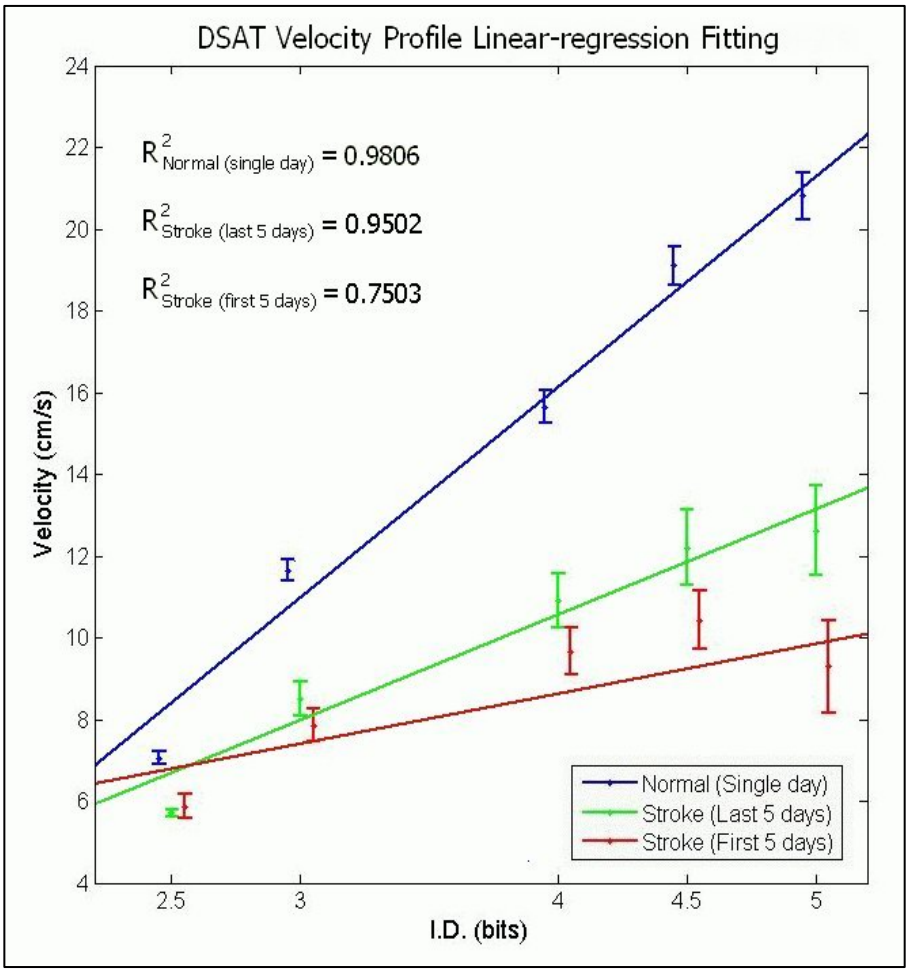

Figure 40. . Linear-regression fitting for DSAT velocity profile. Note the overall better fitting constants here in velocity of DSAT, a similar ovservation as seen in velocity analysis in KSAT

6.3.1.2 MT/ID ratio of stroke group in DSAT test

Similar to KSAT test, stroke subjects' performance in DSAT test over 6 weeks also exhibited noticeable comparative improvements in terms of average MT/ID scores $\left(= \frac{15\ \text{seconds}}{\#\ of\ hits}\right)$ shown in Table 18, calculated as day-wise ratio.

Table 19. DSAT MT/ID score improvements for stroke subjects over 6 weeks.

ID	2.5	3.0	4.0	4.5	5.0
days 1~5	0.74	1.02	1.33	1.78	3.88
days 7~11	0.67	0.96	1.14	1.32	1.57
days 1~5 / days 7~11	1.11	1.07	1.17	1.34	2.47
Averaged MT/ID ratio	**1.43 ± 0.59**				

6.3.1.3 Velocity ratio between first 5 days and last 5 days

Stroke subjects' velocity performance over 6 weeks in DSAT test also exhibited noticeable comparative improvements of velocity per ID $\left(=\frac{\text{Total travel distance per ID}}{15\ seconds}\right)$ shown in Table 20, calculated as day-wise ratio over all stroke subjects. Last 5 days over first 5 days velocity was calculated, showing a 28% improvement in terms of the speed of elbow movements for all ID levels.

Table 20. KSAT velocity improvements for stroke subjects over 6 weeks.

ID	2.5	3.0	4.0	4.5	5.0
$Velocity_{days\ 1\sim5}$	7.25	8.71	11.51	13.80	13.93
$Velocity_{days\ 7\sim11}$	9.27	11.19	14.65	17.51	17.81
$Velocity_{days\ 7\sim11}/Velocity_{days\ 1\sim5}$	1.28	1.28	1.28	1.27	1.28
Averaged Velocity ratio	**1.28 ± 0.01**				

6.4 Conclusion for dynamic SAT test

Grasping an object in a controlled manner without overshooting is one of the omnipresent and fundamental tasks required in activities in daily living (ADL). Yet, their dynamic characteristic of force control by the central nervous system is poorly understood. The present study showed dynamic characteristics of the human motor control system during targeted grasping task with visual feedback. Eight healthy subjects performed dual target task to produce specific force magnitudes in terms of various %MVC (percentile Maximum Voluntary Contraction) while cued by visual feedback from a computer display. A non-linear sensorized cylindrical gripper device was fabricated, consisting of a semi-isometric cylinder with an array of force sensing resistors (FSR) longitudinally aligned on the surface to detect the global force output of cylindrical handgrip, then linearized to represent direct cylindrical palmar force exerted by the finger joints. The required task was to perform a repeated targeting between the two targets in turn as fast as one can in a given time with the grip force. Two alternately posed targets represented high and low force levels each, with the distance between targets increasing by five steps (five different index of difficulties, or ID) in a timed manner. Data was analyzed in terms of measurement time (MT) with force variability, force accuracy and stability by hit scores. Linear-regression characteristics were calculated to show performance log-linearity represented as the fit line slope. Velocity profile was also calculated to show their movement speed changes according to the difficulty levels.

Results exhibited a proportional relationship between force variability and the force magnitude, a trend consistent with other literature (Newell & Carton, 1988). Results also showed a similar

logarithmic relationship between index of difficulty and measurement time (score) with good regression coefficient from normal subject groups (R^2 = 0.90), which agrees well with the well-known kinematic speed and accuracy test (kinematic SAT) described by Fitts' Law, indicating that the dynamic aspects of the Fitts' paradigm also follows log-linearity trend. Stroke subjects' linear regression coefficient for first 5 days was less adherent to linear-regression fitting (R^2 = 0.71), but their last 5 days result showed an even better log-linearity (R^2 = 0.9672) compared to normal's. Stroke group's first 5 days' result followed a cubic fit better with higher coefficient (R^2 = 0.9914) but not reported in the results. A quadratic fitting was also considered and calculated (R^2 = 0.9244), but discarded due to the fact that it is not a monotonically increasing function, which voids the integrity of Fitts' paradigm with speed vs. accuracy trade-offs. These two higher order fitting results was not reported in this research for it was not the main intention of this research to fit the outward behavior at high ID levels from stroke subjects into higher-order regression fittings.

In summary, dynamic force production and matching under visual feedback at the last end-effector level approximately followed Fitts' type behavior for both healthy and hemiparetic groups using the Gripper system. Also stroke subjects dynamic Fitts' type exercise result showed an improved performance by key metrics acquired by the Gripper system. Thus this experiment was successful in producing numerous quantifiable metrics which can be analyzed with ease to investigate the dynamic aspects of human motor control. Also this result can be used effectively in hand grip force control training platform in rehabilitation regime.

7. EXPERIMENT #3: GRIPPER-CUFF CORRELATION

Deciphering the neural code for grasp force is an important challenge for neuro-prosthetic technology (Craelius 2002). The goal of this experiment is to test the ability of high-resolution force myography (FMG) to decode, predict, or reproduce force of hand grasping (Duque, Masset et al. 1995).

7.1 Methods for Gripper-Cuff Correlation

7.1.1 Subject recruitment for Gripper-Cuff Correlation

Six healthy right-handed male adults (age 25.3 ± 4.7 yrs), within university volunteered for this study. Informed consent was gathered from all subjects before the experiment under the provision of Rutgers IRB (internal review board). There were no discomforts or complaints during or after the experiment from all subjects.

7.1.2 Protocols for Gripper-Cuff Correlation

Subjects donned the cuff at their forearm and having the gripper at the same time during the protocol to detect signals from first and second end effectors, the hand and the forearm, respectively. Three protocols were used as shown in Figure 41, to monitor the Cuff signal's reproducibility of the Gripper force signatures.

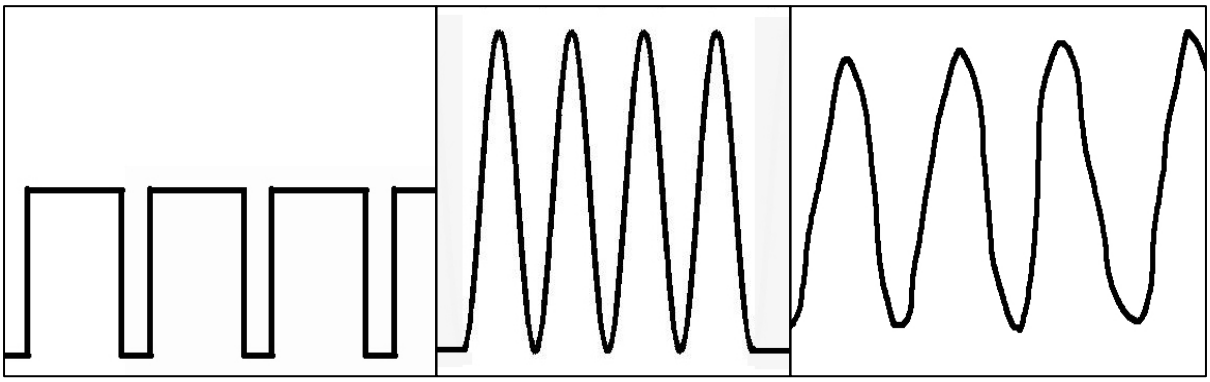

Figure 41. Schematic diagram of the Gripper-Cuff correlation experiment. From left to right; Square matching at mid-force level, sinusoidal matching (two paces), Self-paced sinusoidal force generation.

1. Square matching to test mid-level force stability: square waves at 50% MVC force levels were given to test static consistency and general target variability. Each square was 20 seconds long with 5 seconds of resting periods in between.

2. Sinusoidal wave matching to monitor a closed-loop dynamic control under visual-feedback: Sinusoidal waves of full %MVC force levels were given to see the subjects' dynamic ability to target

and match a moving object with their palmar force. Two sinusoidal target waves with different paces (slow and fast) were given as a visual feedback.

3. Self-select paced sinusoidal wave generation for the open-loop dynamic force generation: While the visual feedback is retracted, self-paced sinusoidal patterns were gathered for their full range of %MVC force levels from the subject to see the smoothness of autonomic force generation characteristics. Note that this protocol was not with the visual targets for this was purely to see the profile of force generation within open-loop motor actions.

7.1.3 Baseline Detection for Gripper-Cuff Correlation

Pre-protocol baseline detection was performed to both the Gripper and the Cuff to adequately represent each individual's unique %MVC ranges onto the force output display on the computer screen. For the Gripper baseline detection, subject was holding the Gripper in dominant hand with their wrist in neutral position, completely relaxed, with palmar force barely enough to hold the Gripper. Then subjects were asked to maximally grasp the Gripper with their full cylindrical grip force to detect their baseline maximum. Those two raw output values were used to scale the visual feedback tank display from 0 to 100 %MVC values.

Baseline detection for the Cuff was performed in the same manner. Absolute deviations from each detection site from the Cuff are squared and summed, then multiplied by a scaling factor β, with the baseline offset factor α, where N is the number of the detection sites, as following equation.

$$\text{FMG output} = \alpha + \beta \cdot \sqrt{\sum_{i=1}^{N} |\text{Pressure}_i(t)|^2} \qquad \text{Equation 8}$$

Using this rectified-summation filter, previous multi-to-one mapping from the Cuff to the Gripper becomes a simpler one-to-one mapping process.

7.2 Results for Gripper-Cuff Correlation

7.2.1 Qualitative correlations of Gripper-Cuff Correlation

Figures 42~44 are representing exemplar waveforms of the Cuff and the Gripper protocols running as square waves, sinusoidal waves, and self-paced sine waves. Ordinate axis represented a normalized arbitrary scaling, showing the Gripper wave (in blue) with as much as 0.5 offset compared to the Cuff wave (red) for display purpose. Important features to notice from these waveforms are the well matched conformality of the Cuff signal (red) mirroring the Gripper signal (blue) along the

waveforms by the features such as onset and offset of the force generations, temporal match of the peak amplitude points, or even the dips in the slopes. These features tell us that the force signal from the Cuff contains much synchronous physiological information comparable to the direct hand force output acquired from the Gripper. This is a very important finding which leads to a possible transfer function between the forearm and the hand, the 2nd last end effector and the last end effector along the neuromotor pathway of our upper limb.

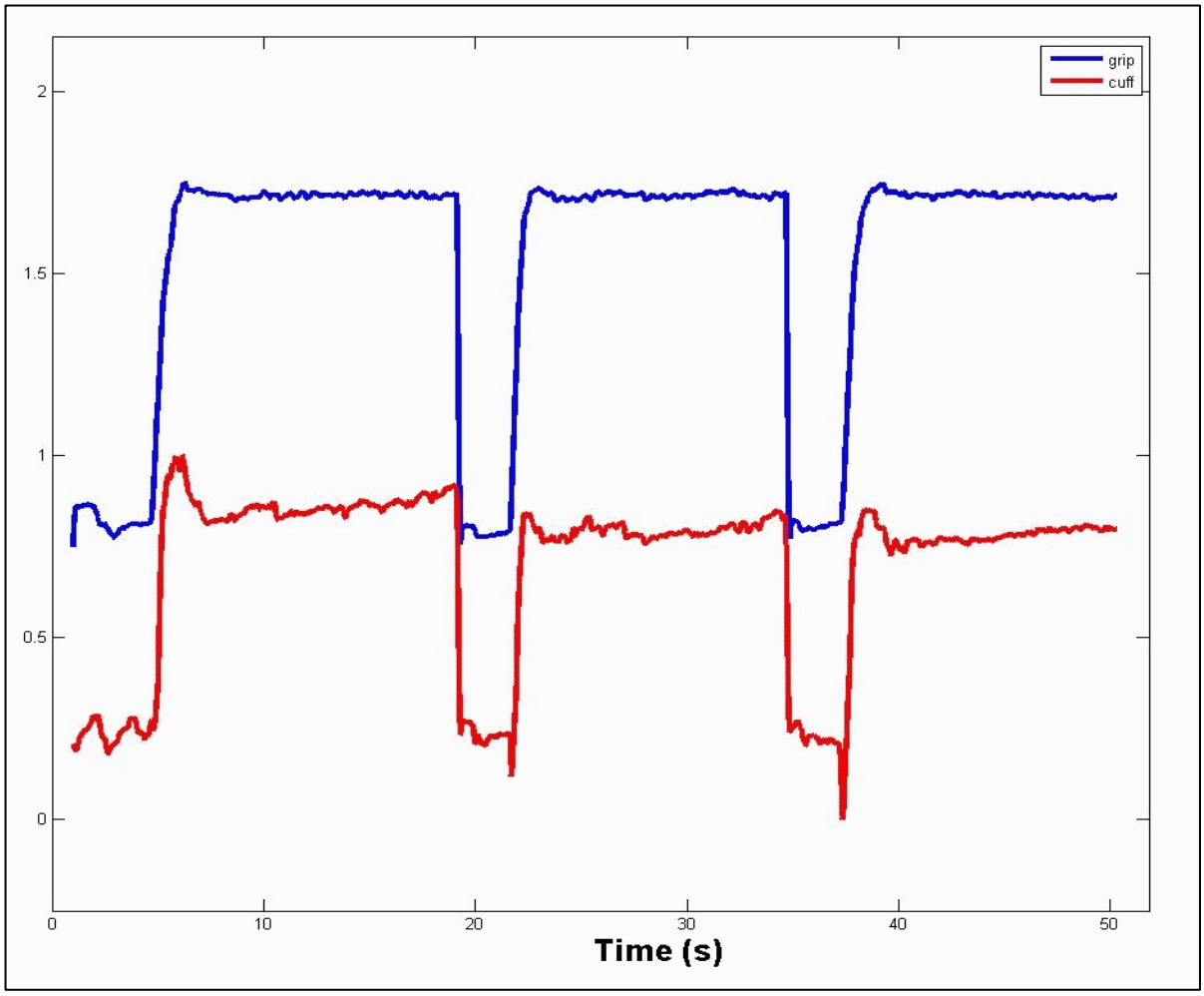

Figure 42. Example waveform from the step protocol showing the gripper output in blue followed by the cuff output in red). Each wave form is normalized then offsetted for display purpose.

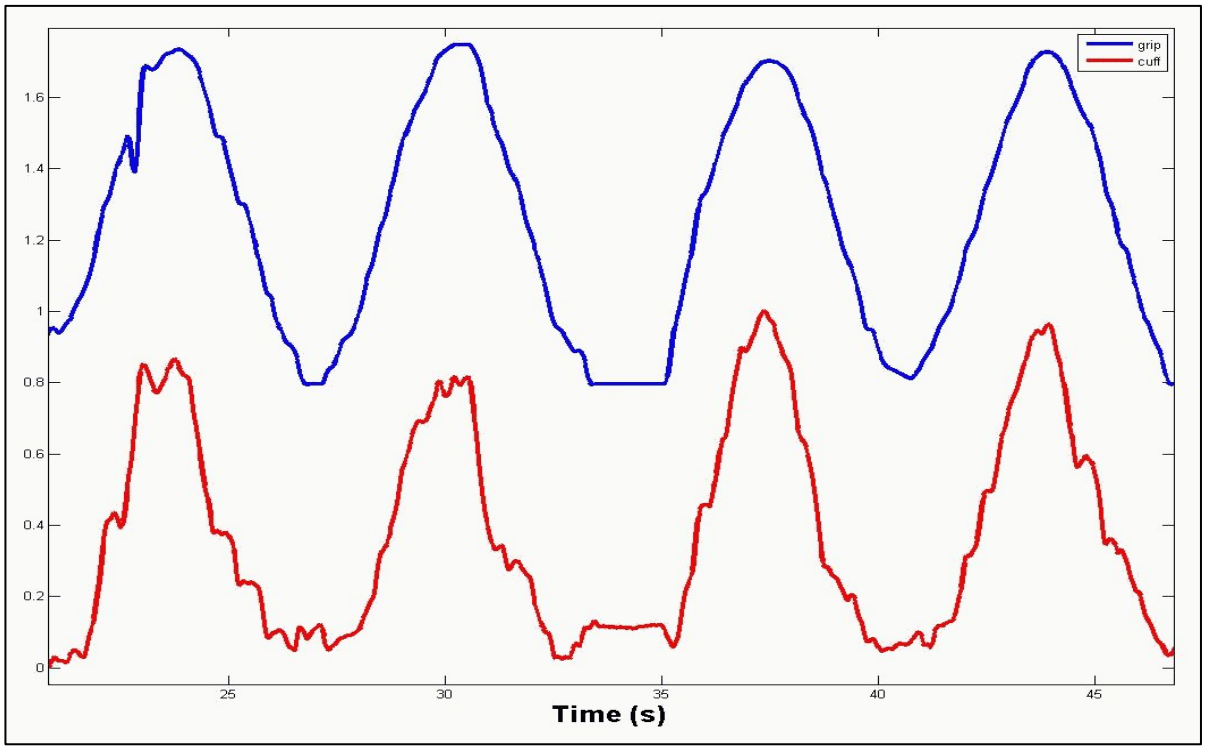

Figure 43. Example waveform from the sine-wave matching protocol (the gripper output in blue is well matched by the cuff signal in red). Each wave form is normalized then offsetted for display purpose.

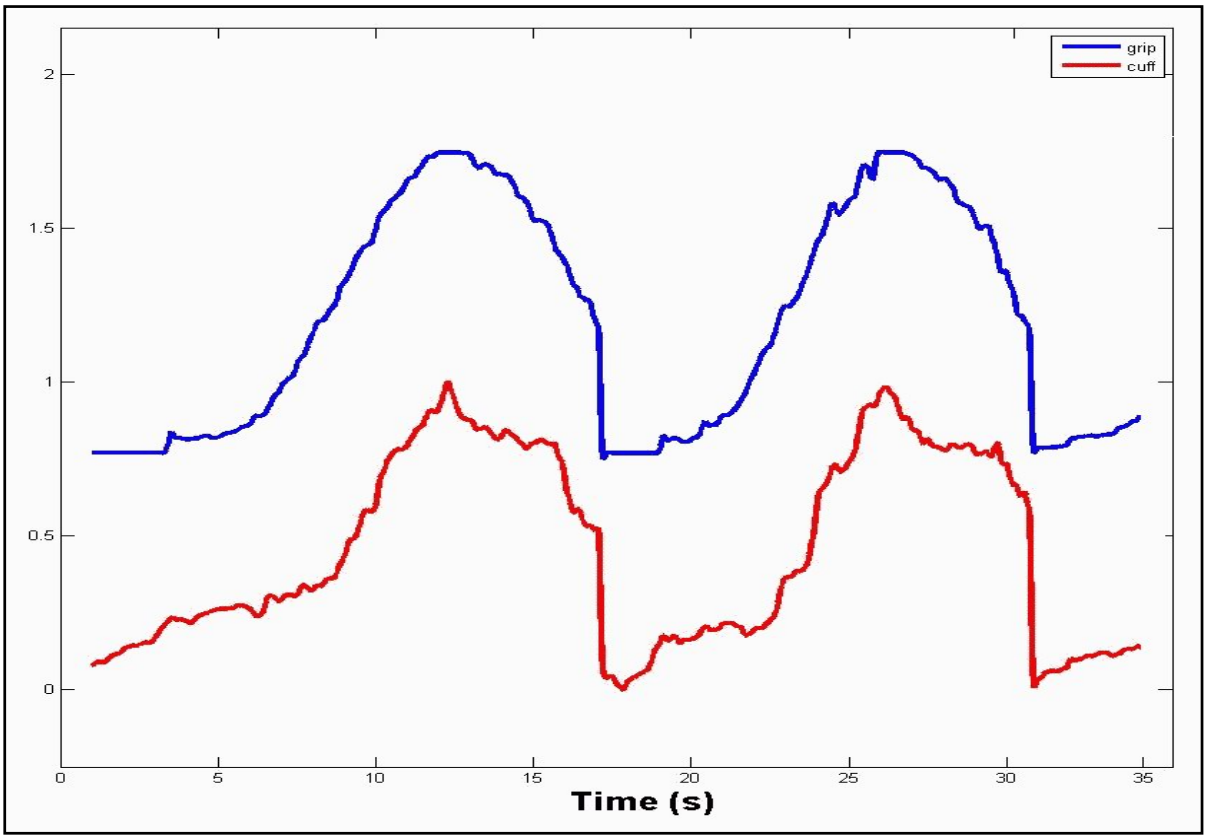

Figure 44. Example waveform from the self-paced sine generation protocol (the Cuff signal in blue shows larger variability in this protocol). Waveforms are normalized and offsetted for display purpose.

7.2.2 Linear Relationship of Gripper-Cuff Correlation

Although the Gripper and the Cuff are not designed to generate amplitudic matching signals, each mounting from each subject constitutes a unique linear relations with very high correlation coefficient, shown in the results. Notice the different intercepts from each lines which indicates the unique characteristics different from each test.

Temporal landmarks correlations of Gripper-Cuff Correlation: Those temporal matching landmarks are extracted and saved as a separate data matrix to calculate the temporal landmark correlation shown in Figure 45 for each subjects over three protocols. All subjects showed good correlation coefficients averaging R^2 value of 0.96 ± 0.05.

Point-to-point correlations of Gripper-Cuff Correlation: Another correlation process, the whole-wave point-to-point correlation was conducted as shown in Figure 46 with relatively agreeable correlation results per protocol with approximate average values ranging approximately from 0.8 to 0.9.

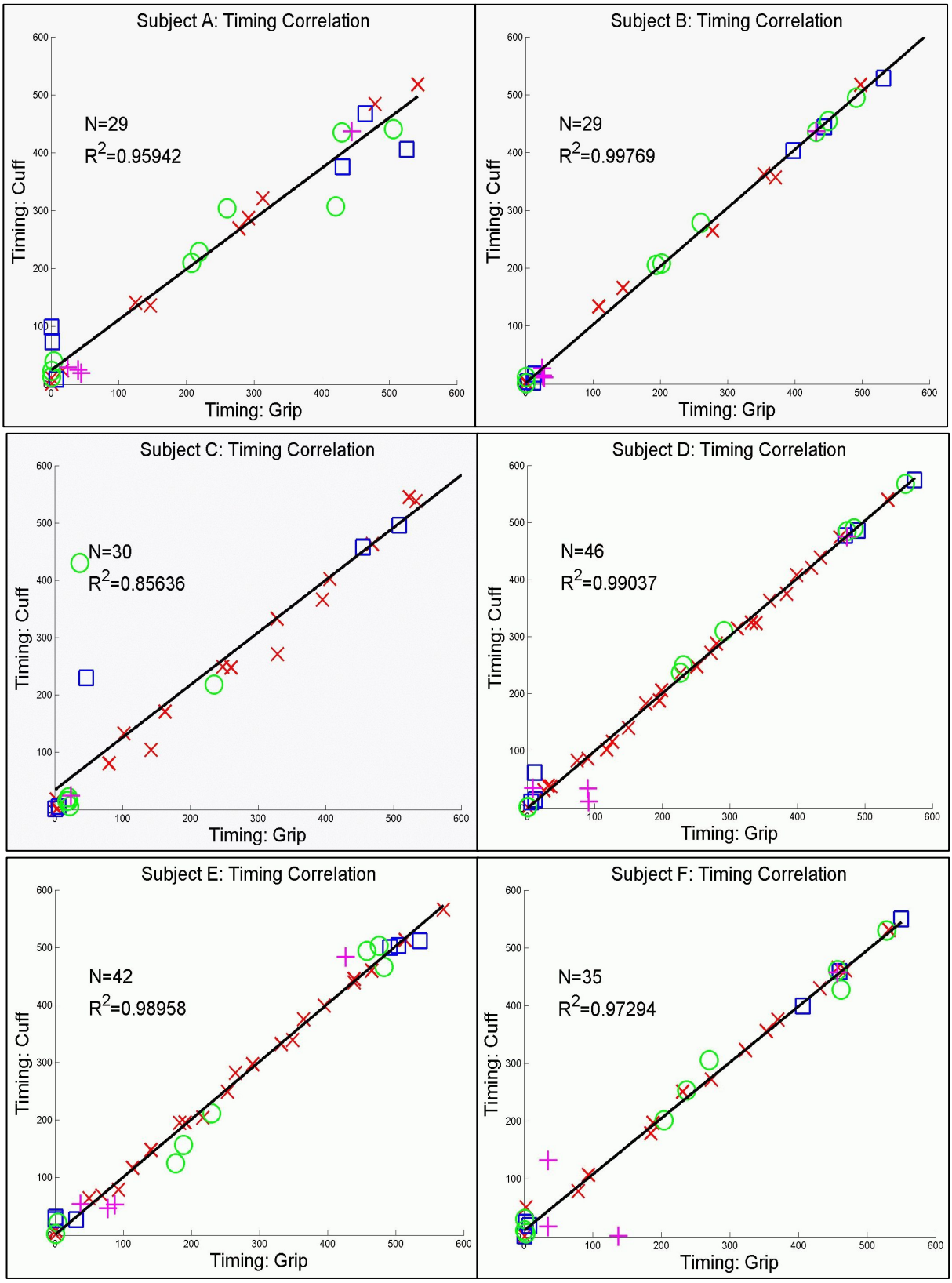

Figure 45. Temporal landmark correlation extracted from all three protocols, showing an averaged correlation value $R^2 = 0.96$. [+:protocol.1(square waves), ×:protocol.2 (slow sine waves), ○:protocol.2'(fast sine waves), □:protocol.3(self-paced sine waves)].

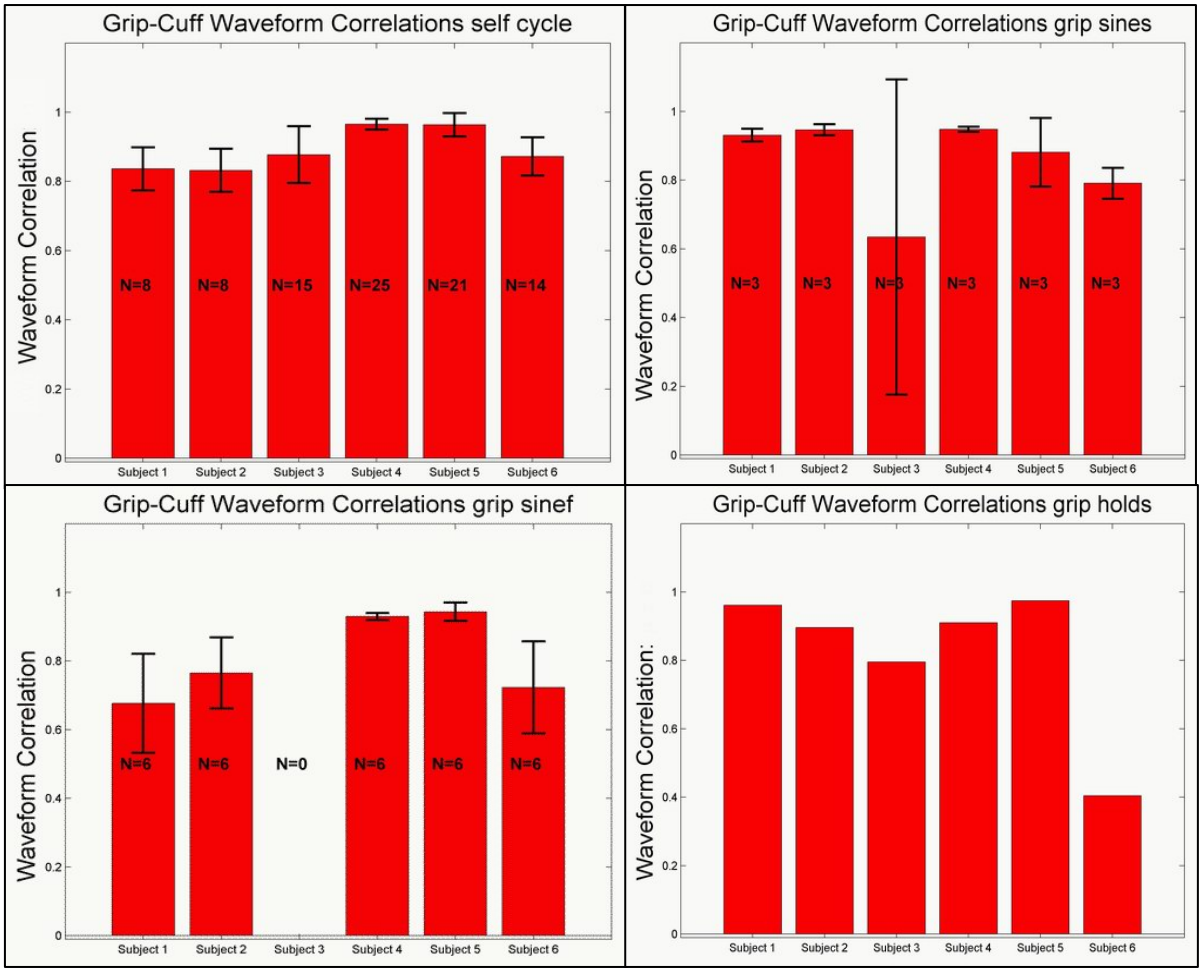

Figure 46. Whole-wave point-to-point correlation results, showing a moderate averaged approximate correlation values of $R^2 = 0.8 \sim 0.9$.

7.3 Conclusion for Gripper-Cuff Correlation

The FMG Cuff was able to mirror the approximate palmar force signal detected by the Gripper with high values of coefficients for both temporal landmarks and whole-wave correlations.

This study evaluated the correlation between these two body parts; the hand (first end-effector) and the forearm (second end-effector), using the Gripper and the force myography (FMG) forearm cuff to detect their muscle activation profiles. FMG of the forearm as a predictor of grip force signature was detected simultaneously with handgrip force signal during various cylindrical grip tasks. Five healthy subjects donned an FMG forearm sleeve device on their dominant side to measure their lower arm myokinetic signal profiles, while they were following protocols to a sensorized cylinder device in their hand as a direct measurement of their handgrip force.

The signal from the forearm sleeve FMG signal is correlated to the sensorized cylinder to see the predictability of FMG signal. Then, the transfer function between forearm muscle activity and direct grip force output from hand was established. Custom programmed protocol with various grip force levels were given to user by a computer display with specific targets to follow via user visual feedback.

Correlation and reproducibility of the hand force signature from extrinsic FMG signal at forearm was sought by comparing two signals from various force producing tasks. Results showed a good correlation between the hand and the forearm force signals, with many prominent temporal landmark features, appearing in synchronous fashion, which enables forearm FMG to be a good candidate to predict and reproduce the handgrip signatures.

Further study regarding the ability of the FMG to correlate and reproduce the direct hand grip would involve developing a transfer function from forearm signal as the input to the palmar grip force as the output in a single input to single output (SISO) manner. From a preliminary experiment using Simulink in Matlab, we expect it to be a second order, and robust enough in such a way that each mounting generates a unique transfer function, which can be acquired in an embedded baseline initialization from the LabVIEW program at the beginning of each run. Between-patient transfer function should be more diversely composed than within-patient variations due to the fact that between patient physiological morphology is much more different than mounting variations within single patient.

These findings can be beneficial to prosthetics design where the functional motor unit and the activation site is not in close proximity, or when the neuromuscular feedback are gathered from proximal body parts as well.

Real challenge lies in seeking the physiomotor theory to describe the differences of force signatures occurring at two motor end-effector sites adjacent to each other along the motor signal conduction pathway from proximal to distal direction while the negative visual feedback is present, acting as a real-time correction. Additionally, deciphering the neural code for grasp force is another important challenge for neuro-prosthetic technology (Craelius 2002). The goal of this type of protocol will be to test the ability of high-resolution force myography (FMG) to decode force of hand grasping (Duque, Masset et al. 1995).

8. DISCUSSIONS

Stroke is the one of the leading causes in the US responsible for long-term disability, and upper extremity rehabilitation regime lags behind lower limb counterparts. The new system developed and evaluated in this research represented by HARI and MAST as a multi-component upper extremity rehabilitation assistive device can be used to fill this void. Over the course of therapy using HARI system, our hemiparetic subjects showed noticeable improvements for elbow mobility and dynamic force control, from qualitatively by a preliminary experiments to the following KSAT and DSAT experiments which showed a agreeable changes in kinematic and dynamic metrics reported by previously quantified results.

Readers should be noted that this approach used in this research was neither to conduct a rigorous clinical study nor to devise a statistical motor theory but to evaluate and develop a better quantifiable upper-limb rehabilitation regime in the context of its systemic ability to interpret on the existing human motor theory which was a modified Fitts' law.

Although these results suggest an efficacy of the system and stroke subjects' functional gain, more in-depth dialogue is needed to identify the reason of these improvements to optimize HARI system further.

8.1 Discussion for Preliminary Experiment

In preliminary results, the efficacy of HARI as an upper limb rehabilitation tool has been evaluated by its ability to quantify human motor control data in wrist, elbow and grip force analysis, that HARI is broadly applicable to upper-limb rehabilitation training. Hemiparetic subjects were easily able to mount the sleeve themselves, and MAST was comfortable enough for all subjects without any complaints or discomforts reported. All subjects showed high interest levels in the visual feedback that they received in response to their finger motion volitions as well as improved range of motion.

8.1.1 Gripper Force Variability

Force variability was tested and showed a proportional relation between the force magnitude and the force variability which agrees well with previous literature. Force variability is defined as a standard deviation of force fluctuation noise (Newell and Carton 1988). A general pattern of force variability over various force levels using the Gripper is shown in Figure 47. It shows a proportionally increasing force variability over force levels, an intuitive phenomenon of human motor system, the

wider and further we move, the more error we get. Just as Fitt's law would say, the faster we move, the less accurate we become (Robertso, Mullinax et al. 1996).

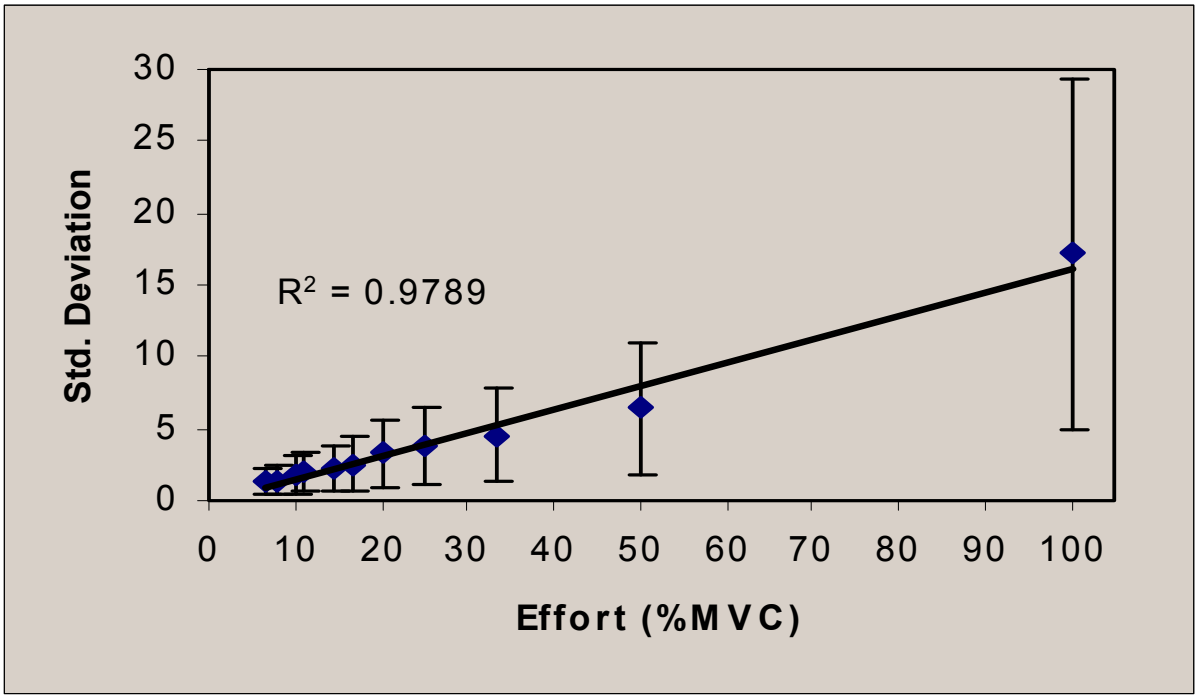

Figure 47. Force variability as standard deviation acquired by the Gripper over various %MVC.

8.2 Discussion for the KSAT Test

Active training of elbow motions for 6 weeks using Fitts' paradigm reported marked improvements from stroke subjects in selected metrics. Whether this result represents true functional improvement caused by a reverted disuse of the affected limb on the upper neuronal level or a task-specific adaptation due to a simple muscle memory at the lower end-effector level cannot be determined in this research. However, the magnitude and the pace of improvement monitored over 6 weeks suggest that adapted Fitts' paradigm implemented in the MAST system is highly productive and encouraging for stroke rehabilitation.

The most important findings from this research came from the performance comparison. The HARI system was successful in producing log-linearity trends of the Fitts' paradigm from both normal and stroke groups. Moreover, stroke group's performance metric showed almost two-fold improvement in linear-regression slope constant along with noticeable improvements in MT score and velocity profiles with decreased variability represented in standard errors. This result told us that even under hemiparetic condition, human motor system can adjust end-effector stiffness to match along the changes of difficulty levels given as a visual feedback in such a way that our neuromuscular

system acts as a suitable low-pass filter to achieve the required goal in minimum possible time within allowable error level.

Although this may suggest actual functional reversal caused by actual reverted disuse of their affected arm and improved plasticity of their motor cortex, it also can be just a simple muscle memory due to task-specific manipulative adaptation. Further study with imaging modalities which can tap into brain activities during reaching and targeting activities such as PET scan, fMRI or fNIRS might answer these questions. For example, Winstein's group conducted a research in 1997 on the monitoring of the brain activity during Fitts' type movements (Winstein, Grafton et al. 1997). They found that the responsible brain area under varying task difficulty are different, a well known characteristics shifts of motor cortex area change patterns. This event-related brain scan results reveal a much better understandings for the functional characteristics of our motor control system. Yet a more comprehensive investigation with a different approach is needed to identify the reason for the improvements regarding the suggested question above.

8.2.1 Corrected MT plot using effective variables (W_e, A_e, ID_e)

Those adjusted target protocol variables (W_e, A_e, ID_e) introduced in the early chapters can be used to describe deviations of MT score plots from perfect linear regression fit lines in SAT test results from stroke subjects if following behavior is visible. At $ID_{2.5}$ as a starting extremity of the whole protocol, subject tends to just barely pass the edges of the targets, resulting in two hit scatter clouds closer than full distance D. Also, MT score deviation at $ID_{5.0}$ (another end of extremity) from same subjects can be explained in a same manner where the subject can reproduce their positions easier when it is closer to two end-reference positions; full-flexion and full extension where the subject can guess where to stop and turn back with relatively more easiness (Soukoreff and MacKenzie 2004).

8.2.2 Exception of Fitts law

8.2.2.1 A rapid-timing task: reversal timing variability

It appears that more accuracy (less variability) with increased speed is possible. In rapid-timing task by ballistic impulsive movements, timing variability actually decreased with increased speed. With fixed time, increasing the target distance made the tester to move faster, resulting a more coherent (less) timing variability, which is in contradiction that movement with slower speed would make more precise target hits (Wright, 1983). Some might argue that it is due to the interchangeable nomenclature regarding 'variability'. There are two types of variability, spatial and temporal. When spatial variability is constrained, some researchers report an increased temporal error (less temporal

variability) for higher IDs, or vice versa. However, it is interesting finding that human motor system changes it's modes of actions to achieve given tasks differently under specific conditions.

8.2.2.2 Role of the placeholders for targets:

Another group reported a violation of the Fitts' law in a structured, linear display of targets with placeholders indicating the possible target locations. Their result showed that the MT to the most distant targets is not longer than MT right before for the second most distant targets, but tends to be shorter. They also observed the role of the placeholders which seems to be attenuating the range effect, and suggested that the visual control mechanism of our hand movements may use allocentric cues, in addition to egocentric, spatial information, in that Fitts' law may only be able to describe egocentric visuomotor movements only (Adam, Mol et al. 2006).

8.2.2.3 Increased consistency from movements with larger amplitude

From normal subjects' MT score result in kinematic SAT, we observed no-trended MT errors from the standard error bars over 5 levels of ID (Figure 29), which seems to be inconsistent with general idea of Fitts' Law. While in dynamic SAT, this inconsistency was not present.

It can be explained in two aspects. First, as target distance increases as ID goes to extremity ($ID_{2.5}$ or ID_5) in kinematic SAT, subject's arm will be closer to full extension or full flexion where it is easier to reproduce as these positions can be achieved with fully differentiated activations of biceps (for full flexion) or triceps (for full extension) with minimal co-contractions between these two muscle groups.

Secondly, as ID goes to its extremity, subjects' motion becomes more and more dramatic as the range of motion gests closer to its full amplitude, which might be altered their modes of reaching from moderate around lover ID to maximal speed around higher ID. In late 1960s, Schmidt reported his findings of this effect, that M.T., absolute error in timing, and other variables becomes more consistent as the subject was instructed to focus more on reaching 'speed', presented in Table 21 as below (Schmidt 1967; Schmidt 1969; Schmidt 1969). The Table shows that variable error acquired from within subject standard deviation of the M.T.s was approximately 44% smaller when subject was specifically instructed to move 'faster' than normal trials. This temporal stability improvement was considered as an example of 'increased effector anticipation' due to the performer's prediction ability in targeting accuracy was experiencing an advantage from rapid movements.

Table 21. Movement Time and other variables as a function of movement distance and swing speed (adapted from Schmidt, 1967, 1969)

	Movement Instructions					
Movement Distance (cm)	Maximal			Moderate		
	MT	Absolute Error	Variable Error of MT	MT	Absolute Error	Variable Error of MT
15	76	20	3	139	24	9
30	123	23	7	209	27	13
45	144	25	7	253	30	12
60	206	28	9	274	41	13
Averages	137	24.0	6.5	219	30.5	11.7

Followed by Schmidt, this second point of view was looked into by other researchers such as Newell, Hoshizaki, Carlton, and Halbert in 1979 shown in the Table 22 below (Newell, Hoshizaki et al. 1979).

Note the decreased VE_t as M.T. also decreases (as velocity increase) from 125.7 to 10.8 milliseconds at 5 cm distance, and from 91.2 to 9.0 milliseconds at 15 cm distance (in bold).

Table 22. Timing errors as a function of M.T. and movement distance.

M.T. (msec)	1000		500		100	
Distance (cm)	5	15	5	15	5	15
Velocity	5	15	10	30	50	150
VEt (msec)	125.7	91.2	74.6	42.8	10.8	9.0
VE/MT (%)	12.6	9.1	14.9	8.6	10.8	9.0

Another interesting investigation about standard deviation was done by Meyer and Rosenbaum, that the standard deviation (S) of any movement's end point are related with the target distance (D) and movement duration (T) with an empirically determined constant k, as following equation (Meyer, Smith et al. 1988; Rosenbaum 1991).

$$S = k\frac{D}{T} \qquad \text{Equation 9}$$

According to this explanation, a rapid (short duration, T_{short}) movement along a long distance (D_{large}) would result a poor consistency (S_{large}), while sufficiently short distance targeting with ample time would be much more accurate.

Obviously, this equation holds for many occasions in motor actions, but no single theory alone cannot explain everything on the monitored increased consistency from larger movement from our results, because more variables should be considered in this research. For example, k should not be a constant from our protocol but an independent variable in finding relationship between standard deviation and target dimension variations, such as, average/peak velocity or acceleration which is not

necessarily referable from D or T. Figure 35~38 shows velocity profiles from normal and stroke subjects' kinematic SAT data. As expected, higher ID targeting yielded a faster movement due to larger target distance.

Note the improved velocity scores from 3 stroke subjects (blue, navy, teal) out of total 4 in Figure 39 and Figure 40. One stroke subject's (red) velocity profile showed a mixed characteristics; same velocity values in $ID_{4.0}$ and $ID_{4.5}$, and somewhat lower velocity values in $ID_{2.5}$, $ID_{4.5}$ and $ID_{5.0}$.

A comparison of velocity profile between normal and stroke subjects' total averages (Figure 36 and 38) is redrawn in Figure 41. Normal subjects' movement was clearly faster for all IDs with higher constancy.

This 2nd derivative information shows well-established physiological phenomenon we see every day; subjects tend to move faster in higher ID regions with longer movement distances.

The widely spread standard deviation represented as error bars from those plots can be explained by the fact that this research utilized a unique visual feedback environment using a virtual instrument in LabVIEW, which offers an indirect interaction without the user physically contacting the screen with the target, but rather the cursor data are inferred from users elbow to display and move the marker on the computer screen. This might have required an additional anticipation or visual delay of the closed-loop targeting during the process of brain-motor control via visual feedback loop. In this regard, some researchers offer a few relevant remarks on virtual target expansion analysis; McGuffin reported that only properly standardized and inferred user performance data outside virtual environment is valid for the *ad-hoc* comparison and analysis because the user is under the additional challenge to predict the trajectory of the cursor through the means of computer (McGuffin 2002). Moreover, it is a general agreement that an accurate cursor prediction is very difficult to achieve in the virtual environment (Zhai, Sue et al. 2002). Note that this research was intrinsically under virtual environment in the form of visual feedback given to all of the users, which would justify the amount of errors being exhibited.

8.2.3 Beyond Fitts' law

Speed vs. accuracy trade-offs in a reaching and targeting movements have been studied for more than a century. Currently, a mutual agreement among researchers exist that Fitts' law would hold for any mobile body parts with which a suitable motor task can be performed (Glencorss and Barrett 1989). Fitts' law is indeed a robust and versatile descriptor which explains the empirical law we abide by when we perform a reaching and targeting movements, with the various aspects of speed vs. accuracy trade-offs.

Seeking for a kinematic, physiological theory: Different human motor control researchers have suggested many variations of Fitts' law, mainly by changing the modes constraint variables, for example, spatially constraining the movement amplitude or target conformations, or temporally constraining the movement time. As a result, few models were tried with kinematic and psychomotor theory to describe beyond Fitts law's empirical success. Plamondon and Alimi's review paper in 1997 displays a number of physiological models to describe the theory behind Fitts' type behaviour (Plamondon and Alimi 1997). Those numerous variations of the Fitts' type equations introduced from their review have their own different models with unique biological parameters selected and constrained for their specific experimental setups, but each individual research seems to describe only a sufficiently smaller part of the whole picture, in that there is no final consensus regarding to a single motor theory on oscillative targeting motion. This long paper concludes at the end that we should explore more in more detail to define some heuristic and experimental conditions to include more global view.

Multi-dimensional Fitts' law: This research applied the Fitts' law into kinematic and dynamic aspects of one-dimensional reaching and targeting setup. But it can be easily expanded to two or three dimensional environments with proper experimental design. For example, MacKenzie and Buxton in 1992 conducted an extended version of Fitts' law into two-dimensional protocol with the introduction of target width and height at the same time and showed in their model that the interpretation of target width and the accompanying formulation for index of difficulty play a critical role in the accuracy of the model (MacKenzie and Buxton 1992). Even though they were using this expansion of Fitts' law to correct their model, it shows the generalization of Fitts' law into possibly wider applications in human motor control research.

8.3 Discussion for the DSAT Test and the Comparison between KSAT and DSAT Tests

DSAT test using the Gripper showed a very high linear regression fit coefficient ($R^2_{\text{normal, DSAT}} \approx 0.95$), indicating a similar or closer logarithmic linearity trend in DSAT compared to KSAT's ($R^2_{\text{normal, KSAT}} \approx 0.90$), thus hypothesis 2 is tested and proven correct. All results agreed well with previous literatures, which suffice us to say that the HARI system with the MAST and the Gripper is a reliable human motor experiment system for kinematic and dynamic motor movement analysis. Further, the nature of speed vs. accuracy trade-off in terms of its theoretical meaning would be an interesting study relevant to this research.

8.3.1 Speed vs. accuracy trade-off as an anti-synergetic behavior

Two conceptual variables, speed and accuracy were compared and found to be showing trade-off characteristics. However, in view of those currently prospering modern trends in theoretical motor control research which deals with the concept of synergy or anti-synergy (Bernstein, 1967), mainly under the within end-effector steady-state force production protocols, which often yields force sharing and enslaving, or asymptotic force controller manifolds (Goodman and Latash 2006), these two concepts of speed vs. accuracy trade-offs can be viewed along with the similar line of scientific insights, that they are an equivalent of anti-synergies or reciprocative behaviors. (Shim, Latash et al. 2005)

Further, these lines of comparative motor researches might be actually dealing with a wider categorical comparison, that speed and accuracy might be a representative metric which comes from a two reciprocal categories of conceptual variables of motor functional metrics between which a more global anti-synergy would form. For example, if we were to add one more independent metric of functional importance, such as smoothness, what kind of synergies or anti-synergies would be formed among those three concepts; speed vs. accuracy vs. smoothness? What if we add one more concepts, such as effort level? (Rosenbaum and Grebory 2002)

The field of theoretical motor control analysis is very deep and sometimes difficult to draw any succinct and well-descriptive conclusion that would precisely depict all the phenomena that we see from a human body. This new field of motor control research will be more accepted and valued widely and possibly yield tangible contributions in the industry and clinical applications in the near future.

8.4 Discussion on the Gripper-Cuff Correlation

It was rather a surprising result that the extrinsic force signature from the Cuff was following the end-effector very well as shown in the temporal landmarks correlation as well as the whole-wave point-to-point correlation. It might be due to the fact that the Cuff's square-summation filter doesn't recognize or distinguish between the co-activation and reciprocal-activation resultant from forearm agonist and antagonist muscle groups. Or it might be because of the evident motor equivalency (Flash and Hogan 1985) which runs through all of the effectors along the neuromuscular pathway. Or it's because of the stationary-state protocol (in spectral domain) to which the CNS favors in producing synergetic actions (Goodman, Shim et al. 2005)

Much can be debated for the ability of the Cuff's good correlation and reproducibility to the last end-effector signal as we already know that the specific brain area is different for low-force precision gripping and high-force power gripping (Winstein, Grafton et al. 1997). But the reason for the FMG be able to mirror the end-effector force signature very well should be thought by seeking the nature of the FMG itself.

Nature of the FMG: Investigating the nature of the FMG would be another interesting aspect of future research; does it detect force or pressure? What is the reason for the volumetric signal being able to be translated to the force generated by the forearm? Considering the fact that the FMG detects the radial volumetric changes exerted as a radial force onto the sensing area inside of the cuff at the mounted site, the force itself should be contemplated over more thoroughly.

The term 'force' has a word sense disambiguation (multiple meanings). It can be used as the general term in physics that force, influence that causes mass to accelerate, such as gravity, friction, or a push. Force is defined by Newton's Second Law as $F = m \cdot a$. This concept of dealing the term force with every possible point of view is not a meaningless trial but can be a fundamentally important attempt when it comes to physiological phenomenon. In physics, only four fundamental forces of nature are defined: strong, electromagnetic, weak and gravitational (in order of decreasing strength). Then where does the physiological force being detected by the FMG Cuff or the Gripper falls into those four categories? Considering the fact that a muscular effort in terms of force is being generated by thousands of sacomeres (z-bands) of the muscle bundles, as a result of action-reaction between myosin and actins, the muscle itself can be viewed as a transducer within our body which transforms electro-chemical energy into a mechanical force. Current methodology implemented in the FMG cannot detect this molecular level of muscular contractions, but only able to detect the resultant volumetric changes exerted radially onto the sensors. Yet, it is capable to detect the final effects of the muscular contractions triggered by the neuromuscular signal originated from the brain with the best possible way.

The motor signal pathway from brain to the distal end effector involves multiple stages of neuromuscular signal conductions and transmissions from proximal predecessors to distal motor units, often with visual and textile feedback. Under a certain motor task such as generating a specific amount of grip force, the person is always under direct control of their last end-effector, their hand. However, considering the top-down motor signal pathway, the neuromuscular signal gathered from second end-effectors or above might contain some important information to predict the signal from the first end effector force signature will be beneficial for designing a robotic prosthesis for amputees.

Additionally, a further research which sees the brain activity levels such as fMRI or PET on different grip-type can reveal a more information on the brain area differentials during targeted gripping tasks over various force levels. As previous literatures on finger digit muscle synergy on the lower force level precision gripping task suggests (Shim and Park 2007), it might show a synergetic behavior at the low force level, followed by possible phase changes (shifts in the modes of force generation) as the task goes more difficult toward higher force levels with an anti-synergetic behavior between forearm agonist and antagonist muscle groups. These kinds of direct comparison between the agonist and the antagonist activations over various force levels using EMG can identify the fundamental utility of the FMG as an alternative or supportive modality with many possibilities in the field of human motor research.

8.5 Discussion on future works

Human motor system is inherently noisy as any other dynamic systems that an infinite amount of uncontrolled variability always exists. It is also known that humans are not capable of producing a perfectly stable force at any force levels, but only be able to produce the end-point targeting movements as the outcome of a noisy control signal filtered after the noise-reducing properties of the biomechanical system (Van Galen and De Jong 1995). The quest to find out the source of this ubiquitous and possibly beneficial neuromotor errors in terms of noise is a deep question to which no single motor theory can clearly answer the whole aspects of human motor control. But all of these heuristic endeavors are not only necessary but also represents the richness of the field and should be continued further.

As an alternative to EMG, MKI using FMG implemented in HARI system offers a non-electrical contact method, which measures residual muscle activity and decodes volitional motions using a simple filtering process that can be readily trained as needed. This modality relaxes the requirement of precise sensor placement, which is an important practical consideration for those who must don and doff their assistive devices daily, where the device placement variation is large and also for experimental setups where the action being detected is more vulnerable to subject motion.

MKI recordings of muscle activity during training provided information comparable to that of EMG regarding pathology and progress. HARI thus serves as a simple interface to a computer that can be used by hemiparetic clients to exploit residual their functionality with achievable tasks.

Future work in upper limb rehabilitation system development would be dealing more proximal body parts as well towards shoulder with upper-arm control to complete the vista of the upper extremity as well as more specific experimentation on individual fingers controls in the distal end.

The MKI is an ideal candidate for hemiparetic subjects to train fine finger controls because even small motions were able to be influence a noticeable changes through the biofeedback interface. The value of myokinetic feedback using FMG has been successfully established in this research, and should be investigated further.

Commercialization of HARI: Even though HARI system still has rooms for improvements, it is safe to say that the system can be commercialized after a minimal streamlining and touch-up processes to hit the market in the near future. This research investigated those early generation prototypes of HARI as well as the most recent version of HARI. Preliminary projection for the cost of the system gives us an approximate production cost comparable to a mid to high end personal computer system. However, this cost does not include the accompanying base software for debugging but only reflects tangible devices and executable programs to run the system on the pc. Nevertheless, the system is expected to significantly cover the current niche rehabilitation market which lacks an affordable home rehabilitation systems targeted for the upper body functionality retraining.

9. REFERENCES

Adam, J. J., R. Mol, et al. (2006). "Moving Farther but faster: An Exception to Fitts' Law." Psychological Science **17**(9): 794-798.

Agnes., R.-B., J. S., et al. (2003). "Hand orientation for grasping and arm joint rotations in healthy subjects and hemi-paretic stroke patients." Brain Research **969**(1): 217-229(13).

Balakrishnan, R. (2004). "Beating Fitts' law: Virtual Enhancements for Pointing Facilitation." Int. J. Human-Comnputer Studies **61**: 857-874.

Bernstein, A. (1967). The Coordination and Regulation of Movements. *Oxford Pergamon* , 77-92.

Craelius, W. (2002). "The bionic man: restoring mobility." Science **295**(5557): 1018-21.

Crossman, E. R. F. W. (1960). "The information-capacity of the human motor-system in pursuit tracking." Quarterly Journal of Experimental Psychology **12**: 1-16.

Curcie, D. J., J.A. Flint, and W. Craelius (2001). "Biomimetic finger control by filtering of distributed forelimb pressures." IEEE Trans Neural Syst Rehabil Eng **9**(1): 69-75.

Duarte, M. and S. Freitas (2005). "Speed-accuracy trade-off in voluntary postural movements." Motor Control **9**(2): 180-196.

Duque, J., D. Masset, et al. (1995). "Evaluation of handgrip force from EMG measurements." Appl. Ergon. **26**: 61-66.

Fitts, P. M. (1954). "The information capacity of the human motor system in controlling the amplitude of movement." Journal of Experimental Psychology **47**: 381-391.

Fitts, P. M. and P. M.I. (1967). "Human performance."

Fitts, P. M. and J. R. Peterson (1964). "Information capacity of discrete motor responses." Journal of Experimental Psychology **67**(2): 103-112.

Fitts, P. M. and B. K. Radford (1966). "Information capacity of discrete motor response under different cognitive sets." Journal of Experimental Psyology **71**(4): 475-482.

Flash, T. and K. N. Hogan (1985). "The coordinate of arm movements: An experimentally confirmed mathematical model." Journal of Neuroscience **5**(2): 1688-1703.

Flint, J., S. Phillips, et al. (2003). "Myo-Kinetic Interface For A Virtual Limb." 2nd International Workshop on Virtual Rehabilitation **2**: 113-118.

Flint JA , S. L. P. S. a. C. W. (2003). "Myo-Kinetic Interface For A Virtual Limb." 2nd International Workshop on Virtual Rehabilitation.

Flint, J. A. (2004, May). A Myokinetic Interface for Identification of Residual Limb Funciton. *Doctoral Dissertation*

Gibbons, J. D. (1985). "Nonparametric Statistical inferences." M. Dekker **2nd ed.**

Glencorss, D. J. and N. C. Barrett (1989). "Discrete movements." In D. Holding (Ed.) Human Skills.

Goodman, S. R. and M. L. Latash (2006). "Feed-forward control of a redundant motor system." Biological Cybernetics **95**(3): 271-280.

Goodman, S. R., J. K. Shim, et al. (2005). "Motor variability within a multi-effector system: exprimental and analytical studies of multi-finger production of quick force pulses." Exp brain Res **163**: 75-85.

Gouiard, Y., & Lafon, M. B. (2004). Fitts' law 50 years later: applications and contributions from human–computer interaction. *International Journal of Human-Computer Studies , 61* (6), 747-750.

Gowland, C., P. Stratford, et al. (1993). "Measuring physical impairment and disability with the Chedoke-McMaster Stroke Assessment." Stroke **24**(1): 58-63.

Kuttiva, M., Flint J, Burdea, G, Craelius, W (2003). "VIA: A virtual interface for the arm of upper-limb amputees." 2nd International Workshop on Virtual Rehabilitation: IWVR **2**: 119-126.

Kuttuva, M., G. Burdea, et al. (2005). "Manipulation Practice for Upper-limb Amputees Using Virtual Reality." Presence **14**(2): 175-182.

Langolf, G. D., Chaffin, D. B., & Foulke, J. A. (1976). An investigation of Fitts' law using a wide range of movement amplitudes. *Journal of Motor Behaviour* , 113-128.

MacKenzie, I. S. (1992). "Movement Time Prediction in Human-computer Interfaces." Proceedings of Graphics Interface: 140-150.

MacKenzie, I. S. and W. Buxton (1992). "Extending Fitts' law to two-dimensional tasks." Proceedings of the ACM Conference on Human Factors in Computing Systems **CHI 92**: 219-226.

McCall, R. B. (1975). "Fundamental Statistics For Pshchology." **2nd ed.**

McGuffin, M. (2002). "Fitts' law and expanding targets: an experimental study and applications to user interface design." Department of Computer Science, University of Toronto.

Meyer, D. E., J. E. Smith, et al. (1988). "Optimality in human motor performance: ideal control of rapid aimed movements." Psychological Review **95**: 340-370.

Newell, K. M., L. E. F. Hoshizaki, et al. (1979). "Movement time and velocity as determinants of movement timing accuracy." Journal of Motor Behavior **11**: 49-58.

Newell, K. M., & Carton, L. G. (1988). Force variability in isometric responses. *Journal of Experimental Psychology: Human Perception and Performance , 14* (1), 37-44.

Plamondon, R. and A. M. Alimi (1997). "Speed/accuracy trade-offs in target-directed movements." Behavioral and brain sciences **20**(2): 279-349.

Robertso, L. D., C. M. Mullinax, et al. (1996). "Muscular fatigue patterning in power grip assessment." Journal of Occupational Rehabilitation **6**(1): 71-85.

Rosenbaum, D. (1991). "Human Motor Control." Academic Press, San Diego, CA.

Rosenbaum, D. A. and R. W. Grebory (2002). "Development of a method for measuring movements-related effort." Exp Brain Res **142**: 365-373.

Schmidt, R. A. (1967). "Motor factors in coincident timing." University of Illinois.

Schmidt, R. A. (1969). "Consistency of response components as a function of selected motor variables." Research Quarterly **40**: 561-566.

Schmidt, R. A. (1969). "Movement time as a determiner of timing accuracy." Journal of Experimental Phychology **79**: 43-47.

Shannon, C. E. and W. Weaver (1949). "The Mathematical Theory of Communication." Univ of Illinois Press, Urbana, Illinois.

Shim, J. K., M. L. Latash, et al. (2005). "Prehension Synergies: Trial-to-trial Variability and Principle of Superposition During Static Prehension in Three Dimensions." J Neurophysiol **93**: 3649-3658.

Shim, J. K. and J. Park (2007). "Prehension synergies: principle of superposition and hierarchical

organization in circular object prehension." Exp Brain Res **In press**.

Soukoreff, W. R. and S. I. MacKenzie (2004). "Towards a standard for pointing device evaluation, perspectives on 27 years of Fitts' law research in HCI (Human-Computer Interface)." Int. J. Human-Comnputer Studies **61**(6): 751-789.

Van Galen, G. P. and W. P. De Jong (1995). "Fitts' law as the outcome of a dynamic noise filtering model of motor control." Human Movement Science **14**: 539-571.

Winstein, C., S. Grafton, et al. (1997). "Motor task difficulty and brain activity: investigation of goal-directed reciprocal aiming using positron emission tomography." J Neurophysiol **77**(3): 1581-1594.

Wright, C. &. (1983). Sources of the linear speed-accuracy tradeoff in aimed limb movements. *Quaterly Journal of Experimental Psychology* , 35A:279-296.

Zhai, S., A. Sue, et al. (2002). "Movement model. Hits Distribution and Learning in Virtual Keyboarding." Proceedings of the ACM Conference on Human Factors in Computing Systems: 17-24.

CURRICULUM VITA

Nam – Hun Kim

EDUCATION

M. S. Rutgers University - Biomedical Engineering May 2004
Thesis Title: *"A Cost Effective System for Optical Topography Imaging Using NIRS (Near Infrared Spectroscopy)"*

M. S. Yonsei University - Solid State Physics Aug 1999
Thesis Title: "*Temperature Dependent Elastic Property of Aluminum Single Crystal Using Ultrasonics and Cryogenics"*

B. S. Yonsei University - Physics Feb 1997
Thesis Title: *"Cryogenics – Technology and Theory to Achieve Zero Kelvin"*

WORK EXPERIENCES

Consultant; Nian-Crae Inc., Somerset, NJ, USA. 2004 Academic Year - Present

Graduate Assistant II; Biomedical Engineering, Rutgers University. 2004 AY - Present

Industrial Internship; Amersham Bioscience. Summer 2004

Graduate Assistant II; Biomedical Engineering, Rutgers University. 2002 - 2004 AY

Research Assistant; Physics, Yonsei University. 2000 - 2001

TEACHING EXPERIENCES

Co-Designer / Teaching Assistant; Biomedical Engineering, Rutgers University. 2003

Teaching Assistant; Physics, Yonsei University. 1997 - 1999 AY

MANUSCRIPTS IN PROGRESS

Nam-Hun Kim, Mike Wininger, William Craelius, *"Characterizing Kinematic and Dynamic Human Motor Control System In Cylindrical Grasp During Alternating Target Task"*.

Nam-Hun Kim, Mike Wininger, William Craelius, *"Temporal Synchronization and Correlation between First and Second End Effectors of Hand Grasping Using Myokinetic Interface With Force Myography (FMG)"*.

CONFERENCE PROCEEDINGS & PRESENTATIONS

Nam-Hun Kim, Michael Wininger, William Craelius, *"Predicting Direct Handgrip Force from Extrinsic Muscle Output with Force Myograpy (FMG)"*, 2007 Northeast American Society of Biomechanics Conference: U of Maryland, USA.

Nam-Hun Kim, Michael Wininger, William Craelius, *"Quantification of Motor Ability in Speed vs. Accuracy Trade-off Test from Hemiparetic Populations"*, 2007 Northeast American Society of Biomechanics Conference: U of Maryland, USA.

Kim N-H, Wininger MT, Craelius W, "*Characterizing Dynamic Human Motor Force Control System in Cylindrical Grasp During Alternating Target Task",* 2006 World Congress on Medical Physics and Biomedical Engineering: Seoul, South Korea. Aug 27-31, 2006.

Kim N-H, Wininger MT, Craelius W, "*Characterizing Force Variability in Human Grasping during Dynamic Force Speed vs. Accuracy Trade-Off (DSAT) task*", 3nd Annual New Jersey Bioengineering Showcase: Woodbridge, NJ. March 10, 2006.

Nam-Hun Kim M.S., James A Flint Ph.D., Jamie Dougherty B.S., Sam L. Phillips C.P., William Craelius Ph.D.
"Quantification of Upper Extremity Control using HARI (Hand and Arm Rehabilitation Interface)",
Poster presentation, BMES Annual Conference, Baltimore, Sep, 2005.

Nam-Hun Kim M.S., John Semmlow Ph.D., Stanley Dunn Ph.D.
"A Cost Effective System for Optical Imaging Using NIRS (Near-Infrared Spectroscopy)",
Poster presentation, BMES Showcase, NJIT Newark, Mar, 2005.

Nam-Hun Kim. A. Chaibi, C. Ketonis, J. Semmlow, & S. Dunn.
"*A Cost Effective System for Optical Imaging*",
Biomedical Engineering Conference, Poster Presentation, April, 2003.

Nam-Hun Kim. A. Chaibi, C. Ketonis, J. Semmlow, & S. Dunn.
"*A Cost Effective System For Optical Imaging*",
Northeastern IEEE Bioengineering Conference in NJIT, Presentation. April, 2003.

Nam-Hun Kim,
"*Temp. Dependent Elastic Property Of Al Single Crystal Using Ultrasonics and Cryogenics",*
A thesis accepted for Master of Science in Physics, Yonsei University, July, 1999.

Nam-Hun Kim.
"*Cryogenics – Technology and Theory to Achieve Zero Kelvin",*
A thesis accepted for Bachelor of Science in Physics, Yonsei University, Dec.,1997.